

**SYNTHESIS AND CHARACTERIZATION OF  
SILVER NANOWIRES VIA POLYOL PROCESS**

**NURUL AZRI KHALISAH BINTI AZNAN**

**DISSERTATION SUBMITTED IN FULLFILLMENT  
OF THE REQUIREMENT FOR THE DEGREE OF  
MASTER OF ENGINEERING SCIENCE**

**DEPARTMENT OF MECHANICAL ENGINEERING**

**FACULTY OF ENGINEERING**

**UNIVERSITY OF MALAYA**

**KUALA LUMPUR**

**2016**

**IN THE NAME OF ALLAH  
THE MOST BENEFICENT & THE MOST MERCIFUL**

University of Malaya

**UNIVERSITY OF MALAYA**  
**ORIGINAL LITERARY WORK DECLARATION**

Name of Candidate: NURUL AZRI KHALISAH BINTI AZNAN

(I.C/Passport No:

Matric No: KGA100075

Name of Degree: MASTER IN ENGINEERING SCIENCE

Title of Project Paper/Research Report/Dissertation/Thesis (“this Work”):

SYNTHESIS AND CHARACTERIZATION OF SILVER NANOWIRES VIA POLYOL  
PROCESS

Field of Study: ADVANCED NANOMATERIALS

I do solemnly and sincerely declare that:

- (1) I am the sole author/writer of this Work;
- (2) This Work is original;
- (3) Any use of any work in which copyright exists was done by way of fair dealing and for permitted purposes and any excerpt or extract from, or reference to or reproduction of any copyright work has been disclosed expressly and sufficiently and the title of the Work and its authorship have been acknowledged in this Work;
- (4) I do not have any actual knowledge nor do I ought reasonably to know that the making of this work constitutes an infringement of any copyright work;
- (5) I hereby assign all and every rights in the copyright to this Work to the University of Malaya (“UM”), who henceforth shall be owner of the copyright in this Work and that any reproduction or use in any form or by any means whatsoever is prohibited without the written consent of UM having been first had and obtained;
- (6) I am fully aware that if in the course of making this Work I have infringed any copyright whether intentionally or otherwise, I may be subject to legal action or any other action as may be determined by UM.

Candidate’s Signature

Date:

Subscribed and solemnly declared before,

Witness’s Signature Date:

Name:

Designation:

# DECLARATION

I, Nurul Azri Khalisah Binti Aznan, hereby declare that except where due acknowledgement has been made; the work presented in this thesis is my own.

Date:

Signature :

Full Name : Nurul Azri Khalisah Binti Aznan

NRIC No. :

Matric No. : KGA 100075

University of Malaysia

# ACKNOWLEDGEMENTS

All Praise Be to Allah S.W.T. for granting me the knowledge, patience, ideas and leading the way to complete my Masters research. Without His bless, I'll not be able to complete my research successfully.

First and foremost I would like to express my sincere gratitude to my supervisor, Associate Professor Dr. Mohd Rafie Bin Johan, for the continuous support of my Master study and related research, for his patience, motivation and immense knowledge. His guidance helped me in all the time of research and writing of this thesis. I could not have imagined having a better supervisor and mentor for my Master study.

Besides my supervisor, I would like to thank my fellow labmates for a good cooperation and help me a lot to conduct the experiments especially the groups of Nano Materials Research, University of Malaya. Many thanks to Advanced Materials lab assistant, Mdm Norzirah who always helps me during the experiments in the lab also other lab assistant, Mr. Mohd Said Sakat who always advice and guide me on how to use the lab instruments. Not to forget the technicians and science officers that helps a lots when using the lab instruments for characterization.

I also would like to appreciate my gratitude to University of Malaya for the PPP (PV059-2011A) grant and also HIR (HIR-MOHE D0000012-16001) grant that help me with the fund to facilitate my research works.

Last but not least, I would like to thank my beloved family; my parents, my brother and sisters for supporting me spiritually throughout writing this thesis and my life in general. And I wish you all the best.

## ABSTRACT

Silver nanowires (AgNWs) were successfully synthesized via polyol process mediated with different mediated and control agents. Morphological studies from Transmission Electron Microscopy (TEM) and Field Emission Scanning Electron Microscopy (FESEM) proved the formation of AgNWs with the diameter sizes in the range between 60 – 100 nm. X-ray Diffraction (XRD) patterns of as-synthesized samples showed the peaks that assigned to the face-centered cubic (FCC) silver (Ag) crystals which according to standard PDF card 04-0783. The peaks at angle  $2\theta$  around  $38^\circ$ ,  $44^\circ$ ,  $64^\circ$  and  $75^\circ$  are corresponding to (111), (200) and (311) crystal planes of the FCC Ag, respectively. Optical studies from UV-vis spectroscopy showed that the spectra have main peaks at wavelength around 410 nm which attributed to the transverse plasmon mode of AgNWs. The spectra also showed another shoulder peaks at wavelength around 350 nm which regarded to the plasmon resonance of long AgNWs.

## ABSTRAK

Wayar nano perak telah berjaya disintesis melalui proses poliol pengantara dengan agen pengantara dan agen kawalan yang berbeza. Kajian morfologi dari mikroskop penghantaran elektron (TEM) dan mikroskop imbasan pelepasan elektron (FESEM) membuktikan pembentukan nanowires perak dengan saiz diameter di antara 60 hingga 100 nm. Pola pembelauan sinar X bagi sampel yang telah disintesis menunjukkan puncak graf yang ditujukan kepada kristal perak berpusat muka kubik berpandukan kad PDF standard 04-0783. Puncak graf pada sudut  $2\theta$  sekitar  $38^\circ$ ,  $44^\circ$ ,  $64^\circ$  dan  $75^\circ$  setiap satunya adalah sepadan dengan planar (111), (200) dan (311) kristal perak berpusat muka kubik. Kajian optik dari spektroskopi Uv-vis menunjukkan spektrum yang mempunyai puncak graf utama pada panjang gelombang sekitar 410 nm yang dikaitkan dengan mod plasmon melintang nanowires perak. Spektrum itu juga menunjukkan satu lagi puncak bahu graf pada panjang gelombang sekitar 350 nm yang dianggap sebagai resonans plasmon bagi panjang nanowires perak.

# TABLE OF CONTENTS

<b>Content</b>	<b>Page</b>
Declaration	i
Acknowledgement	ii
Abstract	iii
Abstrak	iv
Table of Contents	v
List of Paper and Conference from This Work	xi
List of Figures	xii
List of Tables	xvi
List of Symbols and Abbreviations	xvii
<b>Chapter 1 Introduction</b>	
1.1 Backgrounds	1
1.2 Research Motivation	3
1.3 Research Objectives	4
1.4 Scope of Thesis	5



## Chapter 2 Literature Review

2.1	Nanotechnology	6
2.2	Nanomaterials	7
2.3	Nanowires	8
2.4	Silver	9
2.5	Silver Nanowires	10
2.6	Synthesis of Nanomaterials	11
2.7	Synthesis of Silver Nanowires	13
2.8	Polyol Reduction Process	15
2.8.1	Ethylene Glycol (EG)	15
2.8.2	Silver nitrate ( $\text{AgNO}_3$ )	16
2.8.3	Polyvinylpyrrolidone (PVP)	17
2.8.4	Sodium chloride (NaCl)	18
2.8.5	Copper (II) chloride ( $\text{CuCl}_2$ )	19
2.8.6	Ratio between PVP and $\text{AgNO}_3$	20

## Chapter 3 Research Methodology

3.1	Overview	21
3.2	Materials	22
3.3	Synthesis techniques	
3.3.1	Synthesis of AgNWs with reducing agent of 1, 2-Propanediol	23
3.3.2	Synthesis of AgNWs with mediated $\text{CuCl}_2$ mediated	24
3.3.3	Synthesis of AgNWs with mediated agent NaCl at different molar concentration of $\text{AgNO}_3$	25
3.3.4	Synthesis of AgNWs with different control agents (KOH, KCL, $\text{Fe}(\text{NO}_3)_3$ , $\text{H}_2\text{O}$ )	26
3.4	Characterization techniques	
3.4.1	Field Emission Scanning Electron Microscope (FESEM)	27
3.4.2	Transmission Electron Microscope (TEM)	28
3.4.3	X-ray Diffraction (XRD)	29
3.4.4	UV-vis Spectroscopy	30

## Chapter 4 Results and Discussion

4.1	Overview	32
4.2	Synthesis of AgNWs without mediated agent	32
4.2.1	Mechanism formation of AgNWs with reducing agent of 1, 2 – Propanediol	33
4.2.2	Morphological studies	
4.2.2.1	Field Emission Scanning Electron Microscopy (FESEM) Analysis	35
4.2.2.2	Transmission Electron Microscopy (TEM) analysis	38
4.2.3	Structural studies	
4.2.3.1	X-Ray Diffraction (XRD) analysis	44
4.2.4	Optical studies	
4.2.4.1	UV - vis spectroscopy analysis	46
4.3	Synthesis of AgNWs with mediated agent of $\text{CuCl}_2$	49
4.3.1	Mechanism formation of AgNWs with mediated agent of $\text{CuCl}_2$	49
4.3.2	Morphological studies	
4.3.2.1	FESEM analysis	51
4.3.2.2	TEM analysis	54

4.3.3	Structural studies	
4.3.3.1	XRD analysis	56
4.3.4	Optical studies	
4.3.4.1	UV-vis spectroscopy analysis	57
4.4	Synthesis of AgNWs with mediated agent of NaCl	59
4.4.1	Mechanism formation of AgNWs with mediated agent of NaCl	59
4.4.2	Morphological studies	
4.4.2.1	FESEM analysis	62
4.4.2.2	TEM analysis	65
4.4.3	Structural studies	
4.4.3.1	XRD analysis	69
4.4.4	Optical studies	
4.4.4.1	UV-vis spectroscopy analysis	71
4.5	Synthesis of AgNWs via polyol process with different control agent (KOH, KCL, Fe(NO <sub>3</sub> ) <sub>3</sub> , H <sub>2</sub> O)	74
4.5.1	Morphological studies	
4.5.1.1	FESEM analysis	74
4.5.1.2	TEM analysis	77

4.5.2	Structural analysis	
4.5.2.1	XRD studies	80
4.5.3	Optical studies	
4.5.3.1	UV-vis spectroscopy analysis	81
<b>Chapter 5 Conclusion</b>		83
5.1	Suggestions for future work	85
<b>References</b>		
<b>Appendices</b>		

## **LIST OF PAPER ACCEPTED FROM THIS WORK**

1. M. R. Johan, N. A. K. Aznan, T. Y. Soo, H. H. Ing, W. O. Soo, N. D. Singho and F. Aplop. Synthesis and Growth Mechanism of Silver Nanowires through Different Mediated Agents ( $\text{CuCl}_2$  and  $\text{NaCl}$ ) Polyol Process. Hindawi Publishing Cooperation, *Journal of Nanomaterials* (2014).

## **LIST OF CONFERENCE ATTENDED FOR THIS WORK**

1. 3<sup>rd</sup> International Conference on Functional Materials and Devices, 2011, Kuala Terengganu. (ICFMD 2011)
2. 4<sup>th</sup> International Conference on Functional Materials and Devices, 2013. Penang. (ICFMD 2013)

## LIST OF FIGURES

<b>Figure</b>		<b>Page</b>
Figure 2.1	Schematic diagram of Top Down and Bottom Up process	13
Figure 3.1	FESEM machine	27
Figure 3.2	Transmission electron microscope	28
Figure 3.3	X-ray diffraction machine	29
Figure 3.4	UV – Vis spectrophotometer	30
Figure 4.1	FESEM image of as-synthesized sample which has PVP: AgNO <sub>3</sub> molar ratio of 4.5:1 and 5 minutes of injection time.	35
Figure 4.2	FESEM image of as-synthesized sample which has PVP: AgNO <sub>3</sub> molar ratio of 6:1 and 5 minutes of injection time.	36
Figure 4.3	FESEM image of as-synthesized sample which has PVP: AgNO <sub>3</sub> molar ratio of 7.5:1 and 5 minutes of injection time.	36
Figure 4.4	FESEM image of as-synthesized sample which has PVP: AgNO <sub>3</sub> molar ratio of 7.5:1 and 10 minutes of injection time.	37
Figure 4.5	FESEM image of as-synthesized sample which has PVP: AgNO <sub>3</sub> molar ratio of 7.5:1 and 15 minutes of injection time.	37
Figure 4.6	TEM image of as-synthesized sample at PVP: AgNO <sub>3</sub> molar ratio of 4.5:1.	38
Figure 4.7	TEM image of as-synthesized sample at PVP: AgNO <sub>3</sub> molar ratio of 6.0:1.	39
Figure 4.8	TEM image of as-synthesized sample at PVP: AgNO <sub>3</sub> molar ratio of 7.5:1.	39
Figure 4.9	TEM image of as-synthesized sample at injection time of	

	5 minutes.	41
Figure 4.10:	TEM image of as-synthesized sample at injection time of	
	10 minutes.	42
Figure 4.11	TEM image of as-synthesized sample at injection time of	
	15 minutes.	42
Figure 4.12	XRD pattern of as-synthesized sample for molar ratio of 7.5	
	with 15 minutes injection time.	44
Figure 4.13	UV-vis spectra of as-synthesized samples with different molar	
	ratio of the repeating units of PVP and AgNO <sub>3</sub> .	46
Figure 4.14	UV-vis spectra of as-synthesized samples with different	
	injection times.	47
Figure 4.15	FESEM image of as-synthesized sample with CuCl <sub>2</sub>	
	mediated agent at 1000X magnification.	51
Figure 4.16	FESEM image of as-synthesized sample with CuCl <sub>2</sub>	
	mediated agent at 2000X magnification.	52
Figure 4.17	FESEM image of as-synthesized sample with CuCl <sub>2</sub>	
	mediated agent at 10000X magnification.	52
Figure 4.18	FESEM image of as-synthesized sample with CuCl <sub>2</sub>	
	mediated agent at 20000X magnification.	53
Figure 4.19	TEM image of as-synthesized individual AgNW with CuCl <sub>2</sub>	
	mediated agent.	54
Figure 4.20	TEM image revealing the pentagonal cross-sectional of	
	AgNW edge.	54
Figure 4.21	TEM image of typical as-synthesized AgNWs with CuCl <sub>2</sub>	



	mediated agent.	55
Figure 4.22	XRD pattern of as-synthesized sample with $\text{CuCl}_2$ mediated agent.	56
Figure 4.23	UV-vis spectrum of as-synthesized sample with $\text{CuCl}_2$ mediated agent.	57
Figure 4.24	Schematic of a 5-fold twinned pentagonal nanowires consisting of five elongated $\{100\}$ facets and 10 $\{111\}$ end facets.	61
Figure 4.25	FESEM image for as-synthesized samples with 0.025M of $\text{AgNO}_3$ .	62
Figure 4.26	FESEM image for as-synthesized samples with 0.050M of $\text{AgNO}_3$ .	63
Figure 4.27	FESEM image for as-synthesized samples with 0.10M of $\text{AgNO}_3$ .	63
Figure 4.28	FESEM image for as-synthesized samples with 0.20M of $\text{AgNO}_3$ .	64
Figure 4.29	FESEM image for as-synthesized samples with 0.25M of $\text{AgNO}_3$ .	64
Figure 4.30	TEM images of as-synthesized AgNWs with 0.20M of $\text{AgNO}_3$ at different magnification.	66
Figure 4.31	TEM images of as-synthesized AgNWs with 0.25M of $\text{AgNO}_3$ at different magnification.	67
Figure 4.32	XRD pattern of the as synthesized AgNWs at molarity 0.20M of $\text{AgNO}_3$ .	68
Figure 4.33	XRD pattern of the as synthesized AgNWs at molarity 0.25M of $\text{AgNO}_3$ .	69
Figure 4.34	UV- vis spectra for as-synthesized AgNWs at 0.025 and 0.05M of $\text{AgNO}_3$ .	70
Figure 4.35	UV-vis spectra for as-synthesized AgNWs at 0.01, 0.02 and 0.25M of $\text{AgNO}_3$ .	71

Figure 4.36	FESEM image for as-synthesized sample with control agent of KOH.	72
Figure 4.37	FESEM image for as-synthesized sample with control agent of KCl.	73
Figure 4.38	FESEM image for as-synthesized sample with control agent of Fe (NO <sub>3</sub> ) <sub>3</sub> .	73
Figure 4.39	FESEM image for as-synthesized sample with control agent of H <sub>2</sub> O.	74
Figure 4.40	TEM image for as-synthesized sample with control agents of KOH	75
Figure 4.41	TEM image for as-synthesized sample with control agents of KCl.	76
Figure 4.42	TEM image for as-synthesized sample with control agents of Fe (NO <sub>3</sub> ) <sub>3</sub> .	76
Figure 4.43	TEM image for as-synthesized sample with control agents of H <sub>2</sub> O.	77
Figure 4.44	XRD patterns of all as-synthesized samples with different control agents KOH, KCl, Fe(NO <sub>3</sub> ) <sub>3</sub> and H <sub>2</sub> O.	78
Figure 4.45	UV-vis spectra of as-synthesized AgNWs with control agents KOH, KCl, and Fe(NO <sub>3</sub> ) <sub>3</sub> and H <sub>2</sub> O.	79

## LIST OF TABLES

<b>Table</b>		<b>Page</b>
Table 3.1	Samples prepared with different injection times and PVP concentrations.	24
Table 3.2	Samples with different molar concentration of AgNO <sub>3</sub> .	25

University of Malaya

## LIST OF SYMBOLS AND ABBREVIATIONS

Symbol/Abbreviation	Phrase
1-D	One dimensional
AAO	Anodic alumina oxide
Ag	Silver
AgF <sub>2</sub>	Silver (II) fluoride
AgNO <sub>3</sub>	Silver nitrate
AgNPs	Silver nanoparticles
AgNWs	Silver nanowires
Au	Gold
Br	Bromine
Cl	Chlorine
Co	Cobalt
Cu	Copper
CuCl <sub>2</sub>	Copper (II) chloride
EG	Ethylene glycol
FCC	Face centered cubic
Fe	Iron

FESEM	Field Emission Scanning Electron Microscope
Fe(NO <sub>3</sub> ) <sub>3</sub>	Iron (III) nitrate
FWHM	Full width half maximum
H <sub>2</sub> O	Water
I	Iodine
K(AgF <sub>4</sub> )	Potassium tetrafluoroargentate
KCl	Potassium Chloride
KOH	Potassium hydroxide
ml	Milliliter
n	Refractive index
nm	Nanometer
NaCl	Sodium chloride
Ni	Nickel
Pd	Palladium
Pt	Platinum
PVP	Polyvinylpyrrolidone
Si	Silicon
TEM	Transmission Electron Microscope

UV-vis	Ultraviolet visible
XRD	X-ray Diffraction
$\mu\text{l}$	Micro liter
$\theta$	Diffraction angle
$\epsilon$	Permittivity
$\mu$	Permeability
$\lambda$	Wavelength

University of Malaya

# CHAPTER 1

---

## INTRODUCTION

### 1.1 Background

One-dimensional (1-D) metallic nanostructures have drawn a significant amount of research attention recently, because of their unique electrical, optical, thermal, magnetic and catalytic properties (Xingling et al. 2009). 1-D nanostructures are slivers of material constrained in two dimensions to less than 100 nm. Within this category of nanomaterials, researchers discriminate between nanorods with aspect ratios (length/diameter) less than 10, nanowires with aspect ratios greater than 10, and nanotubes with hollow interiors (Chen et al., 2007).

Among various noble metals, silver nanowires (AgNWs) are given much effort on research because of their unique physical and chemical properties, which has been widely used in catalysis (Shi et al., 2004) , optical, electrical (X.-Y. Zhang et al., 2012) and antibacterials. Moreover, silver bulk also exhibit highest electrical and thermal conductivities (You et al., 2009). AgNWs has potential applications on transparent conducting film and electrode of electrochemical capacitor due to its excellent conductivity (Song et al., 2014).

The most widely used method to produce AgNWs is template-directed synthesis that involves hard templates and soft templates and template-free. In the previous study, several papers reported the growth of AgNWs by employing different synthesis method, effect of solvent and the reaction temperature (Sarkar et al., 2010).

In this research, AgNWs was synthesis via polyol process. This polyol process is the most versatile method to produce AgNWs. This polyol process was introduced by (Fievet et al., 1989). Polyol process was described at first as a novel route for preparing finely divided metal powders for easily reducible metal such as copper (Cu), noble metals like gold (Au), palladium (Pd), silver (Ag) and their alloys, or less reducible metals such as cobalt (Co), nickel (Ni), iron (Fe) and their alloys by reduction of inorganic precursors in liquid polyols (Fiévet & Brayner, 2013). Polyol used were either polyhydric alcohols namely  $\alpha$ -diols such as 1,2-ethanediol (ethylene glycol), 1,2-propanediol (propylene glycol), or etherglycols namely di (ethylene) or tri (ethylene glycol).

Polyols are interesting among non-aqueous solvents because like water and monoalcohols, they are hydrogen bonded liquids with high value of relative permittivity. Therefore they are able to dissolve, to some extent in ionic and inorganic compounds. Moreover, polyols, as well as monoalcohols are mild reducing agents but thus reduction can be carried out in such solvents under atmospheric pressure up to 250°C if necessary.

The reaction of the synthesis process involves the reduction of an inorganic salt at an elevated temperature. Polyvinylpyrrolidone (PVP) is added as a stabilizer to prevent agglomeration of the colloidal particles. The versatility of this synthesis includes the ability of polyol to dissolve precursor salts (and ions), it's highly temperature-dependent reducing power and it's relatively high boiling point (for ethylene glycol (EG), it is about 196°C). In particular, the temperature-dependent reducing power of polyol helps synthesizing the colloidal particles over a broad range of sizes, as it gives us the ability to control the nucleation and growth processes through careful regulation of reaction temperature.



## 1.2 Research Motivation

The problem highlighted through this synthesis process is to get large amount of the powder for further characterization. This polyol process had been through some innovation as mediated agent had been introduced to the process. Mediated agents such as copper chloride ( $\text{CuCl}_2$ ) and sodium chloride ( $\text{NaCl}$ ) are added into the reaction of the polyol process (Korte et al., 2008; Tang et al., 2009; Z. Zhang et al., 2011). The results is improved with the additional of this mediated agent.

Beside that the molar ratio of  $\text{AgNO}_3$  to PVP also affected the results on formation of AgNWs. Therefore, it is important to identify the right molar ratio of  $\text{AgNO}_3$  to PVP to get the good result of AgNWs formation.

One of the important steps in this polyol process is the injection of PVP solution into the  $\text{AgNO}_3$  solution. The growth of AgNWs occurs during this step and it is very important to control the injection time as the AgNWs formation is a slow reaction process.

In this research, AgNWs was synthesis via polyol process with different mediated and control agent;  $\text{CuCl}_2$ ,  $\text{NaCl}$ , potassium hydroxide ( $\text{KOH}$ ), potassium chloride ( $\text{KCl}$ ), iron nitrate ( $\text{Fe}(\text{NO}_3)_3$ ) and water ( $\text{H}_2\text{O}$ ). As-synthesized AgNWs was characterized to study their morphological, structural and optical properties using Field Emission Scanning Electron Microscope (FESEM), Transmission Electron Microscope (TEM), X-Ray Diffraction (XRD) and UV-Vis Spectroscopy.

### **1.3 Research Objectives**

The main objectives of this research are listed as below:

- i. To synthesis AgNWs via polyol process using different mediated agent.
- ii. To characterize AgNWs via several analytical technique such as FESEM, TEM, XRD and UV-vis.
- iii. To optimize AgNWs based on their diameter sizes.

University of Malaya

## **1.4 Scope of Thesis**

This thesis is divided into five chapters. Chapter one is an introduction of research on AgNWs synthesized via polyol process and the background. Besides that, the significance and objectives of this research are stated in detail.

Chapter two presents a literature review of synthesis process of AgNWs via polyol process as well as its recent research. The mediated agents used in the synthesis are also reviewed in this chapter.

Chapter three is the research methodology that elaborates in details the experimental works done in this research. Characterization studies are also explained in details.

Chapter four presents all the results and discussion of this research. Analysis studies on morphological, structural and optical from the characterization of as-synthesized AgNWs are discussed thoroughly. Beside that the discussion on mechanism of AgNWs formation synthesized with different reducing agents and different mediated agents is also elaborated in this chapter.

Chapter five concludes the findings of this research as well as recommendation for future works.

# CHAPTER 2

---

## LITERATURE REVIEW

### 2.1 Nanotechnology

Nanotechnology literally means any technology on a nanoscale that has application in the real world (Bhushan, 2010). The term nanotechnology was first use in 1974 by late Norio Taniguchi to refer the ability to engineer materials precisely at the scale of nanometers. Its literally means technology that is very small that has application on the real world. Nanotechnology can be defined as the science and engineering involved in design, synthesis, characterization and application of material and devices whose smallest functional organization in at least one dimension is on the nanometer scale or one billionth of a meter. At these scales, consideration of individual molecules and interacting groups of molecules in relation to the bulk macroscopic properties of the material or device becomes important, since it is control over the fundamental molecular structure that allows control over the macroscopic properties (Silva, 2004).

A more generalized description of nanotechnology was subsequently established by the National Nanotechnology Initiative, which defines nanotechnology as the manipulation of matter with at least one dimension sized from 1 to 100 nanometers. This definition reflects the fact that quantum mechanical effects are important at this quantum-realm scale, and so the definition shifted from a particular technological goal to a research category inclusive of all types of research and technologies that deal with the special properties of matter that occur below the given size threshold. It is therefore common to see the plural

form "nanotechnologies" as well as "nanoscale technologies" to refer to the broad range of research and applications whose common trait is size.

Nanotechnology is a growing field that explores electrical, optical and magnetic activity as well as structural behaviour at the molecular and submolecular level. One of the practical applications of nanotechnology is the science of constructing computer chips and other devices using nanoscale building elements. "Building blocks" for nanomaterials include carbon-based components and organic, semiconductor, metal and metal oxide. Nanoscale structures permit the control of fundamental properties of material without changing the materials' chemical status.

## **2.2 Nanomaterials**

Nanomaterials are defined as materials with at least one external dimension in the size range from approximately 1-100 nanometers. Nano-sized materials are naturally present from forest fires and volcanoes, viral particles, biogenic magnetite, and even protein molecules such as ferritin (Oberdörster, 2004). Recently, anthropogenic sources have also produced nano-sized materials unintentionally from combustion by-products and intentionally as manufactured nanomaterials. Engineered nanomaterials are useful because of their large surface area:mass ratio, which makes them important as catalysts in chemical reactions, and they have desirable properties as drug delivery devices, as imaging agents in medicine, and in consumer products such as sunscreens and cosmetics (Colvin, 2003).

Nanomaterials attracts so much interest because it can have different or enhanced properties compared with those at a bulk size, including increased the chemical reactivity, optical, magnetic or electrical properties. It also gives a much high ratio of surface area to

volume than bulk materials and thus expects to be more reactive (Bhushan, 2010). Nanotechnology aims to exploit these properties to create devices, system and structures with new characteristics and functions.

### 2.3 Nanowires

A nanowire is a nanostructure, with the diameter of the order of a nanometer ( $10^{-9}$  meters). It can also be defined as the ratio of the length to width being greater than 1000. Alternatively, nanowires can be defined as structures that have a thickness or diameter constrained to tens of nanometers or less and an unconstrained length. At these scales, quantum mechanical effects are important - hence such wires are also known as "quantum wires". Many different types of nanowires exist, including superconducting (e.g., YBCO), metallic (e.g., Ni, Pt, Au), semiconducting (e.g., Si, InP, GaN, etc.), and insulating (e.g., SiO<sub>2</sub>, TiO<sub>2</sub>). Molecular nanowires are composed of repeating molecular units either organic (e.g. DNA) or inorganic (e.g. Mo<sub>6</sub>S<sub>9-x</sub>I<sub>x</sub>).

Nanowires have received a great attention due to their special optical, electrical, thermal and magnetic properties with size confinement and dimensionality. The intrinsic properties of nanowires are generally determined by its composition and size (Tang & Tsuji, 2010).

Nanowires are attractive for nanoscience studies and nanotechnology applications. Nanowires have two confined directions compared to other low dimensional systems. However, nanowires still leaving one unconfined direction for electrical conduction. Small diameters of nanowires are expected to display significantly different electrical, optical and

magnetic properties from their 3D crystalline counterpart because of their special density of electronic states.

Properties of nanowires can be improved by exploiting the singular features of the 1D electronic density of state. From applications point of view, nanowires are independently controlled properties for some materials that have critical parameter (Dresselhaus et al., 2003).

## **2.4 Silver**

Silver (Ag) is a metallic chemical element with the chemical symbol Ag and atomic number 47. A soft, white, lustrous transition metal, it has the highest electrical conductivity of any element and the highest thermal conductivity of any metal. The metal occurs naturally in its pure, free form (native silver), as an alloy with gold and other metals, and in minerals such as argentite and chlorargyrite. Most silver is produced as a by-product of copper, gold, lead, and zinc refining.

Ag has long been valued as a precious metal, and it is used to make ornaments, jewellery, high-value tableware, utensils (hence the term silverware), and currency coins. Today, Ag metal is also used in electrical contacts and conductors, in mirrors and in catalysis of chemical reactions. Its compounds are used in photographic film and dilute silver nitrate solutions and other Ag compounds are used as disinfectants and microbiocides. While many medical antimicrobial uses of Ag have been supplanted by antibiotics, further research into clinical potential continues.

Ag is a very ductile and malleable (slightly harder than gold) monovalent coinage metal with a brilliant white metallic luster that can take a high degree of polish. It has the highest electrical conductivity of all metals, even higher than copper, but its greater cost and tendency to tarnish have prevented it from being widely used in place of copper for electrical purposes. Despite this, 13,540 tons were used in the electromagnets used for enriching uranium during World War II (mainly because of the wartime shortage of copper). Another notable exception is in high-end audio cables.

Among metals, pure Ag has the highest thermal conductivity (the non-metal diamond and superfluid helium II are higher) and one of the highest optical reflectivity. (Aluminium slightly outdoes silver in parts of the visible spectrum, and Ag is a poor reflector of ultraviolet light). Ag also has the lowest contact resistance of any metal. Ag halides are photosensitive and are remarkable for their ability to record a latent image that can later be developed chemically. Ag is stable in pure air and water, but tarnishes when it is exposed to air or water containing ozone or hydrogen sulfide to form a black layer of silver sulfide which can be cleaned off with dilute hydrochloric acid. The most common oxidation state of silver is +1 (for example, silver nitrate:  $\text{AgNO}_3$ ); in addition, +2 compounds (for example, silver(II) fluoride:  $\text{AgF}_2$ ) and the less common +3 compounds (for example, potassium tetrafluoroargentate:  $\text{K}[\text{AgF}_4]$ ) are known.

## 2.5 Silver Nanowires

Silver nanowires (AgNWs) represent a particular class of interesting nanostructures to synthesis and study because bulk Ag exhibits the highest electrical and thermal conductivity. The structure and properties of nanowires are controlled by their relatively



high fraction of surface atoms compared to bulk silver. For example, the loading of Ag in polymeric composite could be significantly reduced when nanoparticles of Ag are replaced by nanowires having higher aspect ratio. As the wire diameter is decreased, the fraction of atoms on the wire surface increases.

Various techniques had been attempted for the synthesis of AgNWs, including hard template and solution phase synthesis. (Liu et al., 2005) used anodic alumina oxide (AAO) membrane as template to prepare AgNWs array in solution phase by direct chemical reduction at room temperature. On the other hand, (X. Huang et al., 2011) utilized the nanoscale channels of mesoporous silica SBA – 15 to synthesize AgNWs. However, more researchers adopted direct synthesis by polyol reduction.

## **2.6 Synthesis of Nanomaterials**

Different methods for synthesis of nanomaterials can accommodate precursors from solid, liquid and gas phase. In general, there are two approaches of obtaining the nanomaterials which are “top-down” and “bottom-up” approaches.

“Bottom up” approach involves the assembly of small units into the desired structure. The wide variety of approaches can be split into three categories: chemical synthesis, self-assembly and position assembly. In the bottom-up route, nano to microscale patterned structures are assembled using interaction between molecules or colloidal particles. The strategies for the synthesis of nanomaterials using bottom-up approaches involve the assembly of small units into nanostructures where the small unit arranged according to a well defined shape and architecture. Self-assembly is a bottom-up

production approach which atoms or molecules arrange themselves into ordered nanoscale structures by physical or chemical interaction between the units.

“Top-down” approach involves a larger piece of material are modified by reduce its dimension to give smaller features. It is a technique begins with a macroscopic material and incorporate small-scale details into them. This can be done by using techniques such as precision engineering and lithography. Top-down lithography approach offers arbitrary geometrical designs and good nanometer-level precision and accuracy. Lithography in general involves the patterning of surface through exposure to light, ions or electro, and then subsequent etching and deposition of material on that surface to produce the desired device (Malfatti et al., 2010).

University of Malaysia

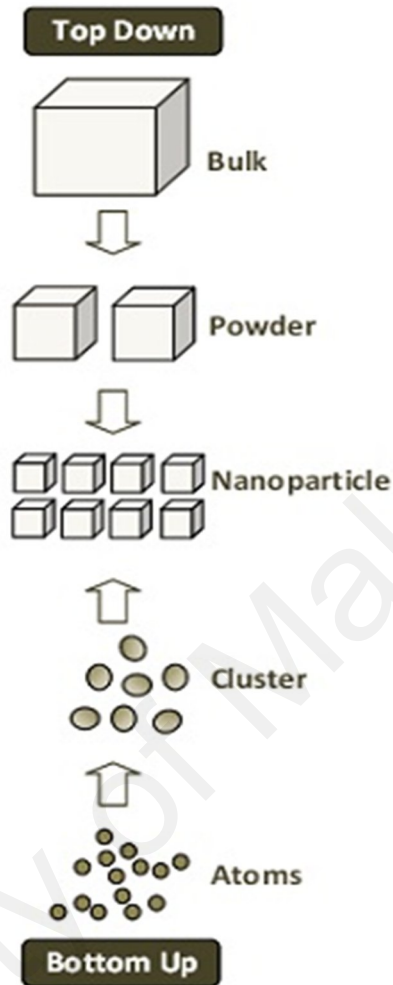


Figure 2.1: Schematic diagram of Top Down and Bottom Up process

## 2.7 Synthesis of Silver Nanowires

Much effort has been devoted to the syntheses of 1D silver nanomaterials. The most widely used method for generating silver nanorods and nanowires is template-directed synthesis that involves hard templates (Day et al., 2005), (Han et al., 2000), (M. H. Huang

et al., 2000), and (Zong et al., 2004) and soft templates (Braun et al., 1998), (Jana et al., 2001), (Murphy & Jana, 2002) and (Shen et al., 2007).

(M. H. Huang et al., 2000) successfully synthesis AgNWs within mesoporous silica SBA-15 by chemical approach which involves  $\text{AgNO}_3$  impregnation, followed by thermal decomposition. (Zong et al., 2004) prepared transparent AgNWs arrays embedded in anodic alumina membrane by a template-based approach combined with alternating current (AC) electrodeposition and subsequent etching of substrate. Gold seed assisted method also been used to produce AgNWs under microwave heating which is low temperature process (Liu et al., 2005). This method produced templateless and polymerless AgNWs with AgNPs.

(You et al., 2009) have reported the synthesis of AgNWs using alcohol-thermal method where  $\text{AgNO}_3$  has been reduced by dodecylamine in ethanol. Polyol process is one of the method that usually been used by many researchers in synthesis the AgNWs. Polyol such as Ethylene glycol (EG) or 1,2-Propanediol is used to reduce  $\text{AgNO}_3$  and Polyvinylpyrrolidone (PVP) as the capping agent (Sun & Xia, 1991), (Sun et al., 2002), (Chen et al., 2006), (Tsuji et al., 2006), (Sarkar et al., 2010), (Tang & Tsuji, 2010) and (Coskun et al., 2011). This polyol process involves the reaction at high temperature.

Mediated agents such as  $\text{NaCl}$  and  $\text{CuCl}_2$  also proposed from some researchers in the synthesis of AgNWs through the polyol process (Korte et al., 2008), (Tang et al., 2009) and (Zhang et al., 2011). These mediated agents facilitated the growth of AgNWs.

## **2.8 Polyol Reduction Process**

Polyol reduction process whereby an organic solvent such as alcohol is used as reducing agent to reduce dissolved inorganic salt. It is commonly done in reflux or boiling system where the alcohol solution of metal is heated and the evaporation solvent is condensed and then fed back to solution.

In this process, the salt precursor is reduced from silver ions to silver. When the Ag atom reaches supersaturation, they agglomerate to form nuclei and seed crystals are formed. The seed formed play a major role in the formation of anisotropic structures. Most nuclei contain twin boundary defects because such defects enable a lower surface energy.

The polyol process offers several advantages. It is versatile whereby different morphology of nanostructures can be obtained by changing the preparation parameters in the system. The morphology could be further well control thorough introducing capping agent. One good example is the synthesis of AgNWs by using PVP as structure-directing reagent developed by (Sun et al., 2002). Besides, large-scale of uniform AgNWs with high aspect ratios is successfully achieved with or without exotic seeds. It is also easy to operate in an air environment.

### **2.8.1 Ethylene Glycol (EG)**

EG is an organic compound. It is colourless and odourless liquid. It is also hygroscopic and completely miscible with many polar solvent such as water, alcohol and acetone. However, its solubility in non-polar solvent is low. EG has two hydroxyl groups

attached to separate carbon atoms in aliphatic chain. It has properties characterizes of alcohol and undergo reaction typical of alcohol. In this research, EG was used as reducing agent reducing agent and solvent as well in the preparation of AgNWs.

### **2.8.2 Silver nitrate ( $\text{AgNO}_3$ )**

Silver nitrate is an organic compound with chemical formula  $\text{AgNO}_3$ .  $\text{AgNO}_3$  is a white crystal inorganic compound look like salt in solid form. This compound is a versatile precursor to many other silver compounds, such as those used in photography. It is far less sensitive to light than the halides. It is an intermediate in the preparation of other silver salts, including the colloidal Ag. Otherwise,  $\text{AgNO}_3$  is least expensive salt of Ag; it offers several other advantages as well. It is non-hygroscopic, in contrast to Ag fluoroborate and Ag perchlorate. It is relatively stable to light. Finally, it dissolves in numerous solvents, including water. The nitrate can be easily replaced by other ligands, rendering  $\text{AgNO}_3$  versatile. Treatment with solutions of halide ions gives a precipitate of  $\text{AgX}$  ( $X=\text{Cl}, \text{Br}, \text{I}$ ). When making photographic film,  $\text{AgNO}_3$  is treated with halides salts of sodium or potassium to form insoluble silver halide in situ in photographic gelatin, which is then applied to strips of tri-acetate or polyester. Similarly,  $\text{AgNO}_3$  is used to prepare some Ag-based explosives, such as the fulminate, azide or acetylide, through a precipitation reaction. It is essential raw material used to prepare Ag nanostructures through chemical reduction process. Treatment of  $\text{AgNO}_3$  with base gives dark grey Ag oxide.

### 2.8.3 Polyvinylpyrrolidone (PVP)

PVP is white to light yellow color appearance of amorphous powder. It is the most widely used surfactant in the synthesis of Ag nanostructures through polyol method. It has been widely used as a protecting agent in liquid state for Ag nanostructures to avoid aggregation.

PVP is a homopolymer with a polyvinyl backbone and its repeat unit contains an amide groups. It shows pyrrolidone rings are attached to the main chain of carbon backbone. One of the outstanding properties of PVP is their universal solubility in hydrophilic and hydrophobic solvent (Folttmann & Quadir, 2008). These structural features make this polymer a good stabilizing role to control the growth rate of nanostructures and to produce desirable nanowires shape.

(Tsuji et al., 2006) studied on the morphology of Ag nanomaterials by changing the chain length of PVP. When the shortest chain PVP was used, spherical particles, triangular, pentagonal, and hexagonal nanoplates and nanorods are produced. The average length of nanorods was 160 nm and the maximum aspect ratio of nanorods was 7. When molecular weight of PVP of 40 k was used, nanorods and nanowires with lengths of 0.5-4  $\mu\text{m}$  are preferentially produced. The maximum aspect lengthly of nanorods and nanowires were 1-20  $\mu\text{m}$  with the longest chain PVP of 360 k was used, and the aspect ratio was 200. These results imply the aspect ratios of nanorods and nanowires increased with increasing the chain length of PVP.

(Luu et al., 2011) present a controllable synthesis of AgNWs and also the effect of PVP concentration and molecular weight on the growth of the AgNWs. The results show that AgNWs successfully synthesized with finely crystallize and has a preferential growth

direction and consists of uniform AgNWs in methanol solution appeared a main peak at 374 nm and a shoulder at 352 nm, both of which corresponding to the surface Plasmon absorption associated with the short axis of the AgNWs. The lower concentration of PVP or shorter chain length often caused incomplete coverage on side wall of AgNWs. They concluded that high PVP concentration and high molecular weight help to control the growth and uniformity of AgNWs.

#### **2.8.4 Sodium chloride (NaCl)**

Sodium chloride also known as salt, common salt, table salt or halite, is an ionic compound with the chemical formula NaCl, representing a 1:1 ratio of sodium and chloride ions. Sodium chloride is the salt most responsible for the salinity of seawater and of the extracellular fluid of many multicellular organisms. In the form of edible or table salt it is commonly used as a condiment and food preservative. Large quantities of sodium chloride are used in many industrial processes, and it is a major source of sodium and chlorine compounds used as feedstocks for further chemical syntheses. A second major consumer of sodium chloride is de-icing of roadways in sub-freezing weather.

In solid sodium chloride, each ion is surrounded by six ions of the opposite charge as expected on electrostatic grounds. The surrounding ions are located at the vertices of a regular octahedron. In the language of close-packing, the larger chloride ions are arranged in a cubic array whereas the smaller sodium ions fill all the cubic gaps (octahedral voids) between them. This same basic structure is found in many other compounds and is commonly known as the halite or rock-salt crystal structure. It can be represented as a face-centered cubic (fcc) lattice with a two-atom basis or as two interpenetrating face centered



cubic lattices. The first atom is located at each lattice point, and the second atom is located half way between lattice points along the fcc unit cell edge.

Thermal conductivity of NaCl as a function of temperature has a maximum of 2.03 W/(cm K) at 8 K ( $-265.15\text{ }^{\circ}\text{C}$ ;  $-445.27\text{ }^{\circ}\text{F}$ ) and decreases to 0.069 at 314 K ( $41\text{ }^{\circ}\text{C}$ ;  $106\text{ }^{\circ}\text{F}$ ).

### **2.8.5 Copper (II) chloride ( $\text{CuCl}_2$ )**

Copper (II) chloride is a chemical compound with the chemical formula  $\text{CuCl}_2$ . It is a light brown solid, which slowly absorbs moisture to form a blue-green dihydrate. The copper (II) chlorides are some of the most common copper (II) compounds, after copper sulfate.

Anhydrous  $\text{CuCl}_2$  adopts a distorted cadmium iodide structure. In this motif, the copper centers are octahedral. Most copper (II) compounds exhibit distortions from idealized octahedral geometry due to the Jahn-Teller effect, which in this case describes the localization of one d-electron into a molecular orbital that is strongly antibonding with respect to a pair of chloride ligands. In  $\text{CuCl}_2 \cdot 2\text{H}_2\text{O}$ , the copper again adopts a highly distorted octahedral geometry, the Cu(II) centers being surrounded by two water ligands and four chloride ligands, which bridge asymmetrically to other Cu centers.

### 2.8.6 Ratio between PVP and AgNO<sub>3</sub>

The morphology and aspect ratio of the AgNWs strongly depended on the molar ratio between PVP and AgNO<sub>3</sub>. Different nanostructures produced with respect to different ratio between PVP and AgNO<sub>3</sub> might cause high coverage of PVP on all faces of the seeds leading to an isotropic growth mode. The low ratio of PVP to AgNO<sub>3</sub> will cause the incomplete coverage of PVP and incomplete formation of AgNWs.

(Zhang et al., 2011) reported high yield preparation of AgNWs by controlling the concentration of PVP and molar ratio relative to AgNO<sub>3</sub>. There were only AgNPs in the samples at molar ratio of PVP/AgNO<sub>3</sub> lower than 2:1. The bigger sizes of nanoparticles of Ag with few nanowires were formed in the sample with molar ratio of 4:1. However, when the molar ratio of PVP/AgNO<sub>3</sub> increases to 8:1, complete formation of AgNWs with lower aspect ratio occurred in the sample.

# CHAPTER 3

---

## RESEARCH METHODOLOGY

### 3.1 Overview

This chapter elaborates in detail the experimental works done in this research. The main objective in this research is to synthesis the AgNWs via polyol process.

Polyol method involves the reduction of a metal salt precursor by a polyol, a compound containing multiple hydroxyl groups at high temperature. The versatility of this synthesis includes the ability of polyol to dissolve precursor salts, it's highly temperature-dependent reducing power and it's relatively high boiling point (for ethylene glycol (EG) is about 196°C). In particular the temperature-dependent reducing power of polyol helps synthesizing the colloidal particles over a broad range of sizes, as it gives us the ability to control the nucleation and growth processes through careful regulation of reaction temperature.

In this research, different mediated and control agents were used in the synthesis process;

- 1) Synthesis of AgNWs with reducing agent of 1,2-Propanediol,
- 2) Synthesis of AgNWs with mediated agent of copper chloride ( $\text{CuCl}_2$ )
- 3) Synthesis of AgNWs with mediated agent sodium chloride ( $\text{NaCl}$ ) at different molar concentration of  $\text{AgNO}_3$
- 4) Synthesis of AgNWs with different control agents (potassium hydroxide ( $\text{KOH}$ ), potassium chloride ( $\text{KCL}$ ), iron nitrate ( $\text{Fe}(\text{NO}_3)_3$ ), water ( $\text{H}_2\text{O}$ ))

The characterization techniques used in this research are also presented in this chapter. The synthesized samples were characterized using, Field Emission Scanning Electron Microscopy (FESEM) and Transmission Electron Microscopy (TEM) for morphological studies, X-ray Diffraction (XRD) for structural studies and Ultraviolet Visible Spectroscopy (UV-vis) for optical studies.

### **3.2 Materials**

The main precursor salt used in this synthesis was silver nitrate ( $\text{AgNO}_3$ ). The polyol used were 1,2-Propanediol and ethylene glycol (EG). These polyol serve as both reducing agent and solvent. Polyvinylpyrrolidone (PVP) was added as a stabilizer to prevent agglomeration of the colloidal particles.

Mediated agents used in this synthesis were copper (II) chloride ( $\text{CuCl}_2$ ) and sodium chloride (NaCl). Different control agents such as potassium hydroxide (KOH), potassium chloride (KCL), iron (III) nitrate ( $\text{Fe}(\text{NO}_3)_3$ ) and distilled water ( $\text{H}_2\text{O}$ ) were also used for synthesis of AgNWs.

### 3.3 Synthesis techniques

#### 3.3.1 Synthesis of AgNWs with reducing agent of 1,2-Propanediol

The procedure started with 10 ml of 1,2-propanediol added into a 50 ml three neck flask and was heated on the electric hotplate at 170°C. The temperature was kept constant temperature for 2 hours. Then 0.5 ml of 1, 2-propanediol solution of AgNO<sub>3</sub> (0.005M) ( $4.25 \times 10^{-4}$  g) was injected into the 1,2-propanediol under vigorous magnetic stirring to form seeds. Two minutes later, 3 ml of 1, 2-propanediol solution of AgNO<sub>3</sub> (0.1M) (0.05 g) and 3 ml of 1,2-propanediol solution of PVP (0.45M) (0.15 g) were added drop wise over a period of 5 minutes simultaneously by using syringe. Immediately upon the addition of the solutions, the entire solution turned from colorless becomes light yellow color. The reaction was continued for 1 hour and was heated in the oven at 170 °C for 30 minutes. After heating, a grey suspension was obtained and was left to cool down to room temperature.

After the reaction was completed, the mixture was diluted by acetone (10 times by volume) and then centrifuged at 3000 rpm for 30 minutes in order to separate polymer from the AgNWs. Then, the mixture was washed by deionized water and centrifuged at 6000 rpm for 20 minutes to remove the byproducts. The washing processes were repeated twice and grey precipitate was obtained and dried in a vacuum oven for 24 hours to obtain the final powder form. Some of the purified products were dispersed in deionized water for further characterization.

Apart from the parameters given above, a parametric studies on the effect of injection times (5, 10 and 15 minutes) and molar ratio of PVP to AgNO<sub>3</sub> (6:1 and 7.5:1) were also conducted as shown in Table 3.1.

Table 3.1: Samples prepared with different injection times and PVP concentrations.

Sample	Injection time (min)	Concentration of PVP (M)
1	5	0.45
2	5	0.60
3	5	0.75
4	10	0.75
5	15	0.75

### 3.3.2 Synthesis of AgNWs with mediated agent of $\text{CuCl}_2$

Firstly, 5 mL of EG was added into a beaker. The EG was heated using silicon oil bath at  $150^\circ\text{C}$  for 1 hour. After 1 hour, 40  $\mu\text{L}$  of 4 mM  $\text{CuCl}_2 \cdot \text{H}_2\text{O}$ /EG solution was added into the preheated EG using syringe and the solution was allowed to heat at  $150^\circ\text{C}$  for another 15 minutes and stirred under magnetic stirring (260 rpm) using hot plate. Next, 1.5 mL of a 114 mM PVP/EG was then added into the beaker, followed by 1.5 mL of a 94 mM  $\text{AgNO}_3$ /EG. The color changed from colorless to yellow after  $\text{AgNO}_3$ /EG was added. Then, the solution was heated for another 1 hour. The color changed from yellow to brownish gray. After 1 hour, the solution was taken out and let it cooled at room temperature.

For characterization, the solution was centrifuged (3000 rpm, 30 minutes) once with acetone and three times with deionized water in order to remove contamination. Finally, the precipitate was preserved in deionized water for characterization.

### 3.3.3 Synthesis of AgNWs with mediated agent NaCl at different molar concentration of AgNO<sub>3</sub>

Firstly, 10 ml EG was refluxed in a three neck round bottom flask and heated up to 210°C for 2 hours. Then, 0.1 M of NaCl in 20 µL EG was added into the refluxed EG. A solution of 0.2 M AgNO<sub>3</sub> in 20 ml EG and a solution of 0.5M PVP in 20ml EG were simultaneously injected at a rate of 0.2ml per minute into the previous solution. After finished the injection, the solution was kept heated for another 90 minutes at 210°C.

The solution was left to cool at room temperature and then was centrifuged at 3000 rpm for 30 minutes. After that, the supernatant liquid was poured away and the grey precipitates were collected and washed for characterization. The experiment was repeated for different molarity of AgNO<sub>3</sub> as shown in Table 3.2.

Table 3.2: Samples with different molar concentration of AgNO<sub>3</sub>.

Sample	Concentration of AgNO <sub>3</sub> (M)	Concentration of PVP (M)
1	0.025	0.05
2	0.050	0.10
3	0.10	0.20
4	0.20	0.40
5	0.25	0.50

### 3.3.4 Synthesis of AgNWs with different control agents (KOH, KCL, Fe(NO<sub>3</sub>)<sub>3</sub>, H<sub>2</sub>O)

Argon was used as the shielding atmosphere to avoid seed oxidative etching process and assure the repeatability of experiments. 5 ml EG was injected into a 50 ml three necked flask and preheated for 30 minutes. 5 ml EG solution of AgNO<sub>3</sub> (0.1 M) was injected within 10 seconds while 5 ml EG solution of PVP (0.3 M, containing control agent) was injected dropwise by syringe within 5 minutes. The reaction then was maintained for 2 hours. The reaction temperature was kept at 180°C and continued stirred during the entire procedure.

The obtained products were diluted with acetone and centrifuged at 4000 rpm for about 30 minutes. After centrifugation, the supernatant was removed by syringe, and washed with the ethanol for two times. These purified products were preserved in ethanol. However, the procedure for the control agent deionized water was different which involved two step polyol process. Firstly, 2 ml of EG was injected into a 50ml three-necked flask and was preheated for 30 minutes. After 30 minutes, 1ml of EG solution of AgNO<sub>3</sub> (0.0002 M) was added into the three necked flask within 5 second, following by addition of 1.0 ml deionized water. After 20 minutes of reaction, 5 ml EG solution of AgNO<sub>3</sub> (0.1 M) was injected into the reaction system by syringe within 10 second. Then 5 ml EG solution of PVP (0.3 M) was injected dropwise by syringe within 5 minutes. The reaction was maintained for the next 2 hours. Next, the centrifugation steps are similar to the centrifugation steps for other control agents.



### 3.4 Characterization techniques

#### 3.4.1 Field Emission Scanning Electron Microscope (FESEM)

Figure 3.1 show the image of FESEM used to characterize morphological studies of as-synthesized samples.



Figure 3.1: FESEM machine

Morphology studies were carried out using Field Emission Scanning Electron Microscope (Carl Zeiss, AURIGA ®) as shown in Figure 3.1. Under vacuum, the electrons

generated by field emission source are accelerated in a field gradient. The beam passes through electromagnetic lenses, focusing onto the specimen. As a result of this bombardment different types of electrons are emitted from the specimen. A detector catches the secondary electron and an image of the sample surface is constructed by comparing the intensity of this secondary electron to the scanning primary electron beam. Finally the image is displayed on a monitor.

### 3.4.2 Transmission Electron Microscope (TEM)

Figure 3.2 show the image of TEM machine used to determine the diameter size of as-synthesized samples.



Figure 3.2: Transmission electron microscope

The diameters of AgNWs were determined using TEM (LIBRA® 120) as shown in Figure 3.2. Prior to using the transmission electron microscope, synthesized samples were dispersed in ethanol and sonicated for 60 minutes to prevent agglomeration on the copper grid. A small drop of suspension was placed onto a 200 Cu Mech holey support film and dried. Then, the copper grid was taped onto 47 nm diameter nucleopore polycarbonate membrane filters. The nucleopore filters were supported by quartz fiber filters. The TEM was operated at an accelerating voltage of 120 kV. The morphological analysis of TEM was operated in bright field mode. The image displayed was then analyzed to obtain the diameter size distribution.

### 3.4.3 X-Ray Diffraction (XRD)

Figure 3.3 shows the image of XRD machine.

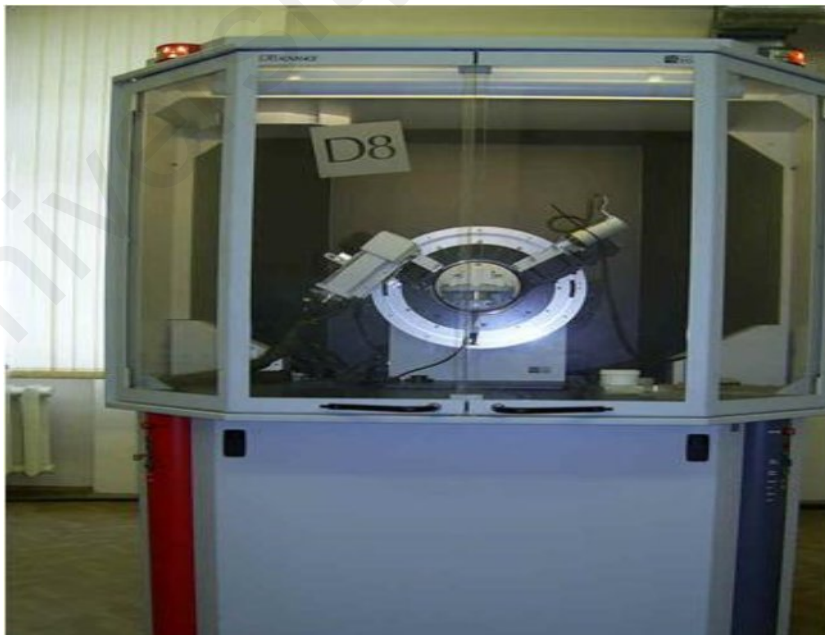


Figure 3.3: X-ray diffraction machine

X-Ray diffraction analysis were carried out using the Philips X' Pert MRD X-ray diffractometer system as shown in Figure 3.3. Measurements were carried out on a portion of the film samples at room temperature. A small portion of film sample was placed onto cleaned microscope slides and then placed in the chamber and scanned for  $2\theta$  between  $15^\circ$ - $60^\circ$ . The X-ray wavelength of  $1.5406 \text{ \AA}$  and values of 60 kV and 60 mA were used in all measurements. The compositions were analyzed by observing the changes in the structures of the samples.

#### 3.4.4 UV-Vis Spectrometer

Figure 3.4 show the image of UV-vis spectrometer.



Figure 3.4: UV – Vis spectrophotometer

In order to understand the optical properties, Cary 50 probe UV-visible spectrophotometer was used as shown in Figure 3.4. The solutions of electrolytes were diluted and filled into a transparent cell, known as cuvette. Cuvette is rectangular in shape with an internal width of 1 cm. The cuvette was placed into the chamber and exposed to UV, visible and near infrared radiation. The absorption spectra were analyzed in a wavelength range between 190 - 800 nm.

University of Malaya

# CHAPTER 4

---

## RESULTS AND DISCUSSION

### 4.1 Overview

This chapter presents the analysis results on morphological, structural, optical and magnetic properties of silver nanowires (AgNWs). Besides that, discussion on mechanism of AgNWs formation synthesized with different reducing agents and different mediated agents is also thoroughly elaborated in this chapter.

This chapter is divided into several subtopics that are;

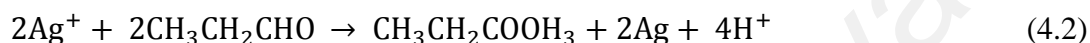
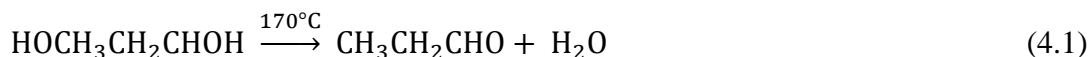
- a) Synthesis of AgNWs with reducing agent of 1,2-Propanediol,
- b) Synthesis of AgNWs with mediated agent of  $\text{CuCl}_2$
- c) Synthesis of AgNWs mediated agent of  $\text{NaCl}$
- d) Synthesis of AgNWs with different control agents ( $\text{KOH}$ ,  $\text{KCL}$ ,  $\text{Fe}(\text{NO}_3)_3$ ,  $\text{H}_2\text{O}$ )

### 4.2 Synthesis of AgNWs without mediated agent

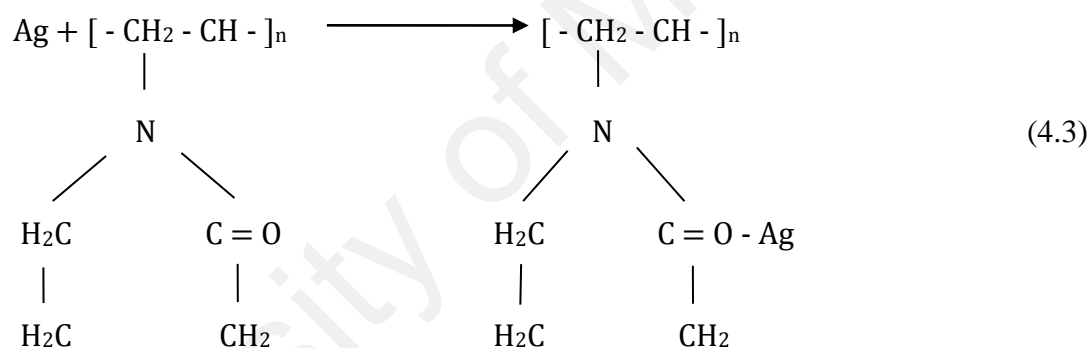
This subtopic is about the analysis results for AgNWs synthesized via polyol process without any mediated agent. The reducing agent used was 1,2-propanediol that also used as solvent in the synthesis while PVP acts as stabilizer or surfactant that control the growth of AgNWs.

#### 4.2.1 Mechanism formation of AgNWs with reducing agent of 1, 2 - Propanediol

The formation of anisotropic AgNWs involves two steps. In the first step, 1,2 propanediol was converted into propionaldehyde at high temperature (170°C) as shown in Equation (4.1). Then it was reduced from Ag<sup>+</sup> to Ag atom as shown in Equation (4.2).



In the second step, AgNO<sub>3</sub> and PVP were added dropwise to the reaction system allowing the nucleation and growth of AgNWs in Equation (4.3).



Ag atoms were nucleated through the homogeneous nucleation process. These silver nanoparticles (AgNPs) were well dispersed because of the presence of a polymeric surfactant PVP that could be chemically adsorbed onto the surfaces of Ag through O – Ag bonding in Equation (4.3). PVP has an affinity toward many chemicals to form coordinative compounds due to the structure of polyvinyl skeleton with strong polar group (pyrrolidone ring). In this case, C = O polar groups were interacted with Ag<sup>+</sup> ions and formed coordinating complex as shown in Equation (4.3). When this dispersion of AgNPs was continuously heated at 170°C, small nanoparticles progressively disappeared to the

benefit of larger ones via Ostwald ripening process (Roosen & Carter, 1998). The critical particle radius increased with temperature. As the reaction continued, the small AgNPs were no longer stable in solution and they started to dissolve and contribute to the growth of larger ones. With the assistance of PVP, some of the larger nanoparticles were able to grow into rod-shaped structures. The growth process would continue until all the AgNPs were completely consumed and only nanowires survived.

University of Malaya



## 4.2.2 Morphological studies

### 4.2.2.1 Field Emission Scanning Electron Microscopy (FESEM) analysis

Figures 4.1 – 4.5 show the FESEM of AgNWs for two different effects.

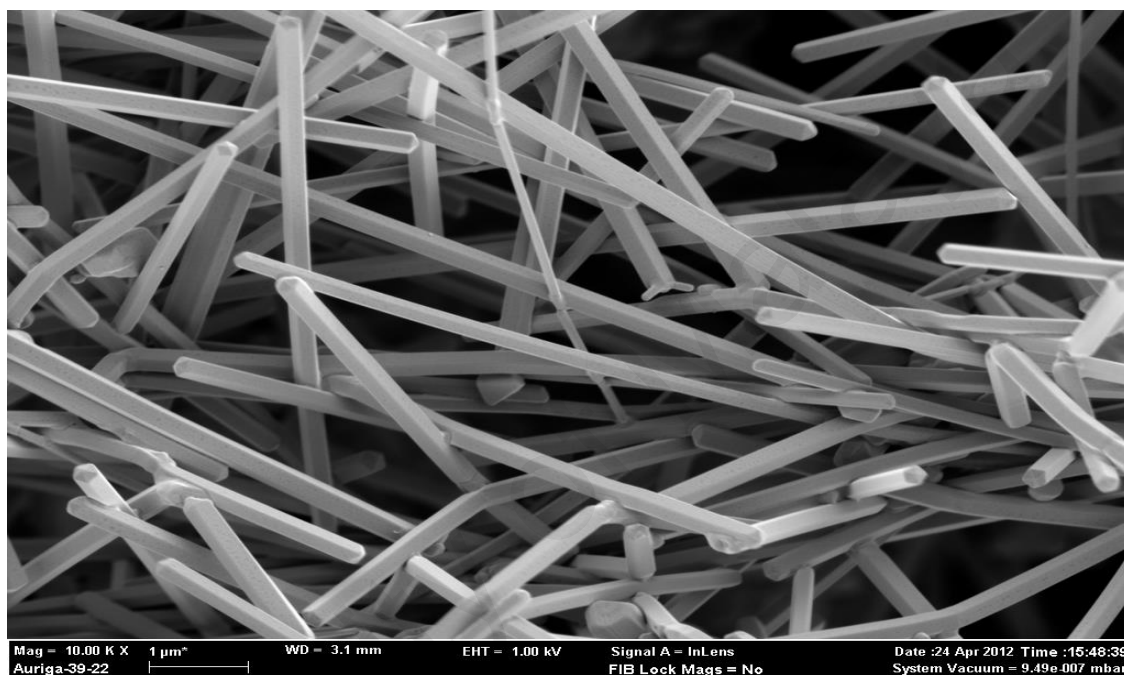


Figure 4.1: FESEM image of as-synthesized sample which has PVP: AgNO<sub>3</sub> molar ratio of 4.5:1 and 5 minutes of injection time.

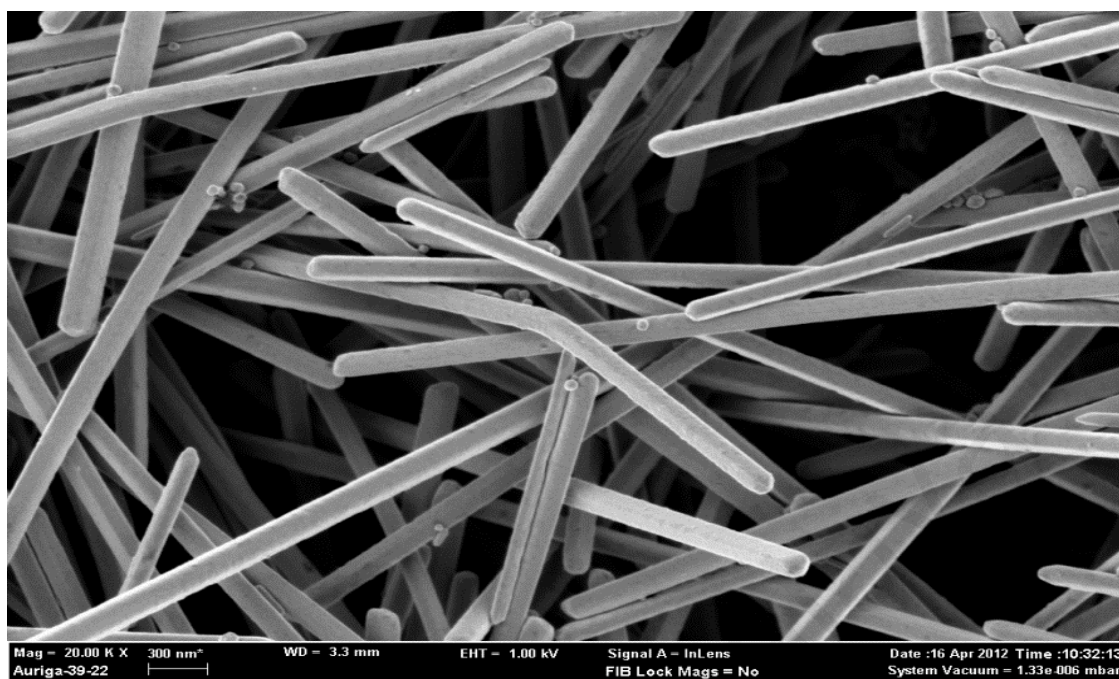


Figure 4.2: FESEM image of as-synthesized sample which has PVP: AgNO<sub>3</sub> molar ratio of 6:1 and 5 minutes of injection time.

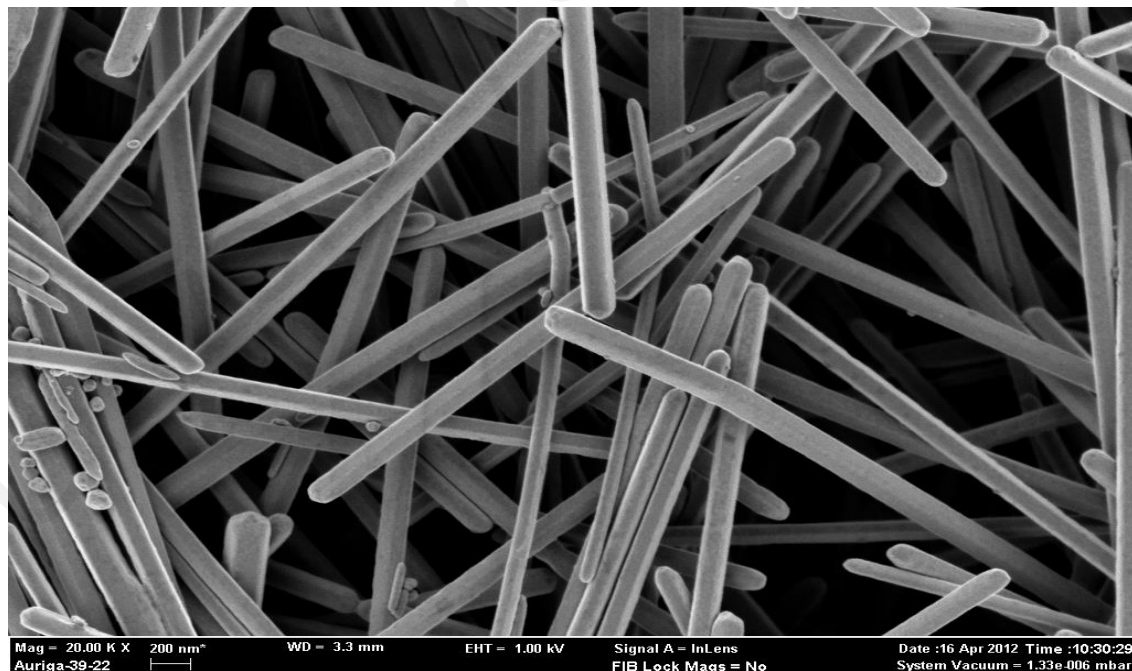


Figure 4.3: FESEM image of as-synthesized sample which has PVP: AgNO<sub>3</sub> molar ratio of 7.5:1 and 5 minutes of injection time.



Figure 4.4: FESEM image of as-synthesized sample which has PVP: AgNO<sub>3</sub> molar ratio of 7.5:1 and 10 minutes of injection time.

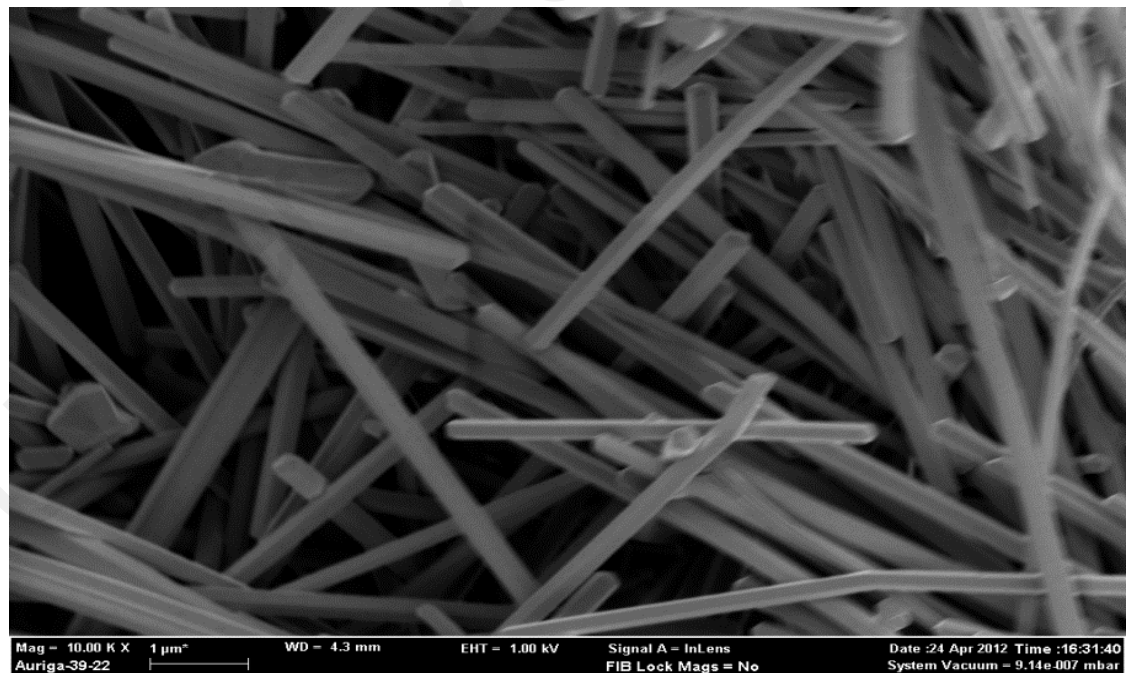


Figure 4.5: FESEM image of as-synthesized sample which has PVP: AgNO<sub>3</sub> molar ratio of 7.5:1 and 15 minutes of injection time.

Figures 4.1 – 4.5 show the FESEM images of as-synthesized samples with different molar ratio of PVP to AgNO<sub>3</sub> and injection time. The FESEM images show that each of the samples contains AgNWs with some low percentages of silver nanoparticles (AgNPs). The morphologies of the AgNWs structures were strongly dependant to the molar ratio of PVP to AgNO<sub>3</sub>. As the molar ratio increased, the diameter sizes of the AgNWs were decreased. At low molar ratio, not all the Ag multitwin particles can grow into nanowires. They were formed large amounts of micrometer sized of Ag particles. However, when the molar ratios were increased, the growth only occurred in [100] direction, thus the diameter size of AgNWs decreased while the length increased.

Besides the molar ratio of PVP to AgNO<sub>3</sub>, the injection time also affected the formation and the diameter size of AgNWs. With the increasing injection time, the diameter sizes of AgNWs were decreased. At lower injection time, extensive Ag cluster were formed due to rapid supersaturation of Ag (Coskun et al., 2011). When the injection time increased, the multitwin particles were grew as thin nanowires, hence decreased the diameter size of AgNWs.

#### **4.2.2.2 Transmission Electron Microscopy (TEM) analysis**

Figures 4.6 – 4.11 show the TEM images of AgNWs for two different effects.

(i) Effect of molar ratio of PVP to  $\text{AgNO}_3$

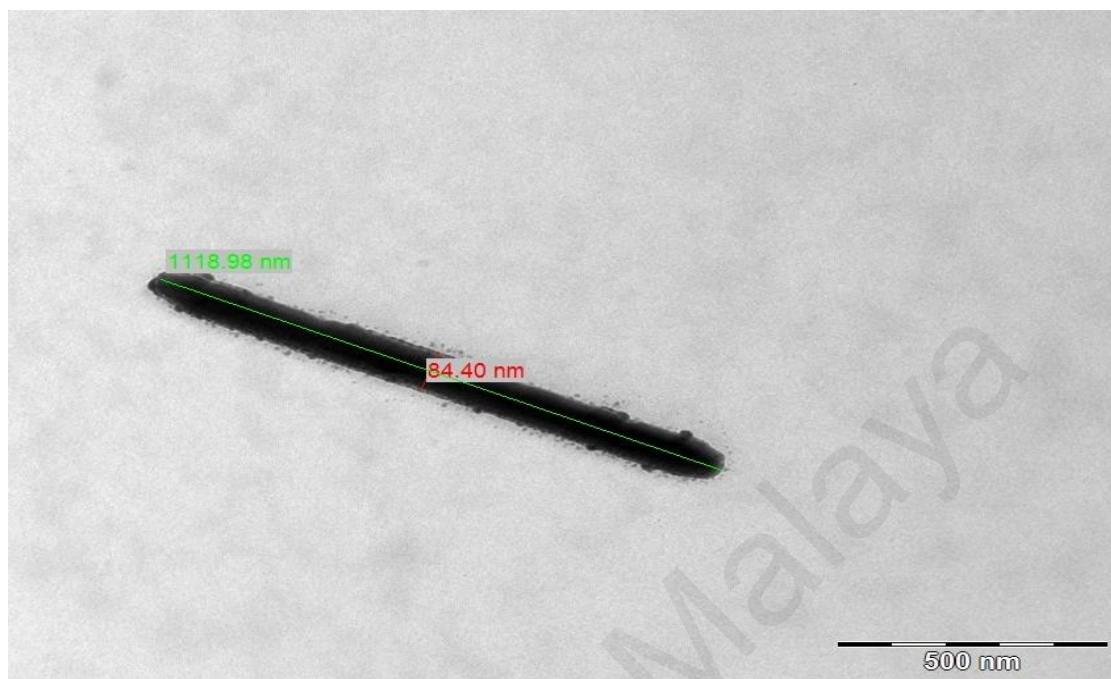


Figure 4.6: TEM image of as-synthesized sample at PVP:  $\text{AgNO}_3$  molar ratio of 4.5:1.

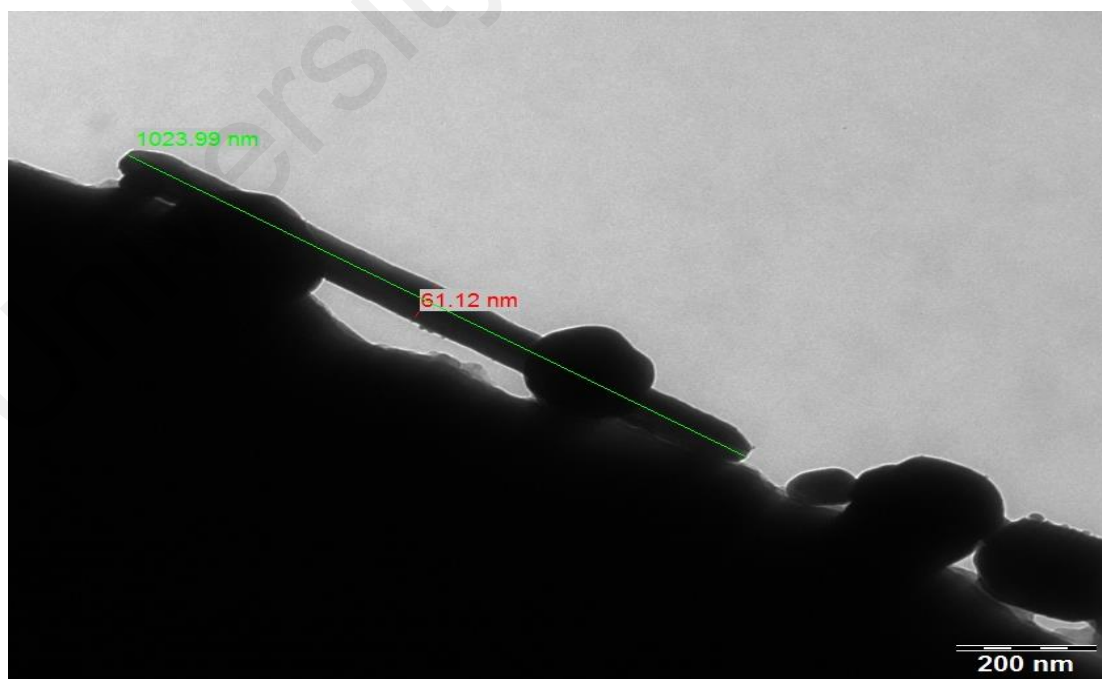


Figure 4.7: TEM image of as-synthesized sample at PVP:  $\text{AgNO}_3$  molar ratio of 6.0:1.

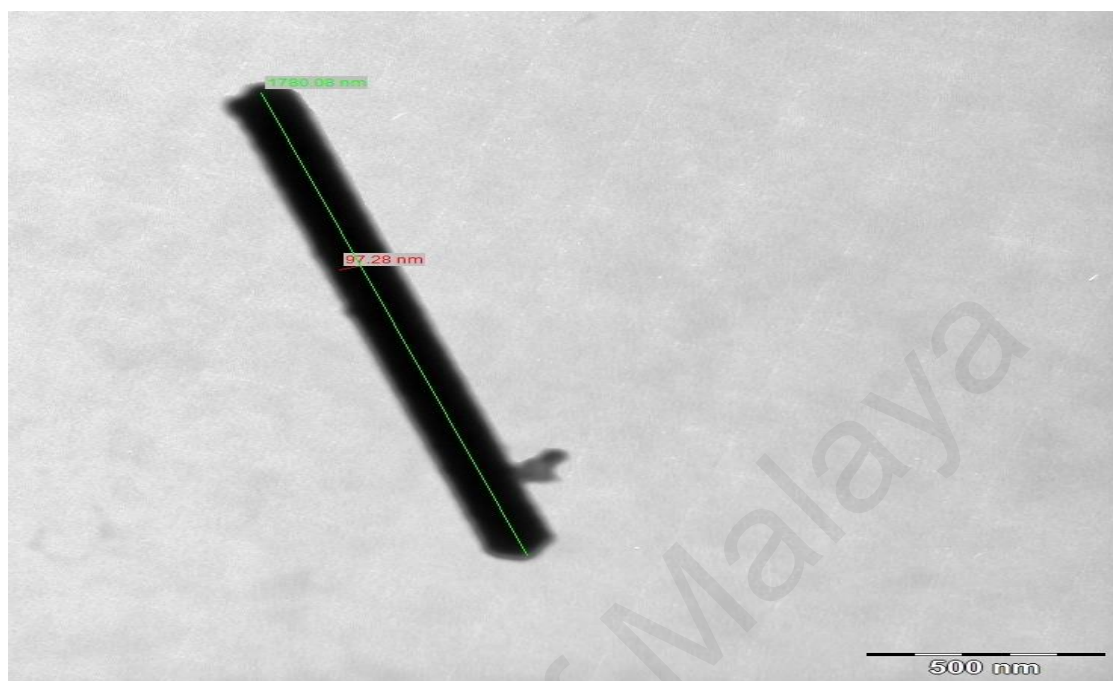


Figure 4.8: TEM image of as-synthesized sample at PVP: AgNO<sub>3</sub> molar ratio of 7.5:1.

Figures 4.6 – 4.8 show the TEM images of the AgNWs which has been synthesized with different PVP:AgNO<sub>3</sub> molar ratios of 4.5:1, 6.0:1 and 7.5:1 at constant 5 minutes injection time respectively. When the molar ratio of PVP:AgNO<sub>3</sub> is 4.5:1, the passivation of faces of multitwin particles were insufficient and AgNWs growth occurred on both {111} and {100} faces (Al-Saidi et al., 2012). Thus, under this condition, AgNWs synthesized at lower molar ratio have large diameter and low aspect ratio (Coskun et al., 2011). TEM image in Figure 4.6 shows that the AgNWs produced with molar ratio of 4.5:1 are 84 nm in diameter and 1119 nm in length, having aspect ratio of 13.3. Thus it can prove that lower molar ratio produced lower aspect ratio of nanowires. Moreover, the multitwin particles cannot grow into nanowires and formed large amounts of micrometer-sized of Ag

particles (Coskun et al., 2011). As the molar ratio of PVP to  $\text{AgNO}_3$  increased to 6.0:1 (Figure 4.7), the diameter of AgNWs were 61 nm and 1024 nm in length, while the aspect ratio is 16.8. On the other hand, for the PVP to  $\text{AgNO}_3$  molar ratio of 7.5:1 (Figure 4.8), the diameter of AgNWs were 97.28 nm and the length was 1780 nm while the aspect ratio has increase to 18.3. From the result obtained, if the molar ratio of PVP to  $\text{AgNO}_3$  increased, the aspect ratio also increased gradually. The optimum molar ratio of PVP to  $\text{AgNO}_3$  was 7.5:1 because under this condition only {100} faces of multitwinned particles were passivated and as the Ag atoms joined active (111) planes, hence longitudinal growth in the [110] direction becomes favorable (Coskun et al., 2011).

**(ii) Effect of injection time**

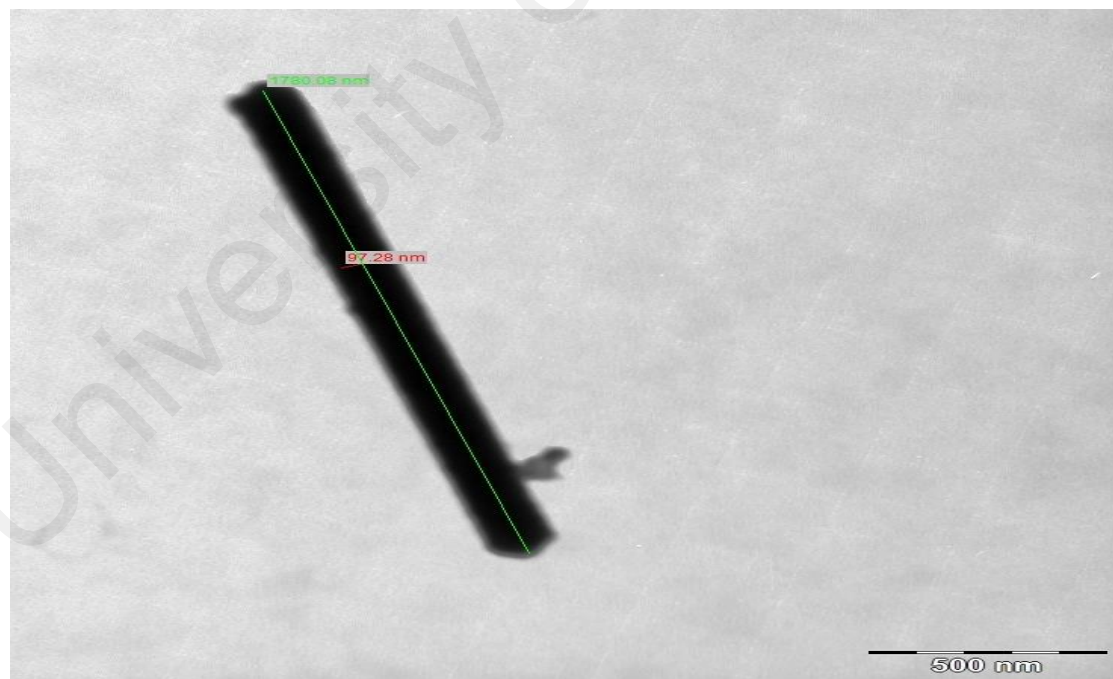


Figure 4.9: TEM image of as-synthesized sample at injection time of 5 minutes.

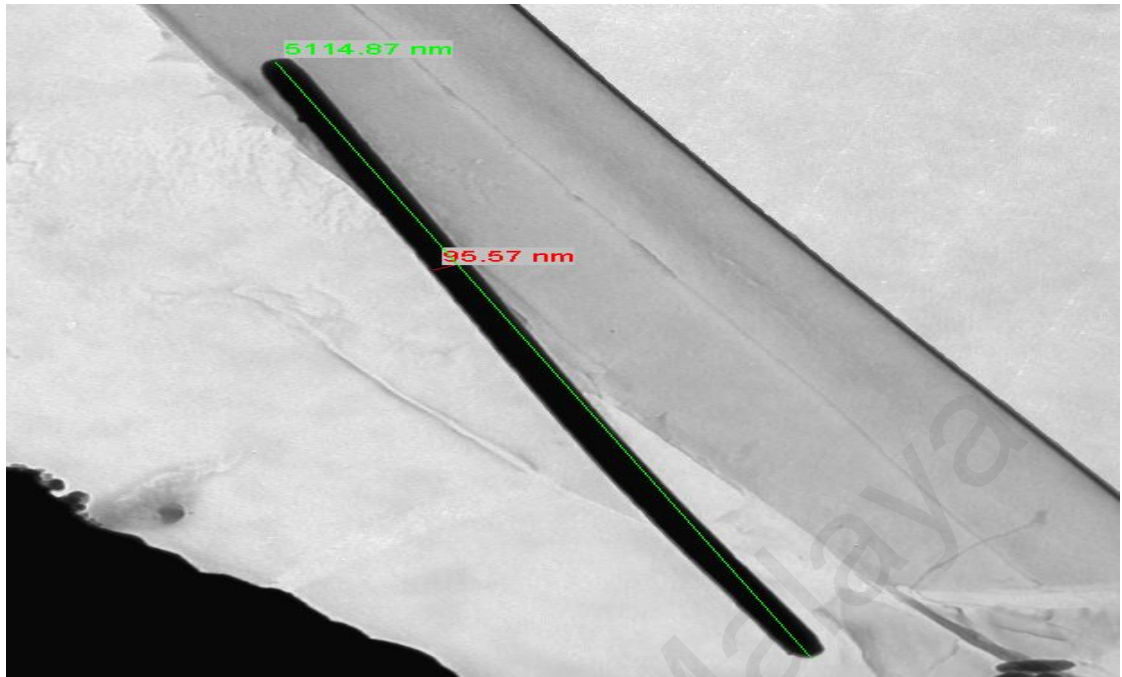


Figure 4.10: TEM image of as-synthesized sample at injection time of 10 minutes.

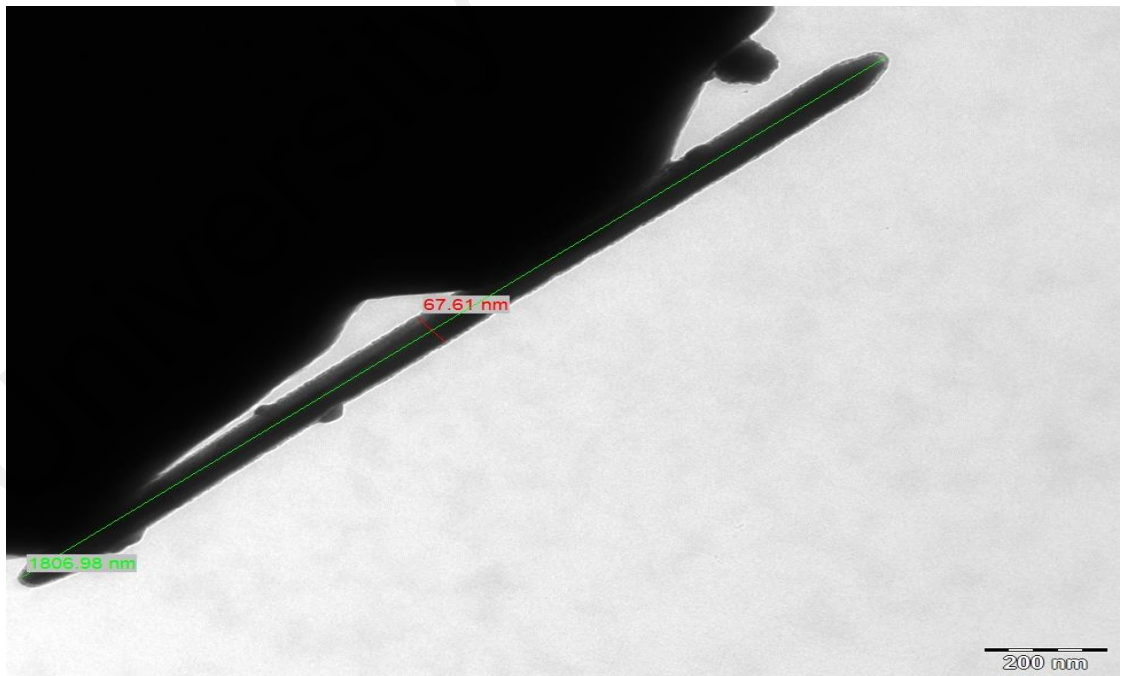


Figure 4.11: TEM image of as-synthesized sample at injection time of 15 minutes.



TEM images of AgNWs synthesized with different injection times of 5, 10 and 15 minutes respectively with constant molar ratio of PVP to AgNO<sub>3</sub> of 7.5:1 are shown in Figures 4.9 – 4.11. For 5 minutes of injection time (Figure 4.9), the diameter of the AgNWs was 97 nm and the length was 1780 nm while the aspect ratio is 18.3. As the injection time increased to 10 minutes (Figure 4.10), the diameter decreased to 96 nm while the length increased to 5115 nm with the aspect ratio was 53.5. For 15 minutes of injection time (Figure 4.11), the diameter decreased to 67 nm and the length was 1807 nm while the aspect ratio was 26.73. At this condition, Ag ion concentration led to the formation of multitwin particles with small diameters. Thus, these multitwin particles grow as a thin AgNWs (Coskun et al., 2011). From the results obtained, it show that the diameter size of AgNWs decreased as the injection time increased.

### 4.2.3 Structural studies

#### 4.2.3.1 X-Ray Diffraction (XRD) analysis

Figure 4.12 shows the XRD pattern of the sample with 7.5 molar ratios and 15 minutes injection time.

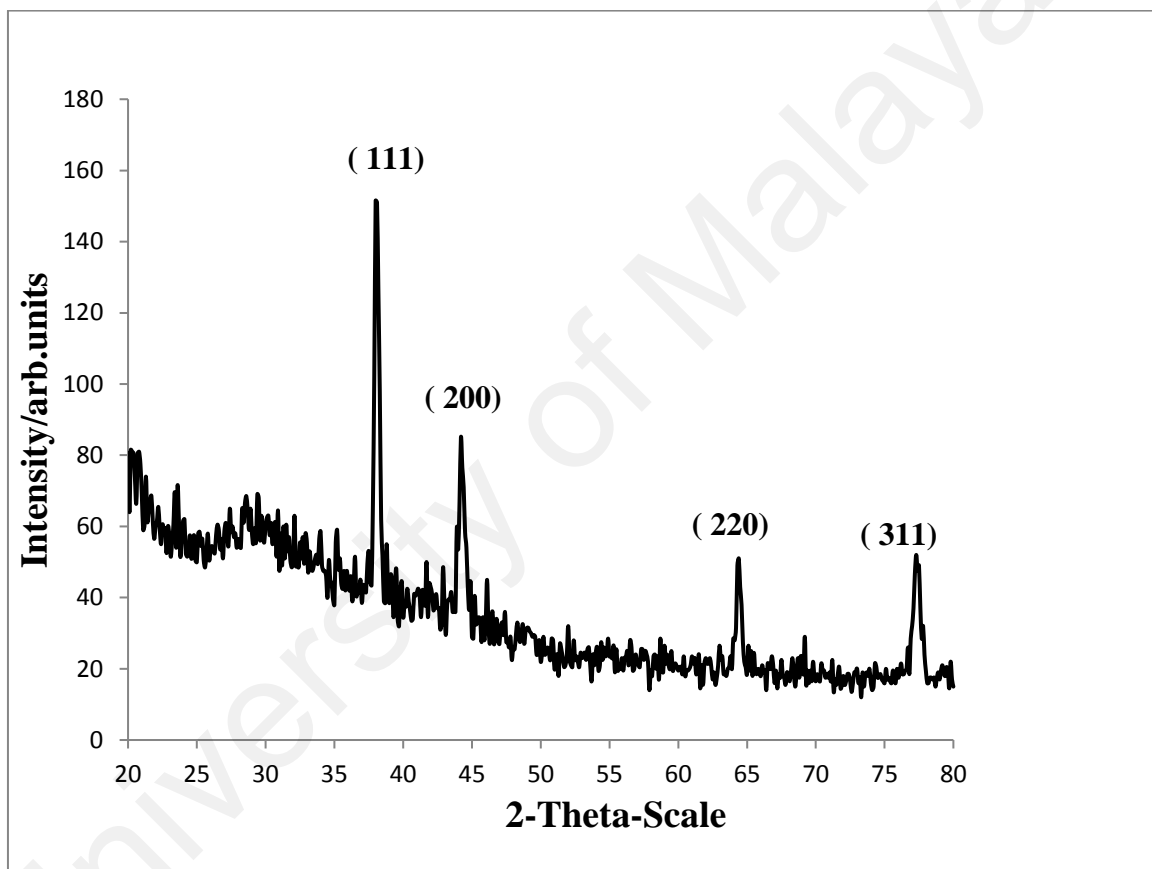


Figure 4.12: XRD pattern of as-synthesized sample for molar ratio of 7.5 with 15 minutes of injection time.

All the diffraction peaks can be assigned as face-centered cubic (FCC) Ag crystals according to standard PDF card 04-0783. The peaks at angle of  $2\theta = 38.1^\circ$ ,  $44.2^\circ$ ,  $64.3^\circ$  and  $77.5^\circ$  correspond to (111), (200), (220) and (311) crystal planes of the FCC Ag, respectively. This indicated that the AgNWs were finely crystallized and successfully synthesized by the polyol process. Besides that, from this pattern the lattice constant was calculated to be 0.4086 nm, which was in agreement with the value of literature (JCPDS 04-0783). Furthermore, it was worth noting that the intensity ratio of the (111) to (200) peaks was higher, indicating the enrichment of {111} crystalline planes in the AgNWs. Since there was no additional diffraction peak detected in Figure 4.12, it explains that the addition of surfactants has limited affect on the purity of AgNWs.

## 4.2.4 Optical studies

### 4.2.4.1 UV - vis spectroscopy analysis

Figure 4.13 shows the variation of absorption wavelength with different molar ratio of PVP to  $\text{AgNO}_3$ .

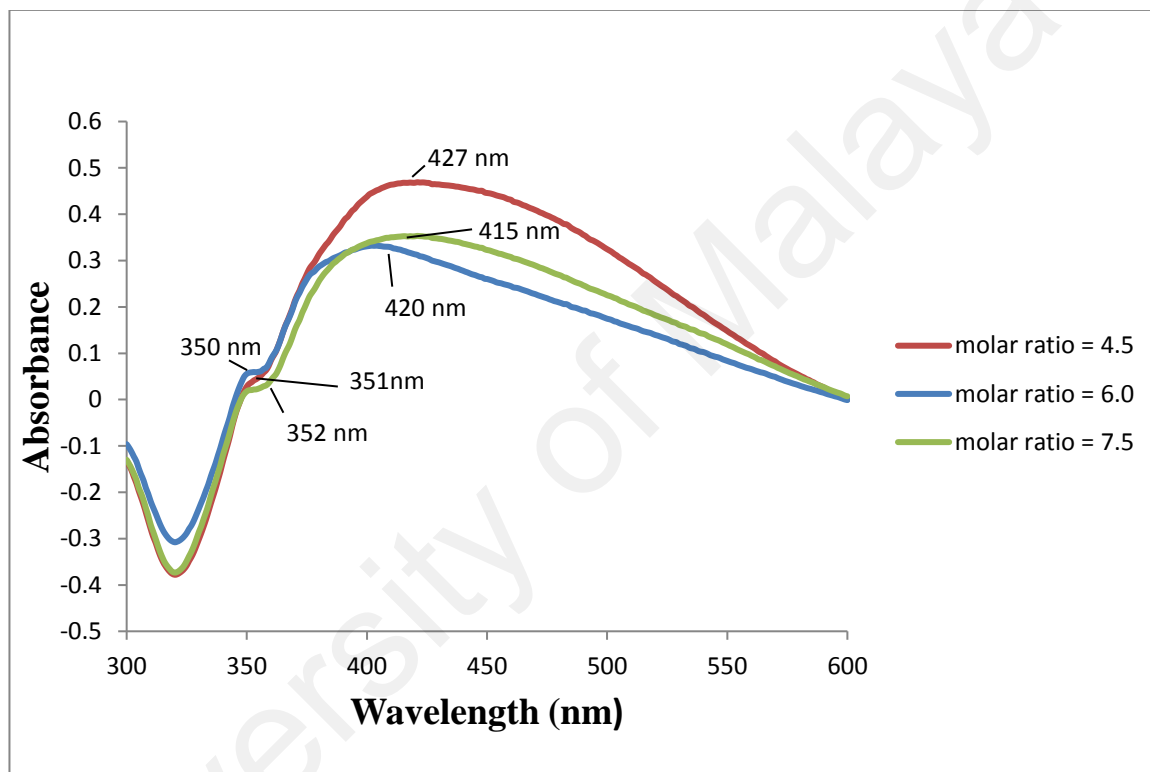


Figure 4.13: UV-vis spectra of as-synthesized samples with different molar ratio of the repeating units of PVP and  $\text{AgNO}_3$ .

The transverse surface plasmon resonance (SPR) band was shifted to blue side occurred around 410 nm. The shoulder weak peak appeared around 350 nm indicating the longitudinal SPR band shifted to the red side. As the molar ratio of the PVP to  $\text{AgNO}_3$  increased from 4.5 to 7.5, the absorption wavelength of transverse SPR band was decreased

from 427 to 415 nm and the absorption wavelength of longitudinal SPR band was unstable. This shows that the diameter of AgNWs of high molar ratio was decreased and the aspect ratio was increased. The weak shoulder peak occurred around 350 nm was belong to the optical signatures of AgNWs. The full width half maximum (FWHM) for molar ratio of 4.5 was 95 nm, FWHM for molar ratio of 6.0 was 63 nm and FWHM for molar ratio of 7.5 was 99 nm respectively. It shows that when value of FWHM increased, the peak becoming broader and diameter distribution of AgNWs was also larger.

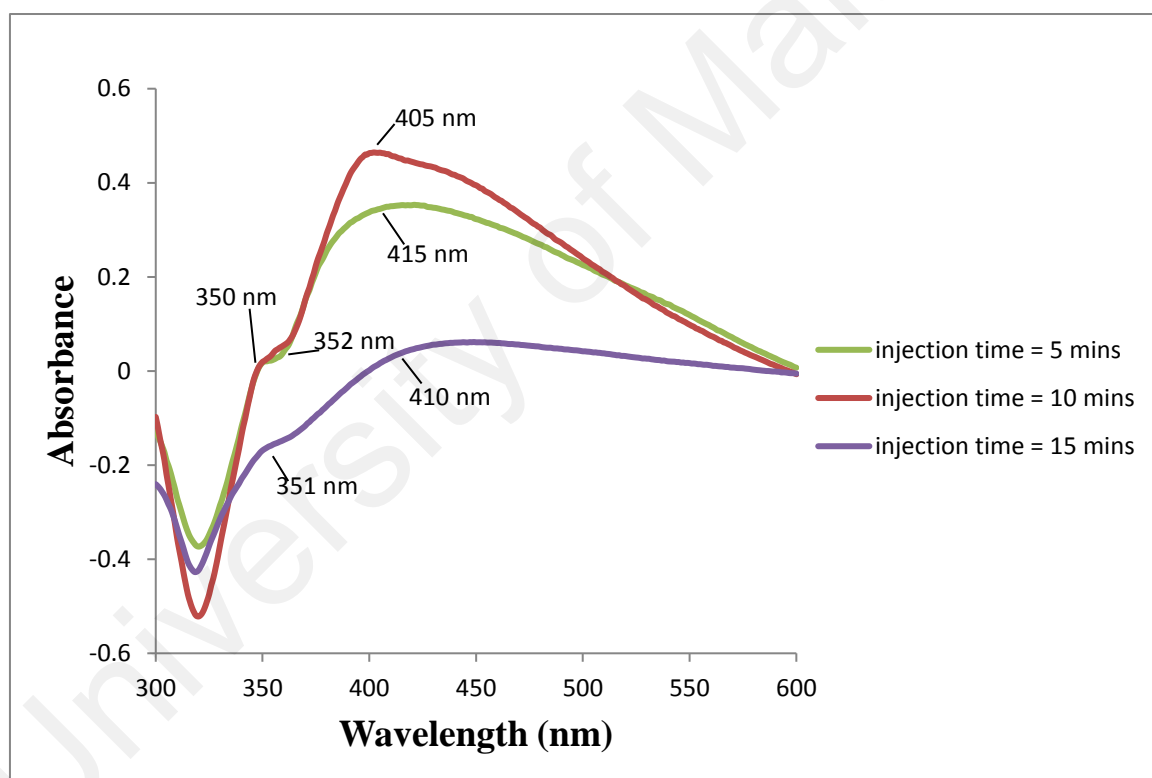


Figure 4.14: UV-vis spectra of as-synthesized samples with different injection times.

Figure 4.14 shows that the AgNWs have different absorption wavelength with different injection times of 5, 10 and 15 minutes respectively. When the injection time was increased from 5 to 10 minutes, transverse of SPR band around 400 nm was shifted to

lower wavelength and it caused the aspect ratio to increase. However by increasing injection time from 10 to 15 minutes, transverse of SPR band was shifted to longer wavelength and it caused the aspect ratio to decrease. The longitudinal of SPR band around 350 nm showed the optical signature of AgNWs. The full width half maximum (FWHM) for injection time of 5 minutes was 99 nm, injection time of 10 minutes was 81 nm and injection time of 15 minutes was 124 nm respectively. It shows that increased the value of FWHM had caused the curve becoming broader and the diameter distribution of AgNWs became larger.

### 4.3 Synthesis of AgNWs with mediated agent of CuCl<sub>2</sub>

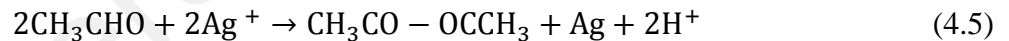
This subtopic is about the analysis results of AgNWs that had been synthesized via polyol process with CuCl<sub>2</sub> as mediated agent. The reducing agent used was ethylene glycol, that was also served as solvent in the synthesis. PVP was used as stabilizer or surfactant that controls the growth of AgNWs.

#### 4.3.1 Mechanism formation of AgNWs with mediated agent of CuCl<sub>2</sub>

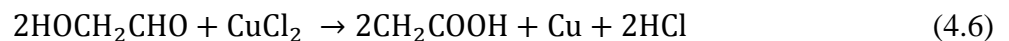
The formation of AgNWs involves several steps. In the initial step, high temperature is crucial for the conversion of ethylene glycol to glycoaldehyde as shown below.



AgNPs were formed by reducing Ag<sup>+</sup> ions with glycoaldehyde as shown below.



It was found that a small amount of Cl<sup>-</sup> must be added to a polyol synthesis to provide electrostatic stabilization for the initially formed Ag seeds (Hu et al., 1999).



In addition to electrostatically stabilizing the initially formed Ag seeds, the high Cl<sup>-</sup> concentrations during CuCl<sub>2</sub> mediated synthesis help to reduce the concentration of free

$\text{Ag}^+$  ions in the solution through the formation of  $\text{AgCl}$ . Subsequent, it will slowly release the  $\text{Ag}^+$  effectively. This facilitates the high yield formation of the thermodynamically more stable multiply twinned Ag seeds that are required for wire length. Valency metal ions ( $\text{Cu}^{2+}$ ) were reduced by EG to low valence ( $\text{Cu}^+$ ) which in turn reacted with and scavenged adsorbed atomic oxygen from the surface of AgNPs. Here,  $\text{Cu}^{2+}$  can remove oxygen from the solvent which prevents twinned seeds dissolved by oxidative etching and scavenging adsorbed atomic oxygen from the surface of the Ag seeds, facilitating multiply twinned seeds growth (Korte et al., 2008).

In the final step,  $\text{AgNO}_3$  and PVP were added dropwise to the reaction system allowing the nucleation and growth of AgNWs as shown in Equation (4.6). AgNPs were well dispersed because of the presence of PVP, a polymeric surfactant that could chemically adsorb onto the surfaces of Ag through O – Ag bonding. As the reaction continued, the small AgNPs were no longer stable in solution and they started to dissolve and contribute to the growth of larger ones. When multiple twinned form the nanoparticles during a nuclei period, the PVP was bounded preferentially on {100} then {111} (Al-Saidi et al., 2012). This inhibited the growth along {111} direction. So the growth took place only in the {110} direction resulting in the fivefold twinned nanowires.



## 4.3.2 Morphological studies

### 4.3.2.1 FESEM analysis

Figures 4.15 – 4.18 show the FESEM images of as-synthesized AgNWs at different magnification.

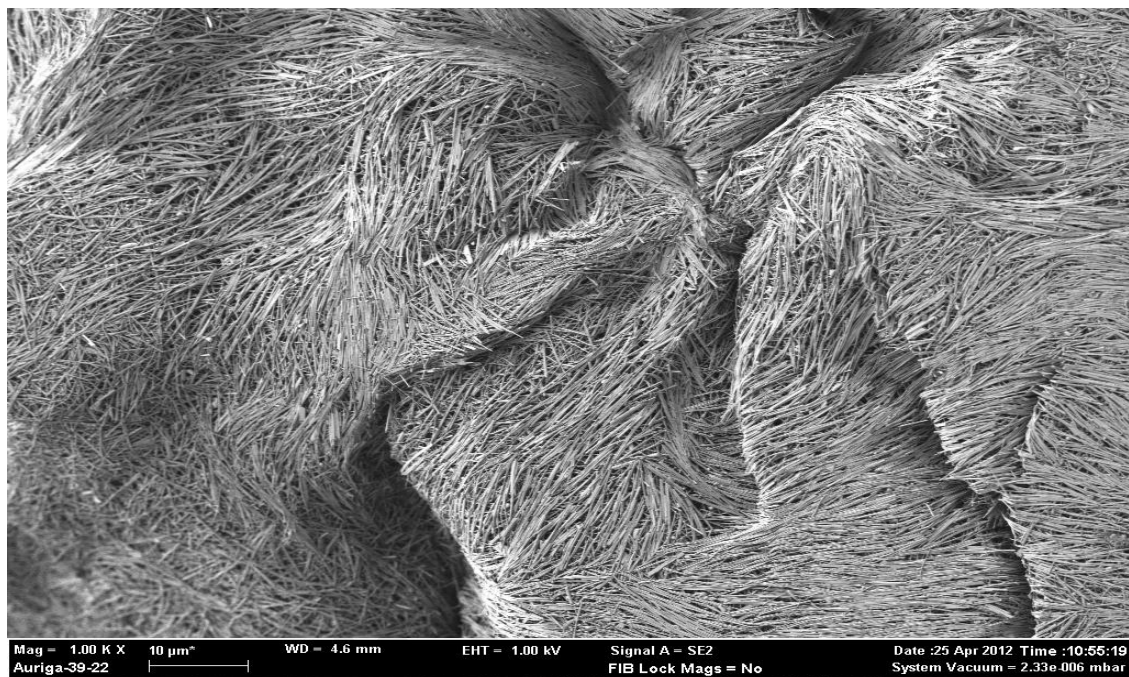


Figure 4.15: FESEM image of as-synthesized sample with  $\text{CuCl}_2$  mediated agent at 1000X magnification.



Figure 4.16: FESEM image of as-synthesized sample with  $\text{CuCl}_2$  mediated agent at 2000X magnification.

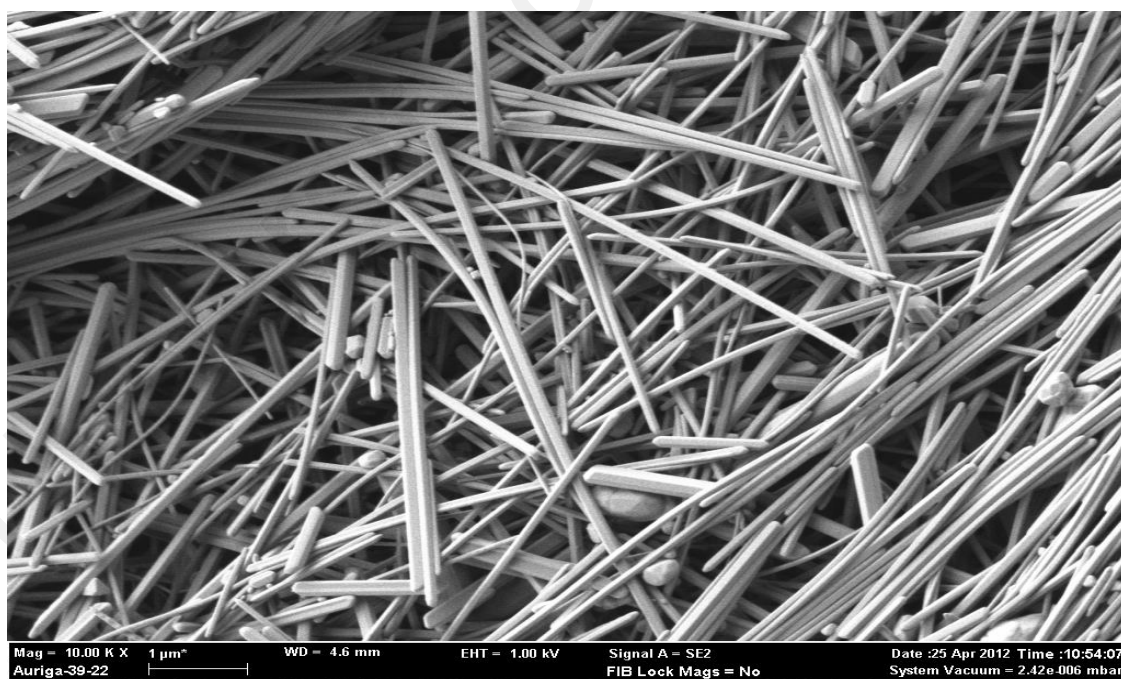


Figure 4.17: FESEM image of as-synthesized sample with  $\text{CuCl}_2$  mediated agent at 10000X magnification.

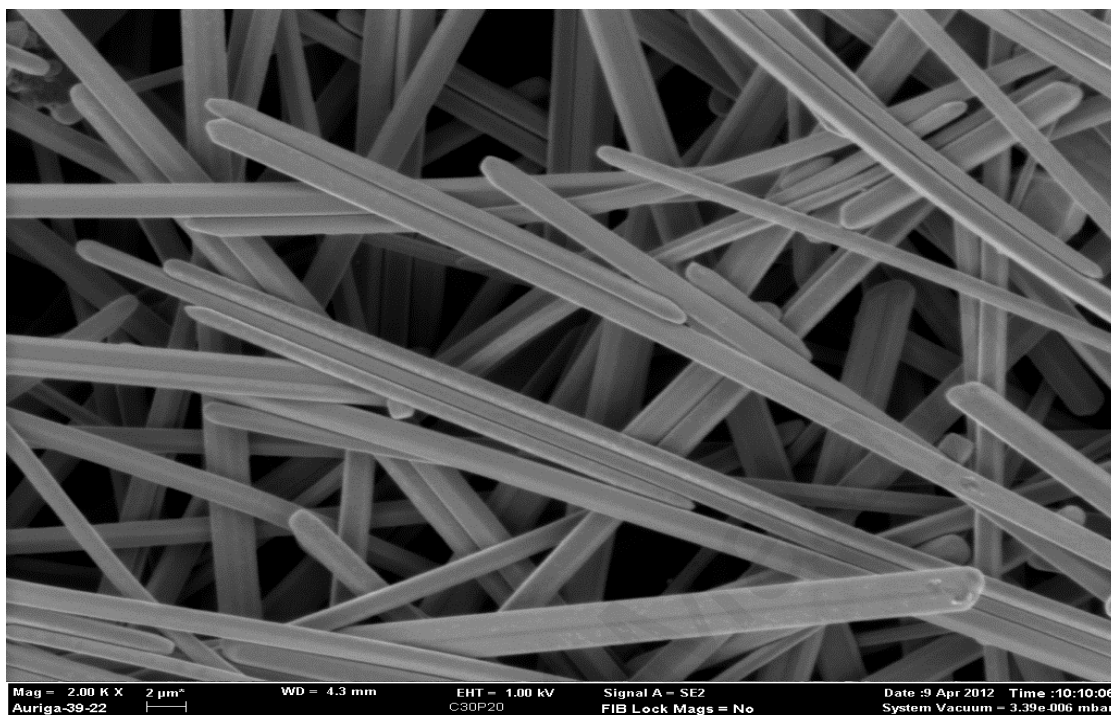


Figure 4.18: FESEM image of as-synthesized sample with  $\text{CuCl}_2$  mediated agent at 20000X magnification.

These images indicate that the sample was comprised of entangled AgNWs. It was observed that the diameter of the AgNWs was not homogenous throughout the samples. Most of AgNWs diameters were categorized in the range of 61-70 nm. The formation of AgNWs was completed with the mediated agent of  $\text{CuCl}_2$  due to the Ostwald ripening process. All the Ag particles were successfully growth in [100] direction lead to the formation of AgNWs (Al-Saidi et al., 2012).

### 4.3.2.2 TEM analysis

Figures 4.19 – 4.21 show the TEM images of as-synthesized AgNWs with  $\text{CuCl}_2$  mediated agent.

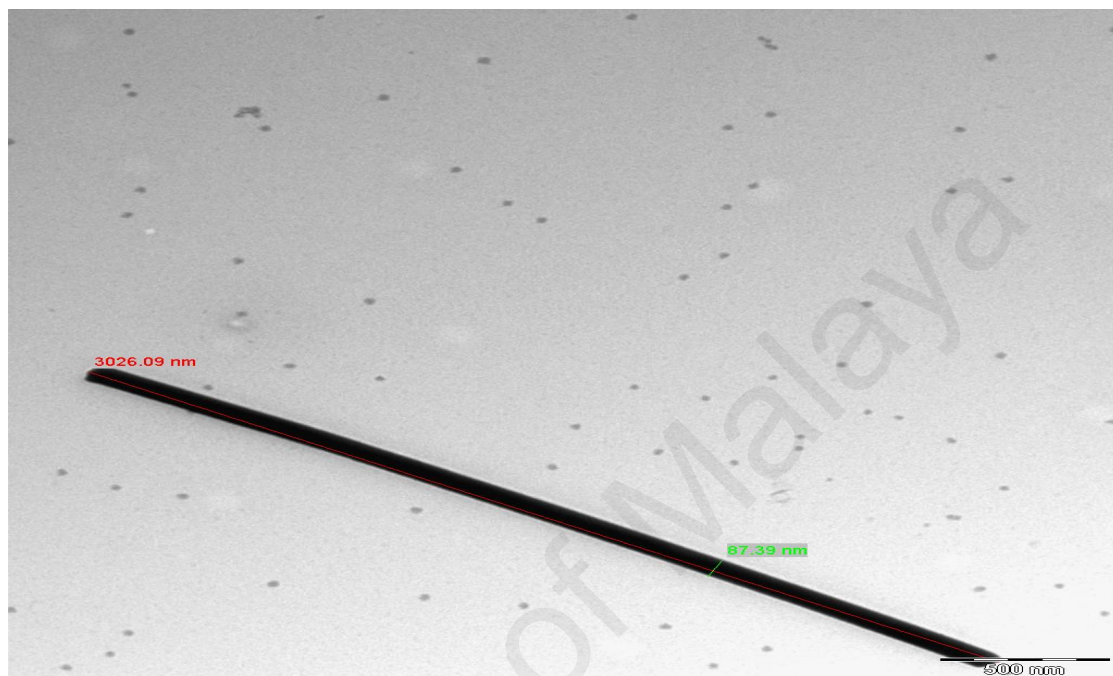


Figure 4.19: TEM image of as-synthesized individual AgNW with  $\text{CuCl}_2$  mediated agent.

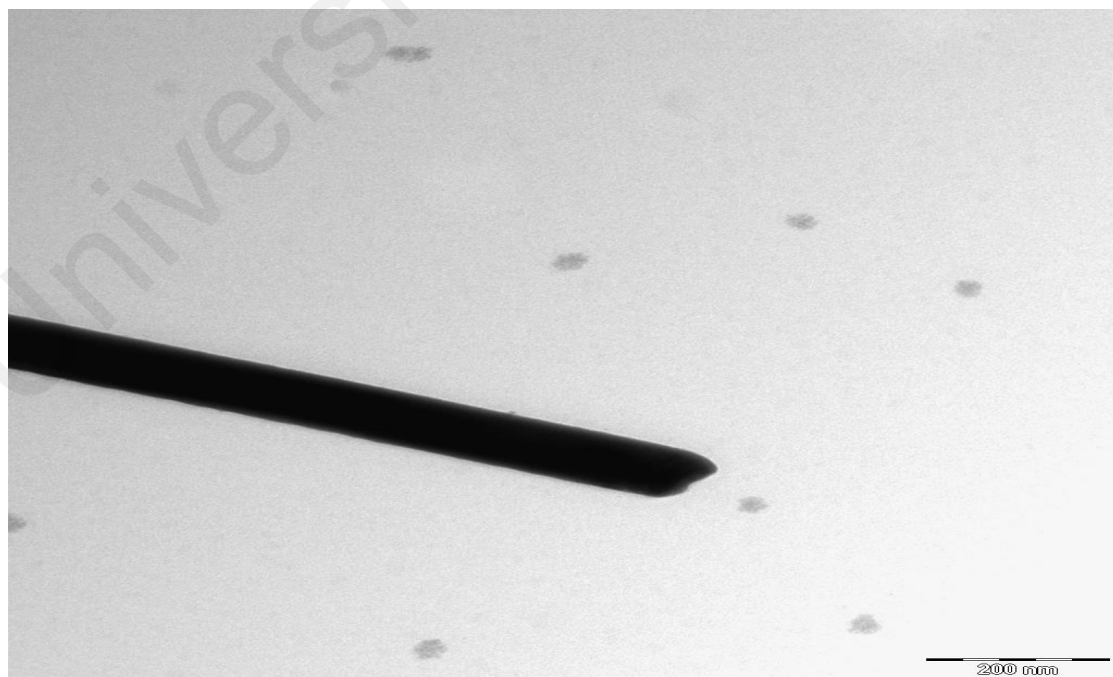


Figure 4.20: TEM image revealing the pentagonal cross-sectional of AgNW edge.



Figure 4.21: TEM image of typical as-synthesized AgNWs with  $\text{CuCl}_2$  mediated agent.

The diameter of AgNWs is about 87nm with  $3\mu\text{m}$  length. The aspect ratio is 1:35 indicated that the length of AgNWs is 35 times greater than the diameter. The pentagonal cross-sectional of a AgNWs edge is shown in Figure 4.20. The result obtained from TEM is in a good agreement with previous work (Korte *et al.*, 2007). Figure 4.21 shows the TEM image of several AgNWs in the sample. The formation of AgNWs started with Ag seeds that reduced from  $\text{AgNO}_3$  by the EG. Sufficient molarity of  $\text{AgNO}_3$  and PVP with mediated agent of  $\text{CuCl}_2$  allowed the Ag particles to transform into nanowires by the Ostwald ripening process. During the process, Ag particles were grew in the [100] direction that led to the formation of AgNWs.

### 4.3.3 Structural studies

#### 4.3.3.1 XRD analysis

Figure 4.22 shows the XRD pattern of as-synthesized sample with mediated agent of  $\text{CuCl}_2$ .

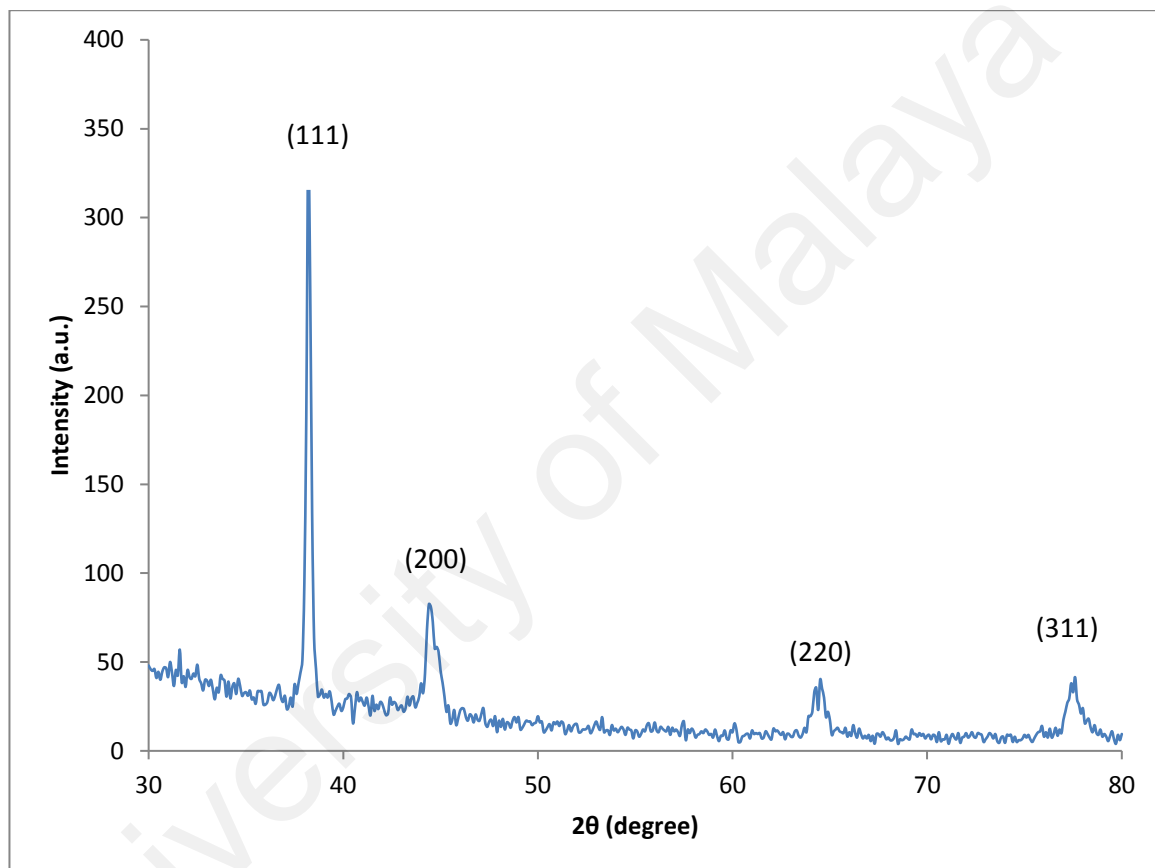


Figure 4.22: XRD pattern of as-synthesized sample with  $\text{CuCl}_2$  mediated agent.

It is observed that all the reflection peaks can be indexed to face-centered cubic (FCC) Ag. The XRD pattern reveals that the synthesis AgNWs through polyol process comprise of pure phase.

The sharp and strong peaks show that AgNWs are highly crystalline in nature. Four distinct peaks of AgNWs are located at angle of  $2\theta = 38.02^\circ$ ,  $44.40^\circ$ ,  $64.60^\circ$  and  $77.60^\circ$

which are corresponding to (111), (200), (220) and (311) plane. The lattice constant ( $a$ ) analysed from the XRD pattern is 4.07724 Å. This value is almost approaching the literature value of 4.086 Å (Sun *et al.*, 2002).

The ratio of intensity between (111) and (200) peaks reveals a relatively high value of 3.2 compared to the theoretical ratio value of 2.5 (Sun *et al.*, 2002). This high value of ratio indicate the enchancement of {111} crystalline planes in the AgNWs.

#### 4.3.4 Optical studies

##### 4.3.4.1 UV-vis spectroscopy analysis

Figure 4.23 shows the UV-vis spectrum for as-synthesized sample with mediated agent of  $\text{CuCl}_2$ .

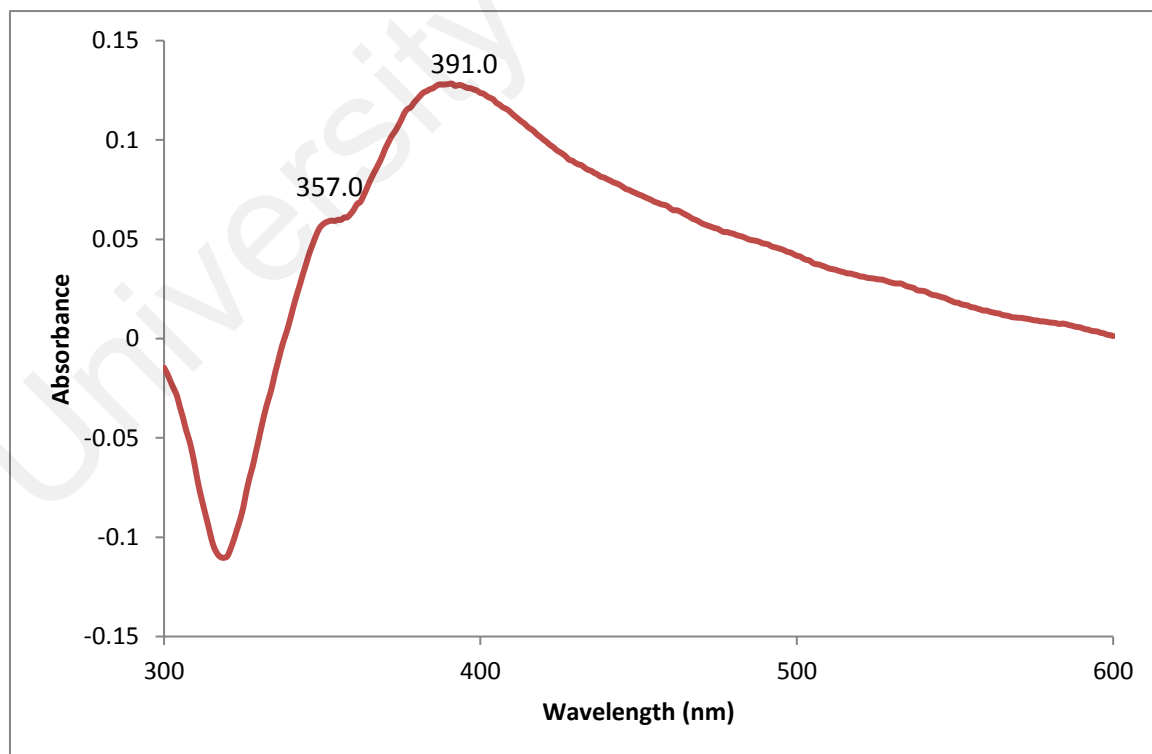


Figure 4.23: UV-vis spectrum of as-synthesized sample with  $\text{CuCl}_2$  mediated agent.

It was observed that there were two peaks occurred in the UV-vis spectrum in Figure 4.23. The shoulder peak at ~357 nm can be attributed to the plasmon response of the relatively long AgNWs which is similar as bulk Ag meanwhile, the absorption peak at 391 nm possibly attributed to the transverse plasmon mode of AgNWs (You *et al.*, 2009).

University of Malaya

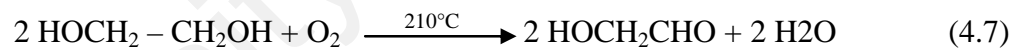


#### 4.4 Synthesis of AgNWs with mediated agent of NaCl

This subtopic is about the analysis results for AgNWs synthesized via polyol process with mediated agent of NaCl. The reducing agent used for this section is ethylene glycol NaCl. Different molar concentration of AgNO<sub>3</sub> used was 0.025 M, 0.05 M, 0.1 M, 0.2 M and 0.25 M.

##### 4.4.1 Mechanism formation of AgNWs with mediated agent of NaCl

The formation of anisotropic AgNWs involves a number of steps. In the first step, high temperature is crucial for the conversion of ethylene glycol to glycoaldehyde as shown in equation (4.7).



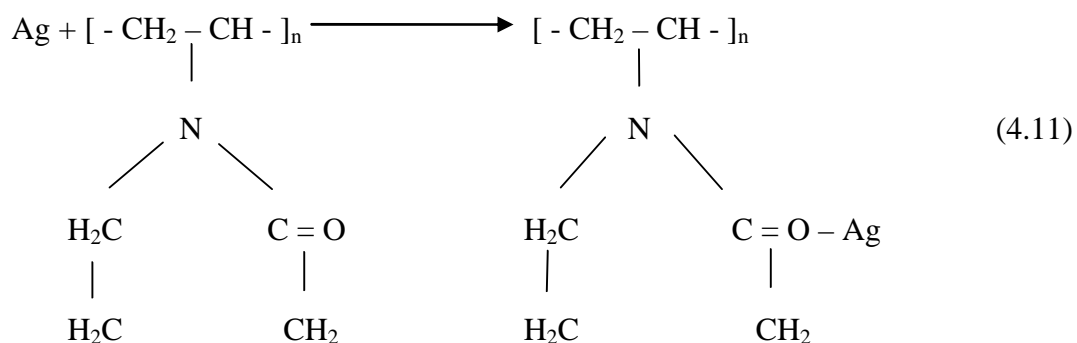
AgNPs start to form via homogeneous nucleation by reducing AgNO<sub>3</sub> with glycoaldehyde as shown in Equation (4.8).



It was found that chloride ions (Equation (4.9) & (4.10)) stabilized AgNPs against aggregation (Hu et al., 1999). This stabilization may also prevent the growth of these nanoparticles. As a result, nanoparticles that can grow will dissolve via Oswald ripening.



The high  $\text{Cl}^-$  concentration during NaCl mediated synthesis, helps to reduce the concentration of free  $\text{Ag}^+$  in the solution through the formation of AgCl nanocrystallites. This decrease in free  $\text{Ag}^+$  during initial Ag seed formation and subsequent slow release of  $\text{Ag}^+$ , effectively. This facilitates the high yield formation of the thermodynamically stable multiply twinned Ag seeds. So, AgCl precipitate that forms in the early stages of the reaction serves as a seed for multitwinned particles. The formed AgCl nanoparticles can be reduced slowly and decreased reaction rate makes anisotropic growth of AgNWs favourable (Korte et al., 2008). Meanwhile,  $\text{Na}^+$  can remove oxygen from the solvent which prevents twinned seeds dissolved by oxidative etching and scavenging adsorbed atomic oxygen from the surface of the Ag seeds, facilitating multiply twinned seeds growth. In the final step,  $\text{AgNO}_3$  and PVP were added dropwise to the reaction system allowing the nucleation and growth of AgNWs.



AgNPs were well-dispersed because of the presence of PVP, a polymeric surfactant that could chemically adsorb onto the surfaces of Ag through O – Ag bonding (Equation 4.11). When the dispersion of AgNPs was continuously heated at 210°C, some of the AgNPs started to dissolve and grow as larger nanoparticles via the mechanism known as Oswald ripening (Roosen et al., 2004). With passivation of some facets of particles by PVP, some nanoparticles can grow into multitwin particles. PVP is believed to passivate {100} faces of these multitwin particles and leave {111} planes available for anisotropic growth at [110] direction (Saidi et al., 2012) (Figure 4.24). As the addition of Ag<sup>+</sup> continues, multitwin particles grow into AgNWs.

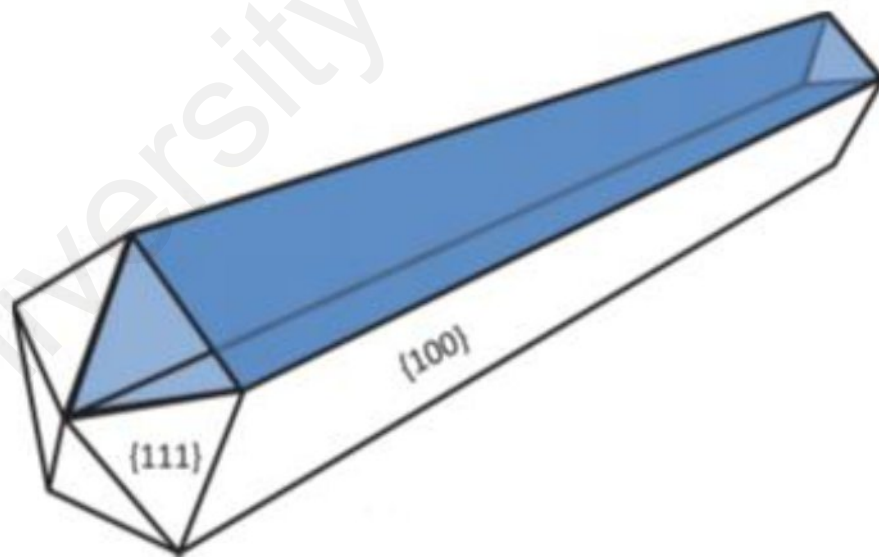


Figure 4.24: Schematic of a 5-fold twinned pentagonal nanowires consisting of five elongated {100} facets and 10 {111} end facets.

## 4.4.2 Morphological studies

### 4.4.2.1 FESEM analysis

Figures 4.25 – 4.29 show the FESEM images of as-synthesized samples mediated with NaCl at different molar of  $\text{AgNO}_3$ .

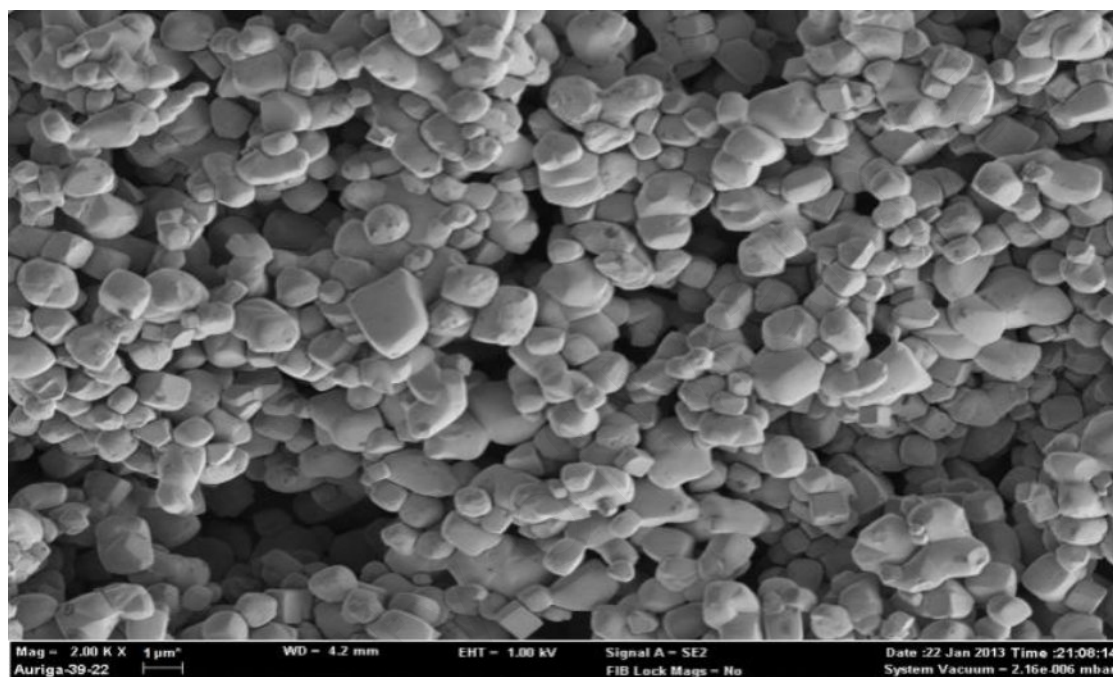


Figure 4.25: FESEM image for as-synthesized samples with 0.025 M of  $\text{AgNO}_3$ .

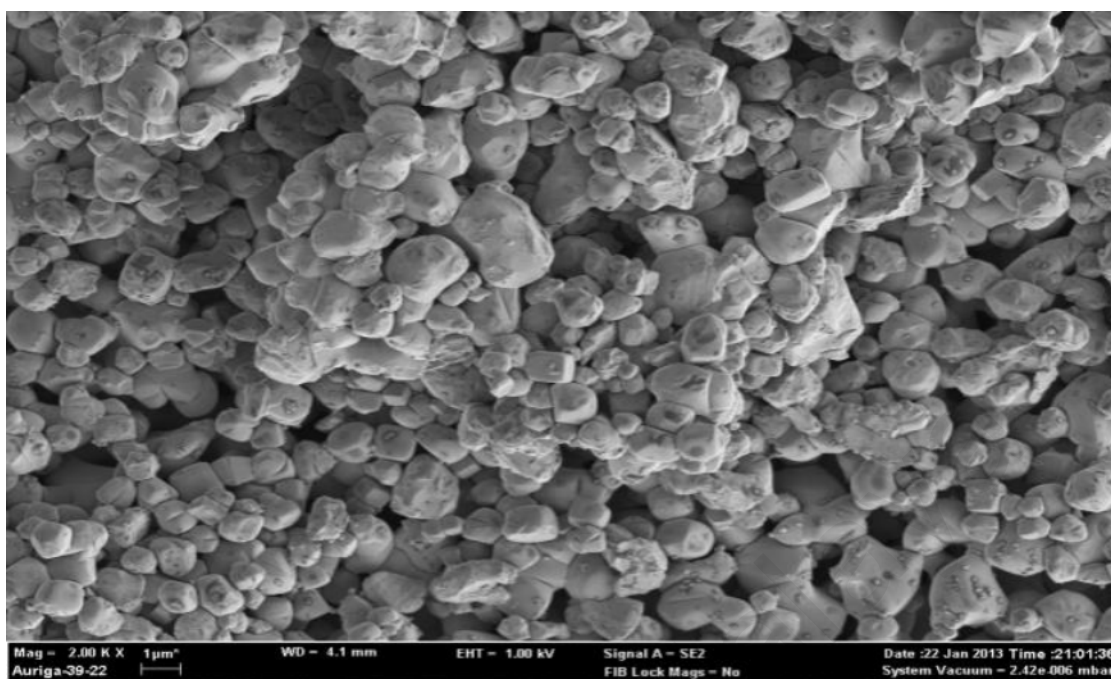


Figure 4.26: FESEM image for as-synthesized samples with 0.050 M of  $\text{AgNO}_3$ .

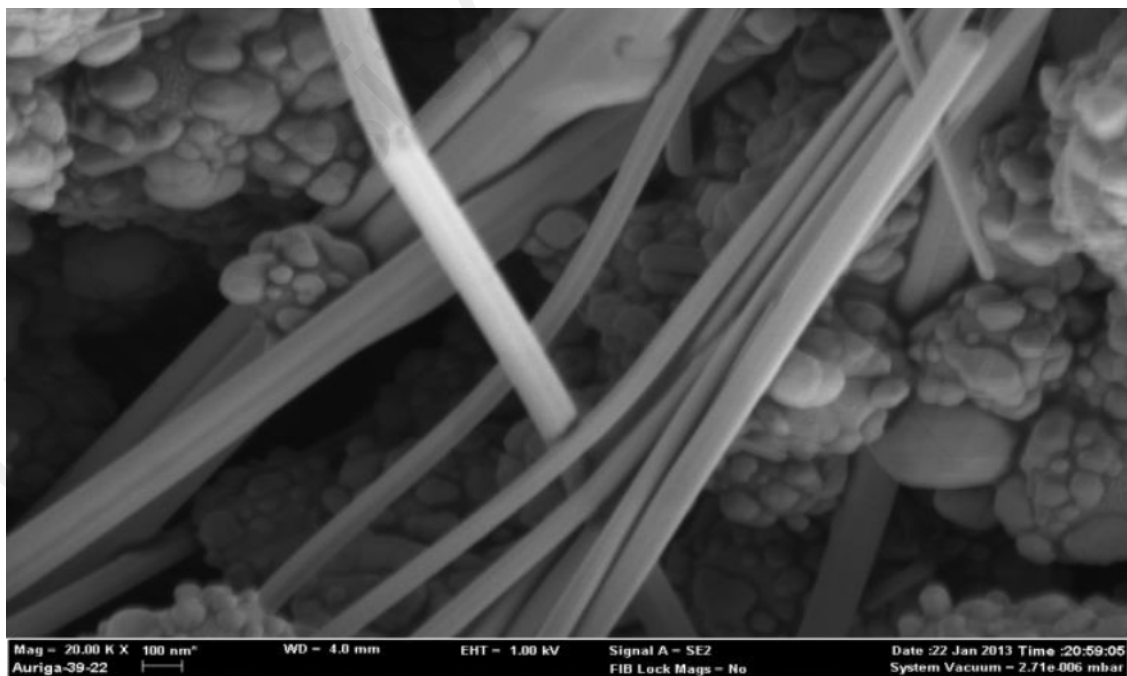


Figure 4.27: FESEM image for as-synthesized samples with 0.10 M of  $\text{AgNO}_3$ .

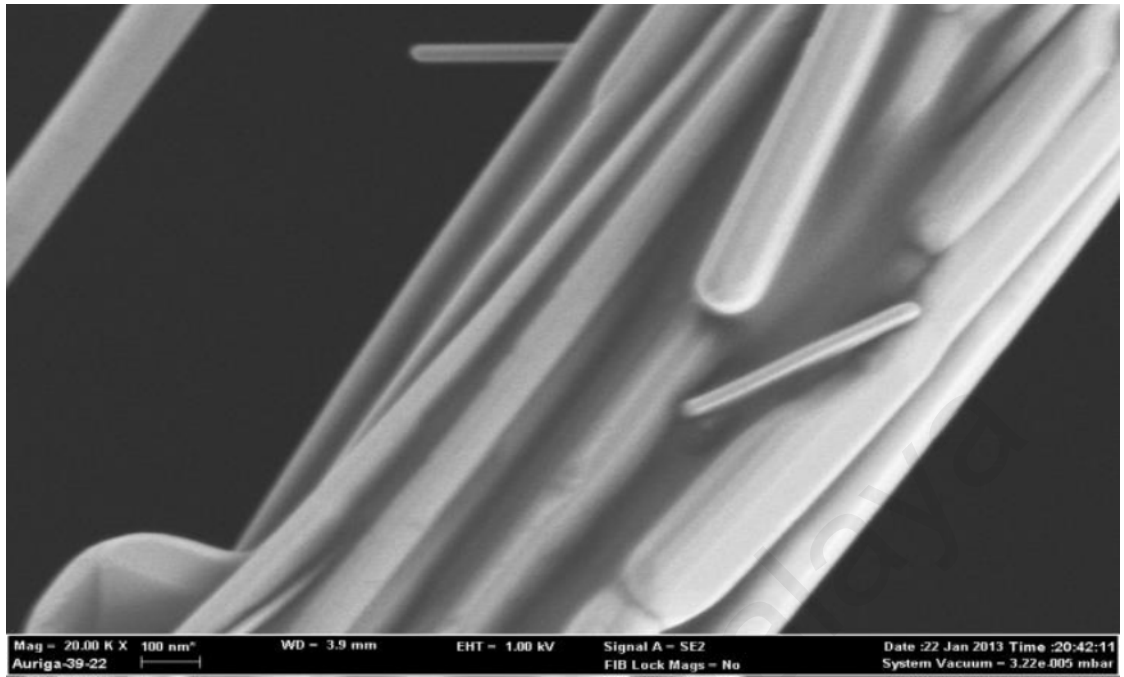


Figure 4.28: FESEM image for as-synthesized samples with 0.20 M of  $\text{AgNO}_3$ .

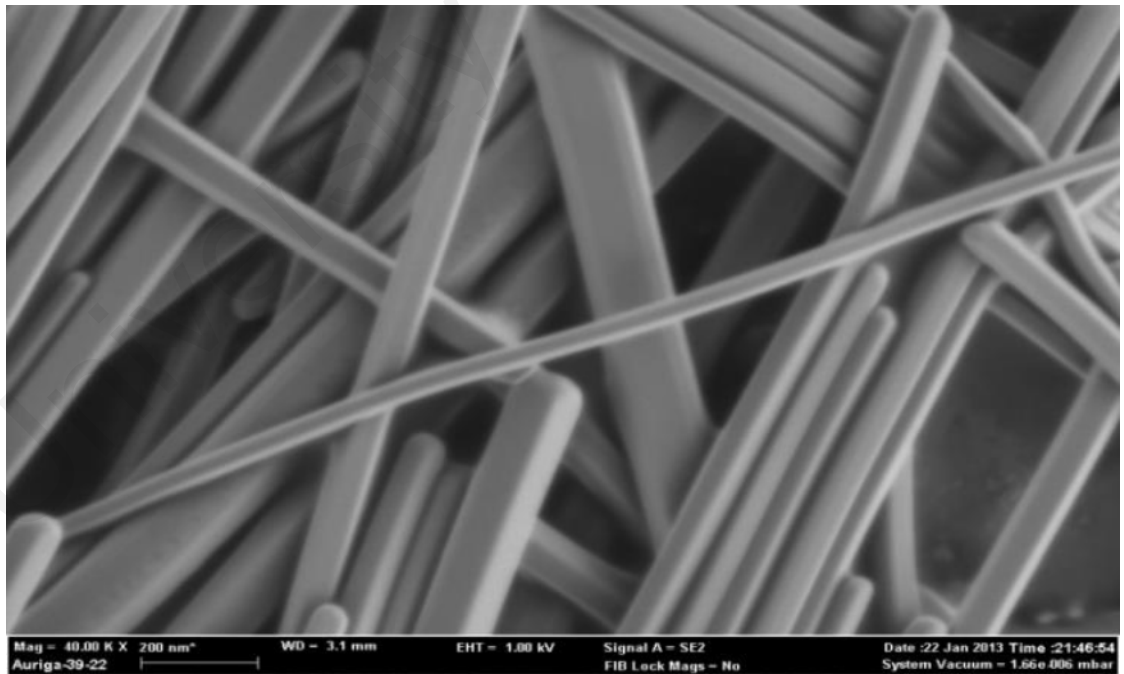


Figure 4.29: FESEM image for as-synthesized samples with 0.25 M of  $\text{AgNO}_3$ .

From the images, these show that samples with 0.025 and 0.05 M of  $\text{AgNO}_3$  formed Ag particles with spherical shape as shown in Figure 4.25 and 4.26. Large size diameters of particles were formed due to insufficient the passivation of {100} faces of multitwin particles and thus Ag structures growth occurred on both {111} and {100} faces (Coskun et al., 2011). Moreover, the multitwin particles that could not grow into nanowires agglomerated and formed large amounts of micrometer-sized Ag particles.

However, at 0.10 M of  $\text{AgNO}_3$ , the particles started to transform into nanowires. With increasing molarity of  $\text{AgNO}_3$  at 0.2 and 0.25 M, Ag particles were completely formed nanowires. The diameter sizes of AgNWs were decreased with increasing molarity of  $\text{AgNO}_3$ . At these conditions, enough amount of PVP molecules were covered all the Ag particles and also responsible for blocking anisotropic growth (1D) of AgNWs (Coskun et al., 2011) as shown in Figure 4.28 and 4.29.

#### **4.4.2.2 TEM analysis**

Figures 4.30 (a) and (b) show TEM images of as-synthesized AgNWs at 0.20 M  $\text{AgNO}_3$  at different magnification while Figures 4.31 (a) and (b) show the TEM images for as-synthesized AgNWs at 0.25 M of  $\text{AgNO}_3$  at different magnification.

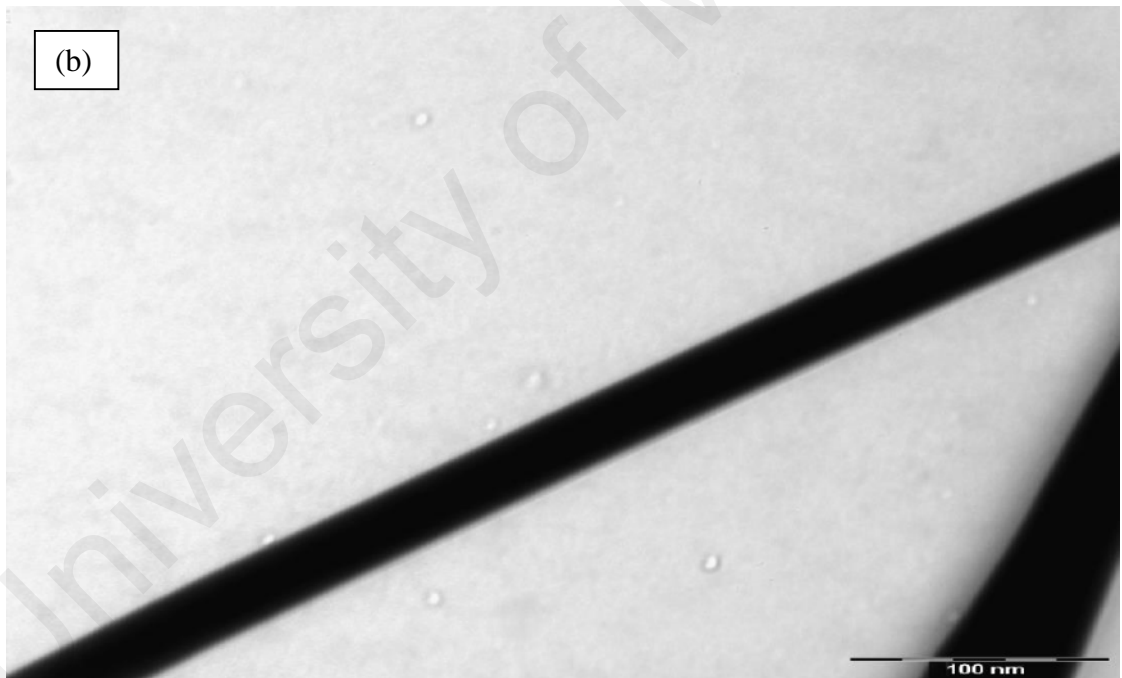
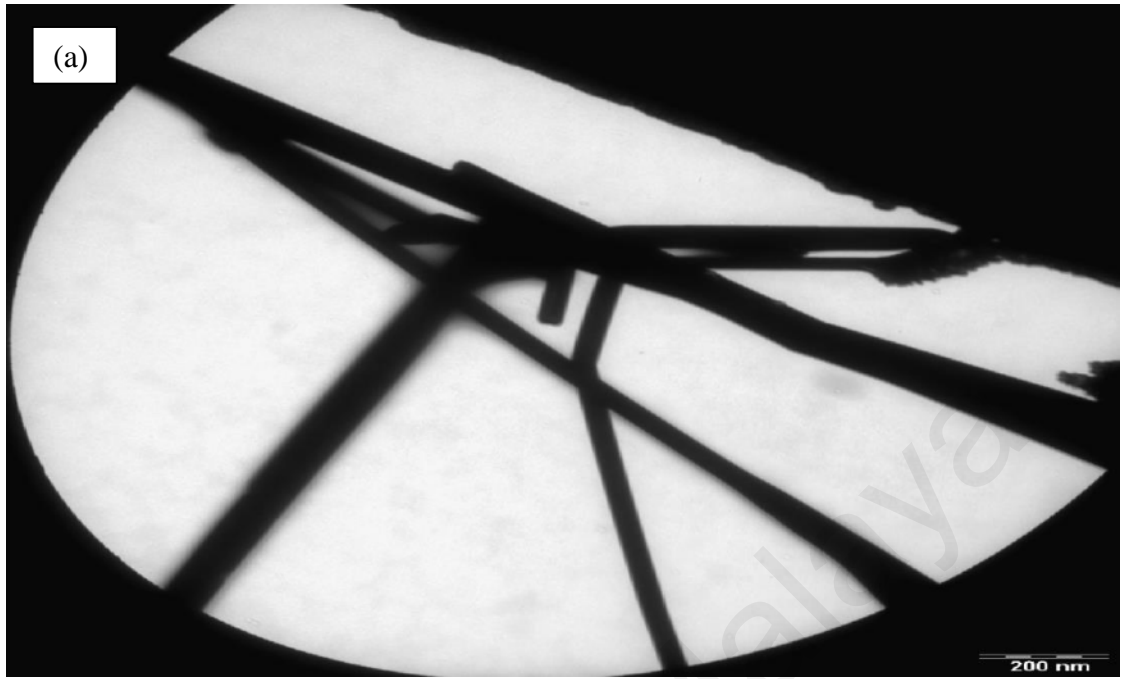


Figure 4.30: TEM images of as-synthesized AgNWs with 0.20 M of  $\text{AgNO}_3$  at different magnification.



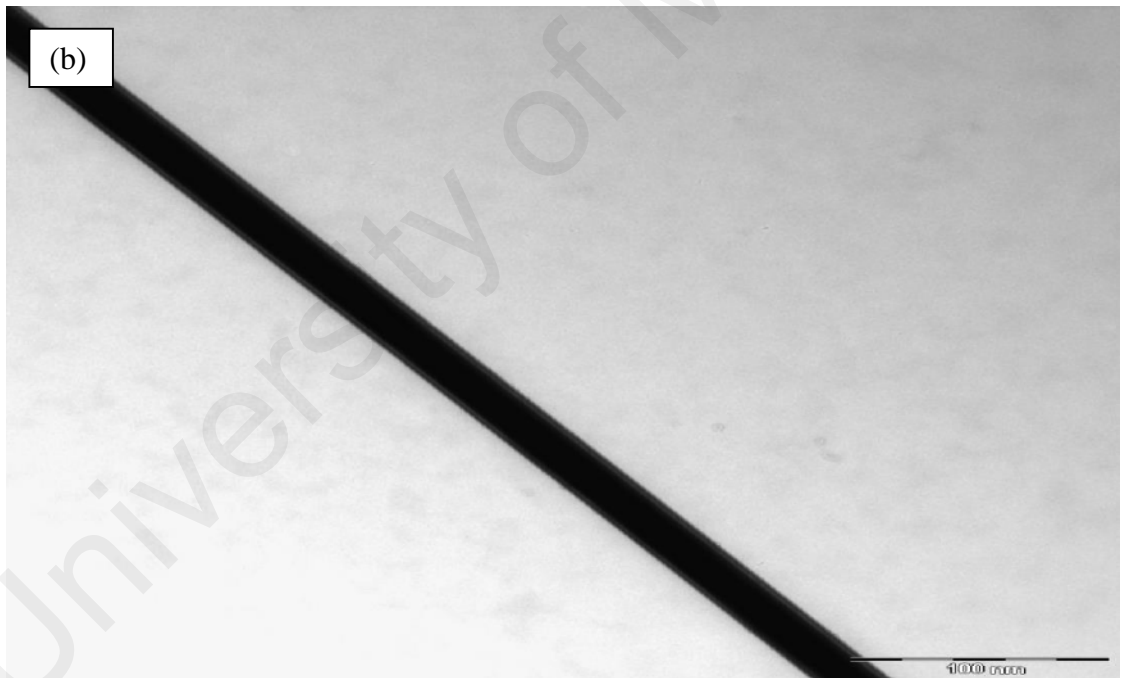
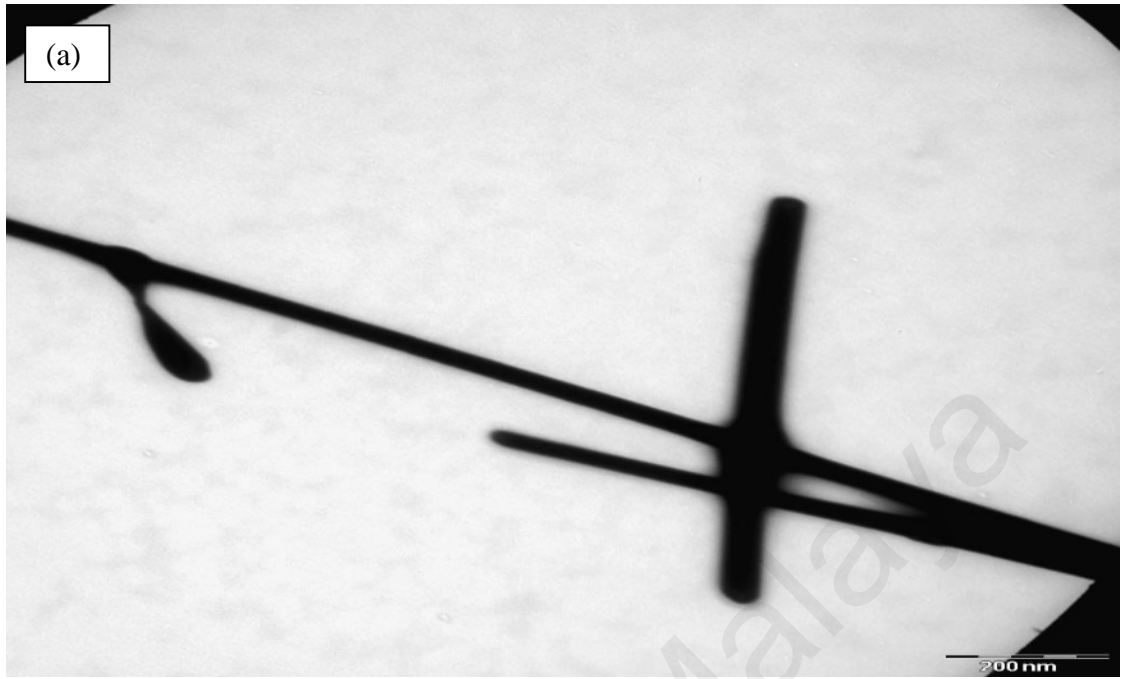


Figure 4.31: TEM images of as-synthesized AgNWs with 0.25 M of  $\text{AgNO}_3$  at different magnification.

The TEM images in Figure 4.30 (b) and 4.31 (b) show long and straight rod shape of an individual AgNWs. The diameter of AgNWs for sample with 0.20 M AgNO<sub>3</sub> is in the range of 60 to 100 nm. Meanwhile, the diameter of AgNWs for sample with 0.25 M AgNO<sub>3</sub> decreased to 30 – 70 nm. The diameter sizes of AgNWs were decreased with the increasing of molarity of AgNO<sub>3</sub>.

The formation of AgNWs occurred due to the growth of Ag particles known as Ostwald ripening process. PVP that acted as stabilizer was responsible to control the growth of Ag particles in [110] direction to form AgNWs. Therefore with the increasing molarity of AgNO<sub>3</sub> and PVP, there were sufficient passivation of {100} faces of multitwin particles and the growth in longitudinal decreased the diameter size of AgNWs.

### 4.4.3 Structural studies

#### 4.4.3.1 XRD analysis

Figures 4.32 – 4.33 show the XRD patterns of as-synthesized at different molarity of  $\text{AgNO}_3$ .

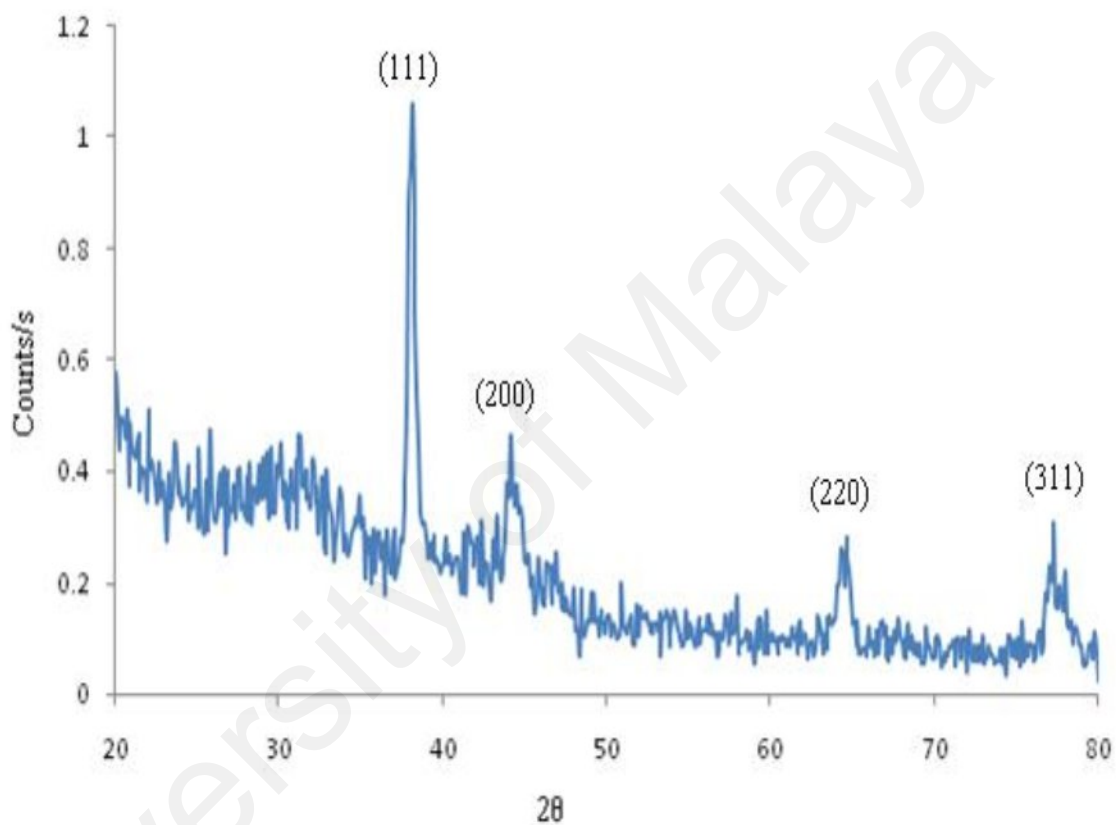


Figure 4.32: XRD pattern of the as synthesized AgNWs at molarity 0.20 M of  $\text{AgNO}_3$ .

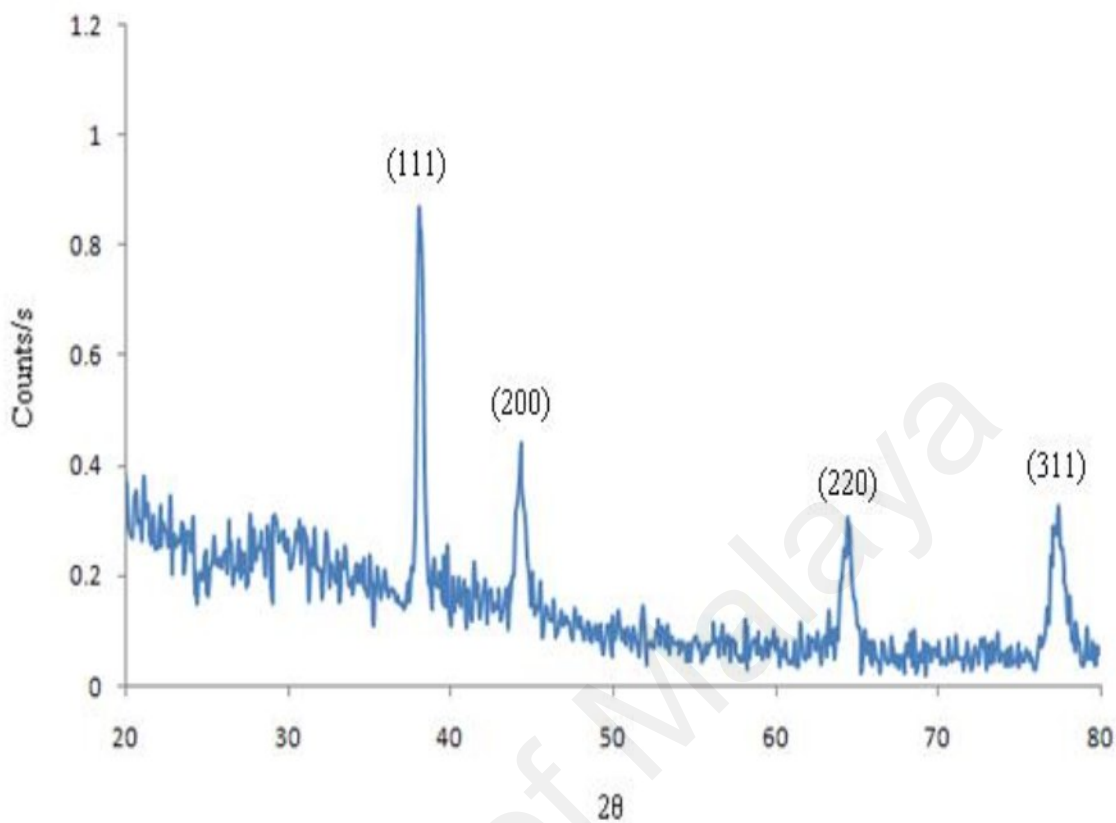


Figure 4.33: XRD pattern of the as synthesized AgNWs at molarity 0.25 M of  $\text{AgNO}_3$ .

Both figures exhibit four diffraction peaks corresponding to the face centre cubic (FCC) phase structure of Ag. No phase transition was occurred with the increasing molar concentration of  $\text{AgNO}_3$ . It is worth noting that the intensity ratio between (111) and (200) peaks exhibits a relatively value of 2.05 while the theoretical ratio is 2.5 (Sun et al., 2002). However, the intensity for (111) plane was slightly decreased for sample with 0.25 M  $\text{AgNO}_3$  indicated that it become less crystalline at higher molar of  $\text{AgNO}_3$ .

#### 4.4.4 Optical studies

##### 4.4.4.1 UV-vis spectroscopy analysis

Figures 4.34 – 4.35 show the absorption spectra for as-synthesized AgNWs at various molar of  $\text{AgNO}_3$ .

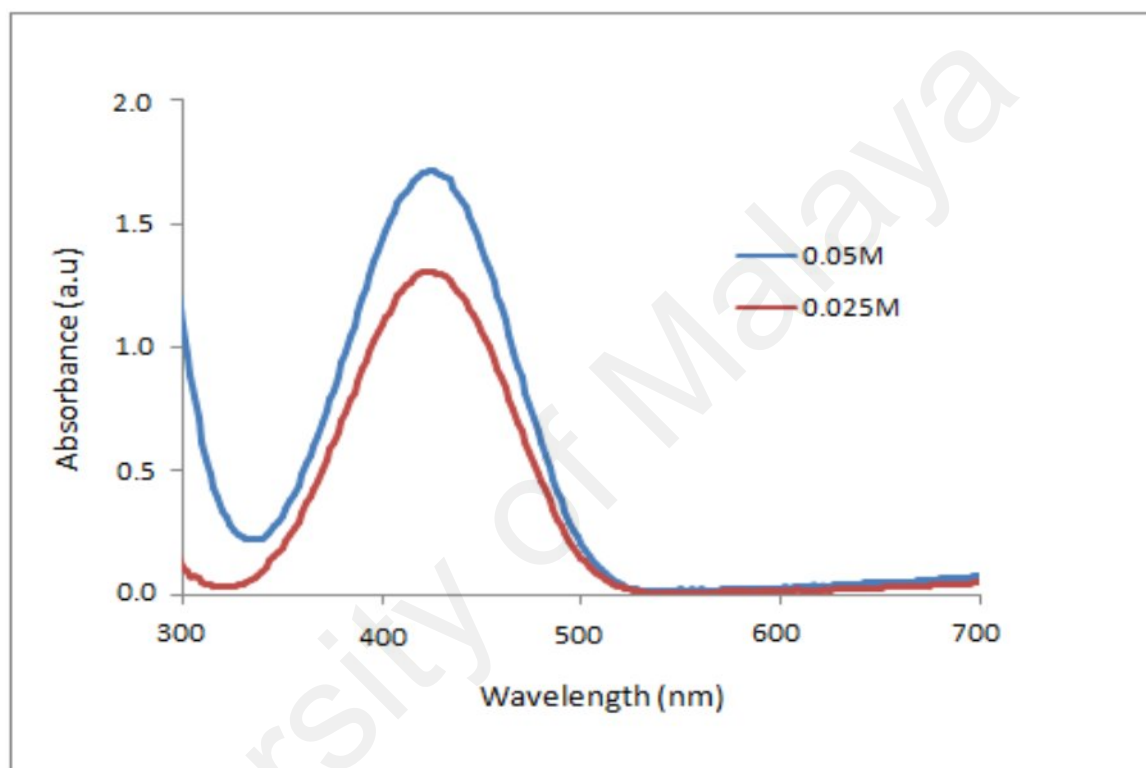


Figure 4.34: UV- vis spectra for as-synthesized AgNWs at 0.025 and 0.05 M of  $\text{AgNO}_3$ .

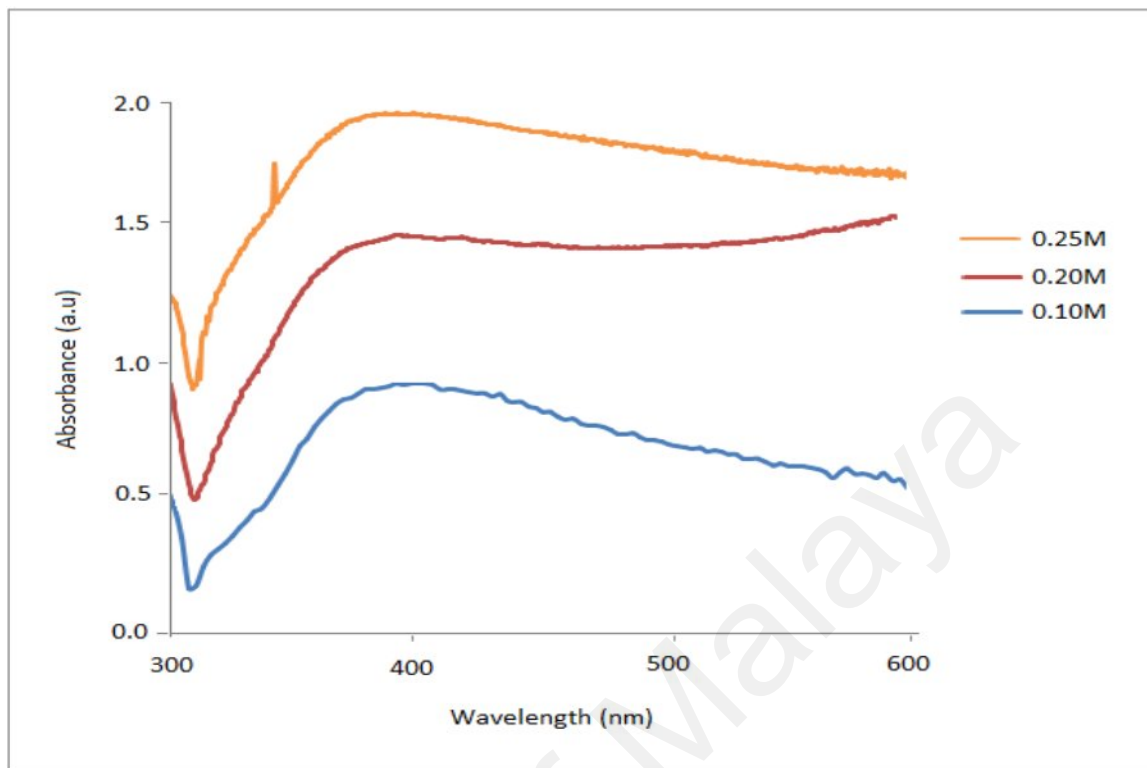


Figure 4.35: UV-vis spectra for as-synthesized AgNWs at 0.01, 0.02 and 0.25 M of  $\text{AgNO}_3$ .

Figure 4.34 shows the absorption spectra of synthesized AgNPs with very low molarity of  $\text{AgNO}_3$ . SPR peaks for both samples occurred at 420 nm indicating the present of AgNPs. The symmetrical shape of both SPR peaks indicating narrow particle size distribution. Meanwhile, sample with lower molarity of  $\text{AgNO}_3$  (0.025 M) shows less absorbance than sample with high molarity of  $\text{AgNO}_3$  (0.05 M) indicating different yield of AgNPs.

Figure 4.35 shows the absorption spectra of as-synthesized AgNWs with high molarity of  $\text{AgNO}_3$ . There were two main peaks at wavelength around 350 nm and 400 nm. The weak peak at 350 nm, also known as shoulder peak was attributed to the longitudinal

SPR of AgNWs while the other main peak at 400 nm was attributed to the transverse mode Plasmon of AgNWs (You et al., 2009).

University of Malaya

## 4.5 Synthesis of AgNWs via polyol process with different control agent (KOH, KCL, Fe(NO<sub>3</sub>)<sub>3</sub>, H<sub>2</sub>O)

### 4.5.1 Morphological studies

#### 4.5.1.1 FESEM analysis

Figures 4.36 – 4.39 show the FESEM images for all as-synthesized samples with different control agent.

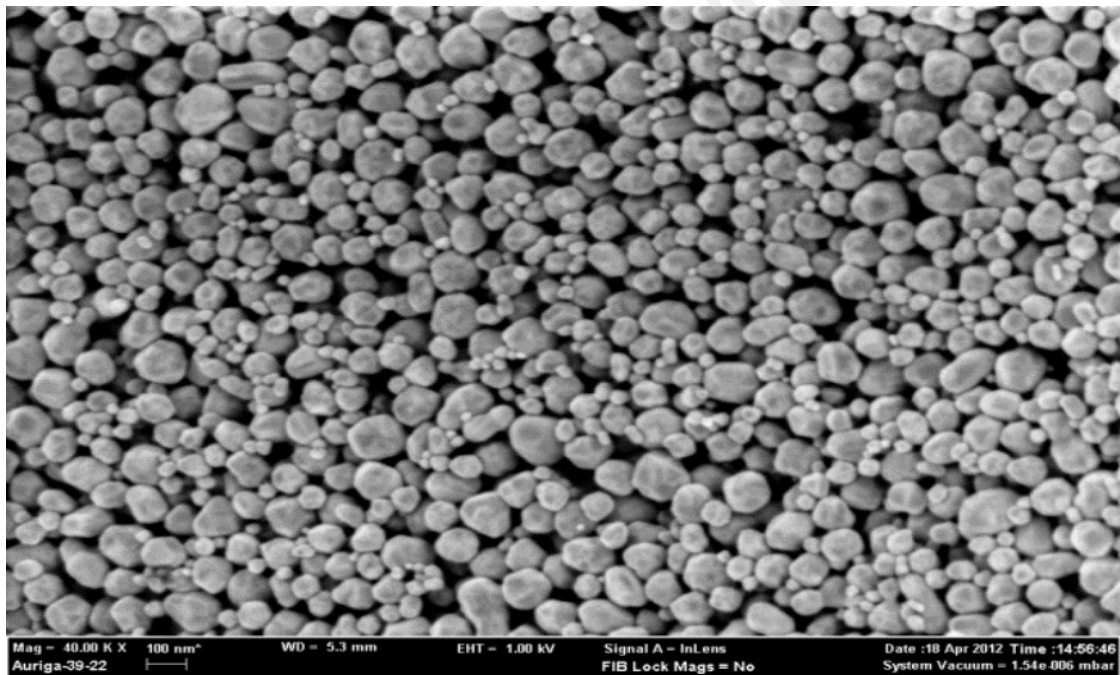


Figure 4.36: FESEM image for as-synthesized sample with control agent of KOH.



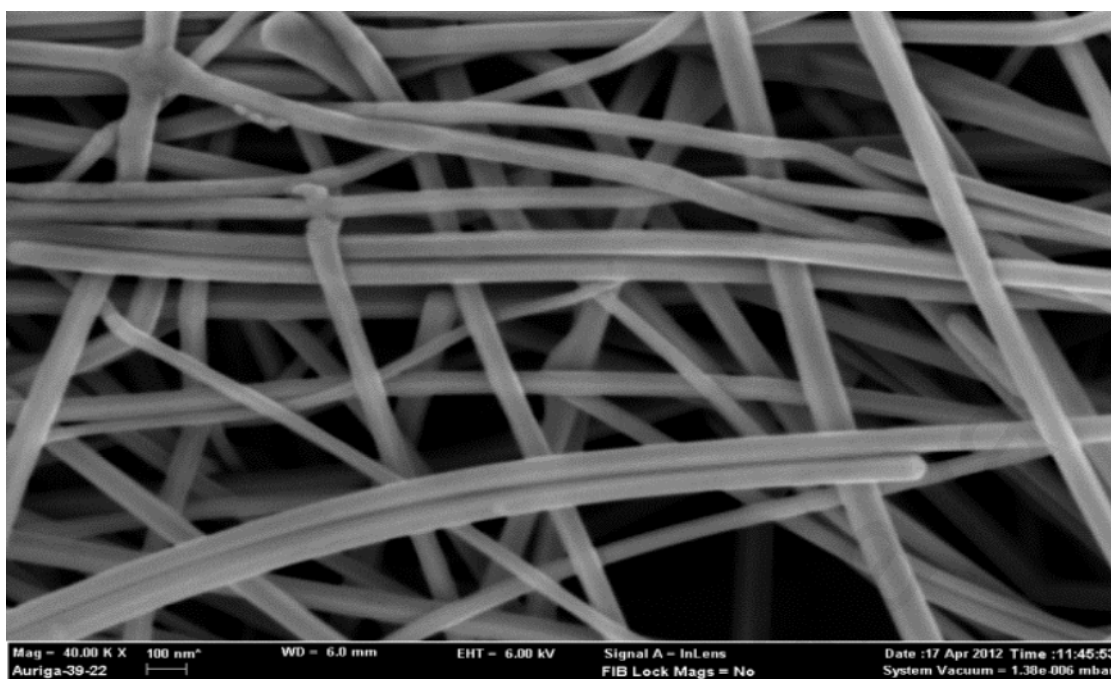


Figure 4.37: FESEM image for as-synthesized sample with control agent of KCl.

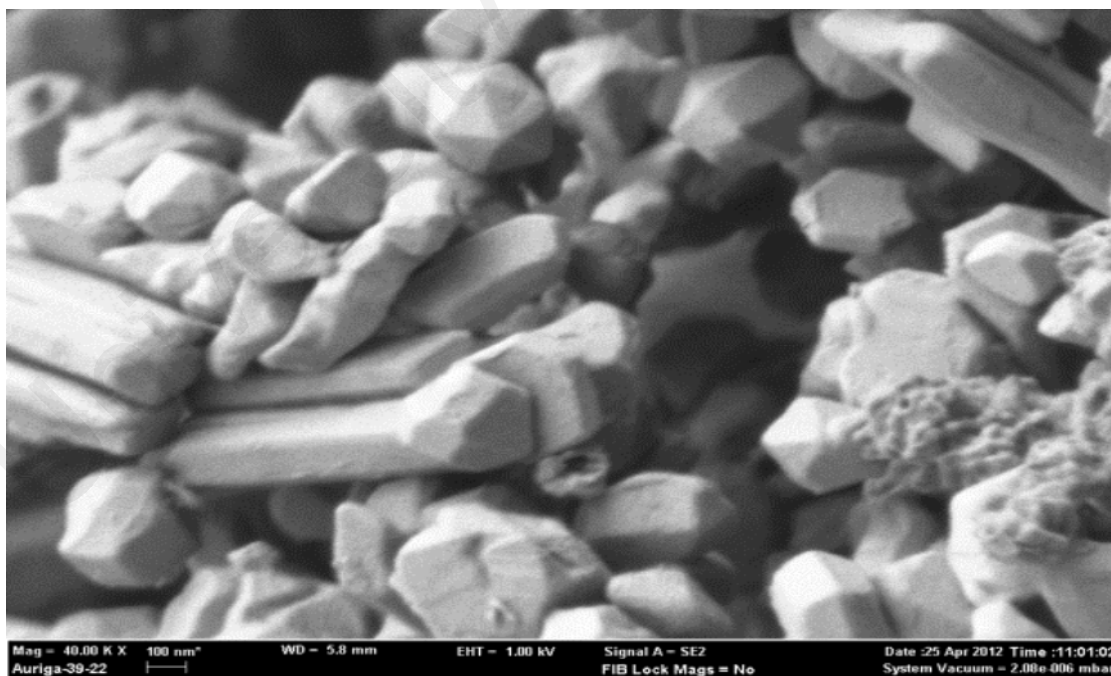


Figure 4.38: FESEM image for as-synthesized sample with control agent of  $\text{Fe}(\text{NO}_3)_3$ .

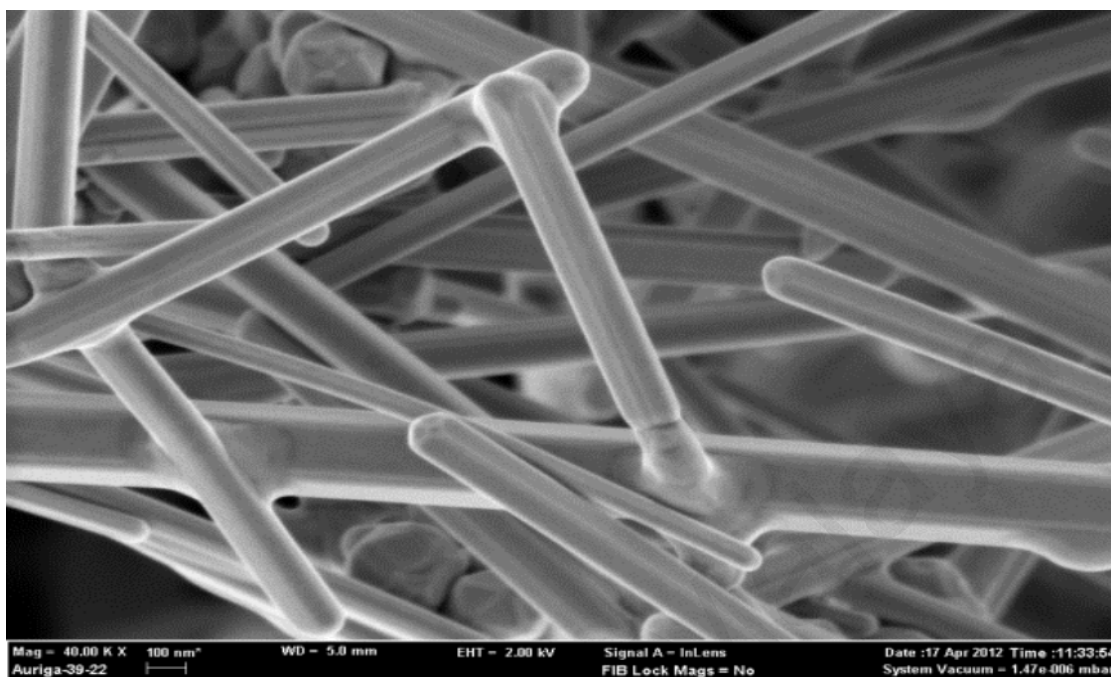


Figure 4.39: FESEM image for as-synthesized sample with control agent of H<sub>2</sub>O.

AgNWs were successfully synthesized using control agent KCl and deionized water. Meanwhile, a pentagonal shape or five – fold symmetry cross sectional shape was observed for control agents KOH and Fe(NO<sub>3</sub>)<sub>3</sub>. This indicated the formation of multiply twinned nanoparticle (MTP) of Ag, which was the early stage of AgNWs formation before its growth. For the case of control agent KOH, the five-fold symmetry cross sectional shape of structures proved the incomplete process of formation of AgNWs (Chen et al., 2006).

For the case of control agent Fe(NO<sub>3</sub>)<sub>3</sub>, the overall uniformity of the structure was low due to some over-growth rod-shape structures and small cubic-shape structures. The failures in fabrication of AgNWs for the case of control agents KOH and Fe(NO<sub>3</sub>)<sub>3</sub> was due to the reaction temperature since precision in controlling the temperature was critical in the polyol process. The different failure conditions for both control agent KOH and Fe(NO<sub>3</sub>)<sub>3</sub>

were due to higher yielding ratio of AgNWs for control agent  $\text{Fe}(\text{NO}_3)_3$  than that of control agent KOH. As a result, some wire-like shape structure such as rod can be observed for control agent  $\text{Fe}(\text{NO}_3)_3$ .

#### 4.5.1.2 TEM analysis

Figures 4.40 – 4.43 show the TEM images for as-synthesized samples with different control agents.

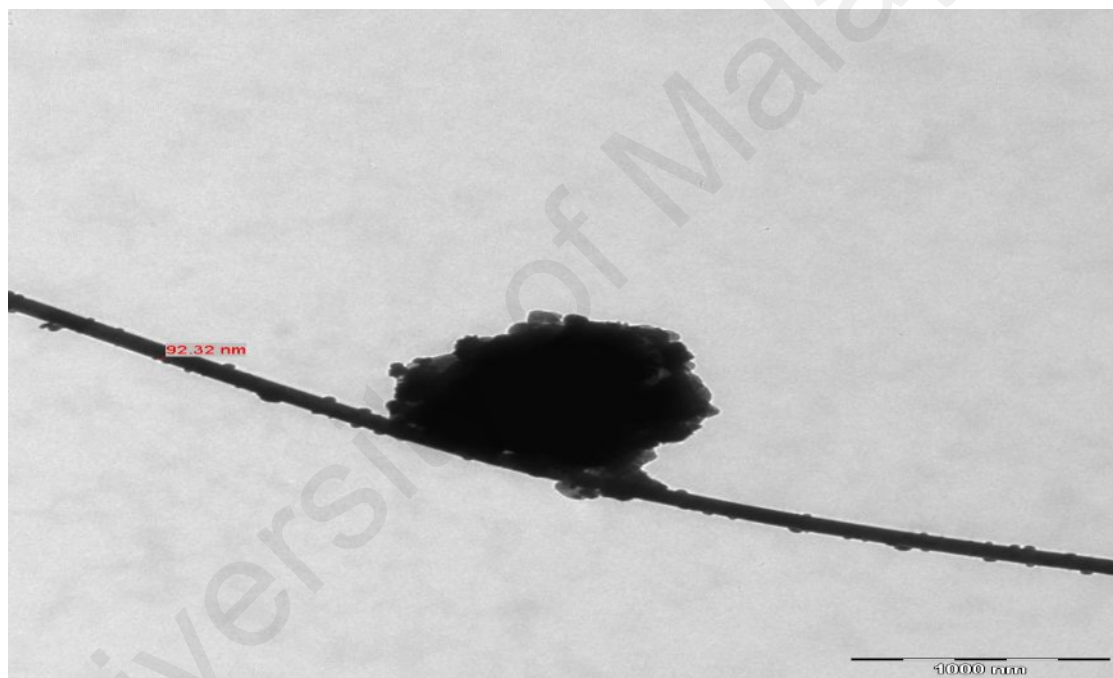


Figure 4.40: TEM image for as-synthesized sample with control agents of KOH



Figure 4.41: TEM image for as-synthesized sample with control agents of KCl.

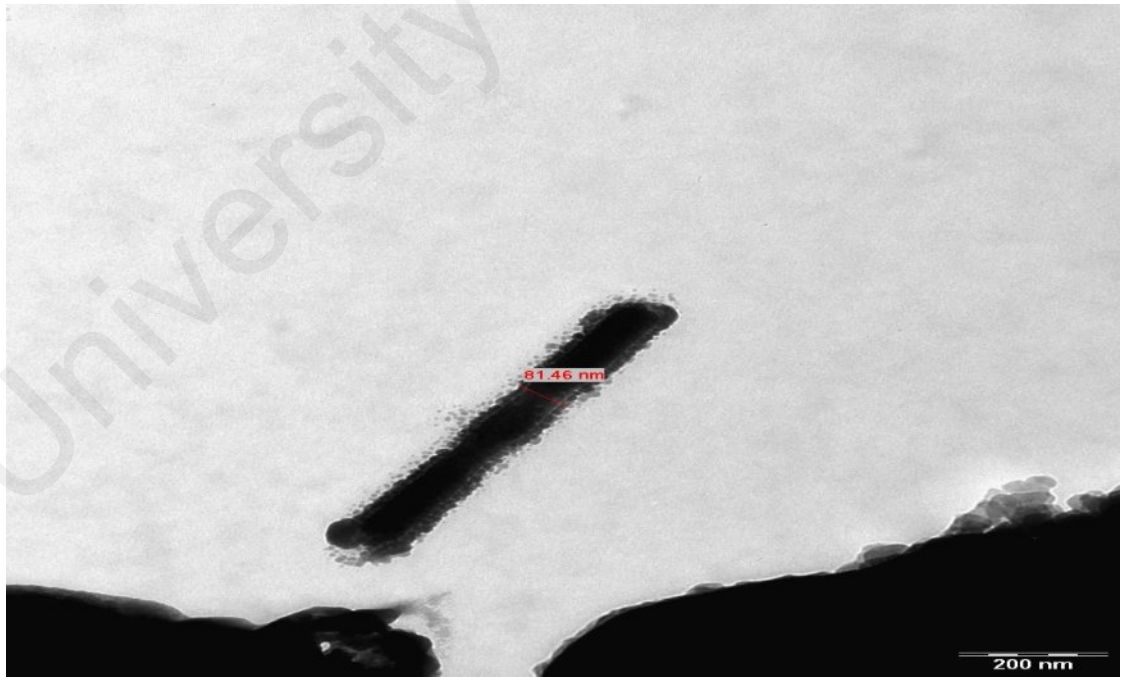


Figure 4.42: TEM image for as-synthesized sample with control agents of  $\text{Fe}(\text{NO}_3)_3$ .

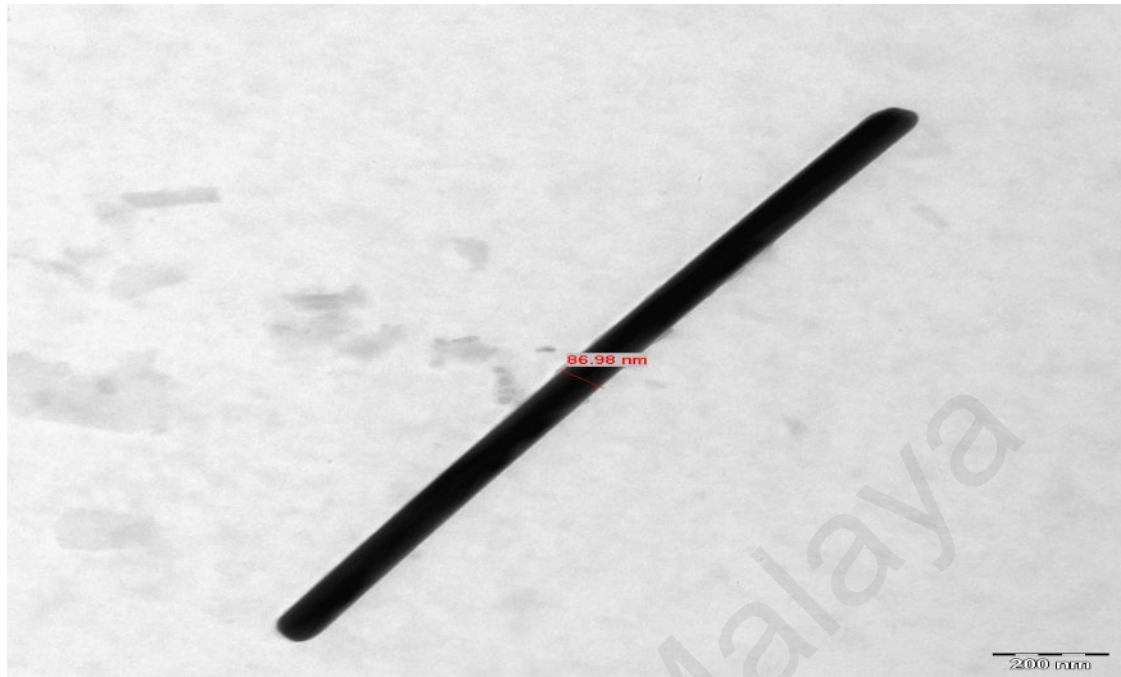


Figure 4.43: TEM image for as-synthesized sample with control agents of H<sub>2</sub>O.

All the images show the wire-like shape structure. The as-synthesized AgNWs with control agents of KCl, Fe(NO<sub>3</sub>)<sub>3</sub> and H<sub>2</sub>O with the exception of control agent KOH were having diameter near to theoretical value. It was observed that AgNPs with diameter of 66 nm in Figure 4.40. This indicated that an incomplete growth process of AgNW for control agent KOH. Temperature was the factor for the change of AgNW diameter from 60 to 90nm for the case of control agent KOH and non-uniform surface structure of AgNW for the case of control agent Fe(NO<sub>3</sub>)<sub>3</sub>. AgNWs with desirable diameter have been successfully synthesized by adding control agent KCl and H<sub>2</sub>O in polyol synthesis.

## 4.5.2 Structural analysis

### 4.5.2.1 XRD studies

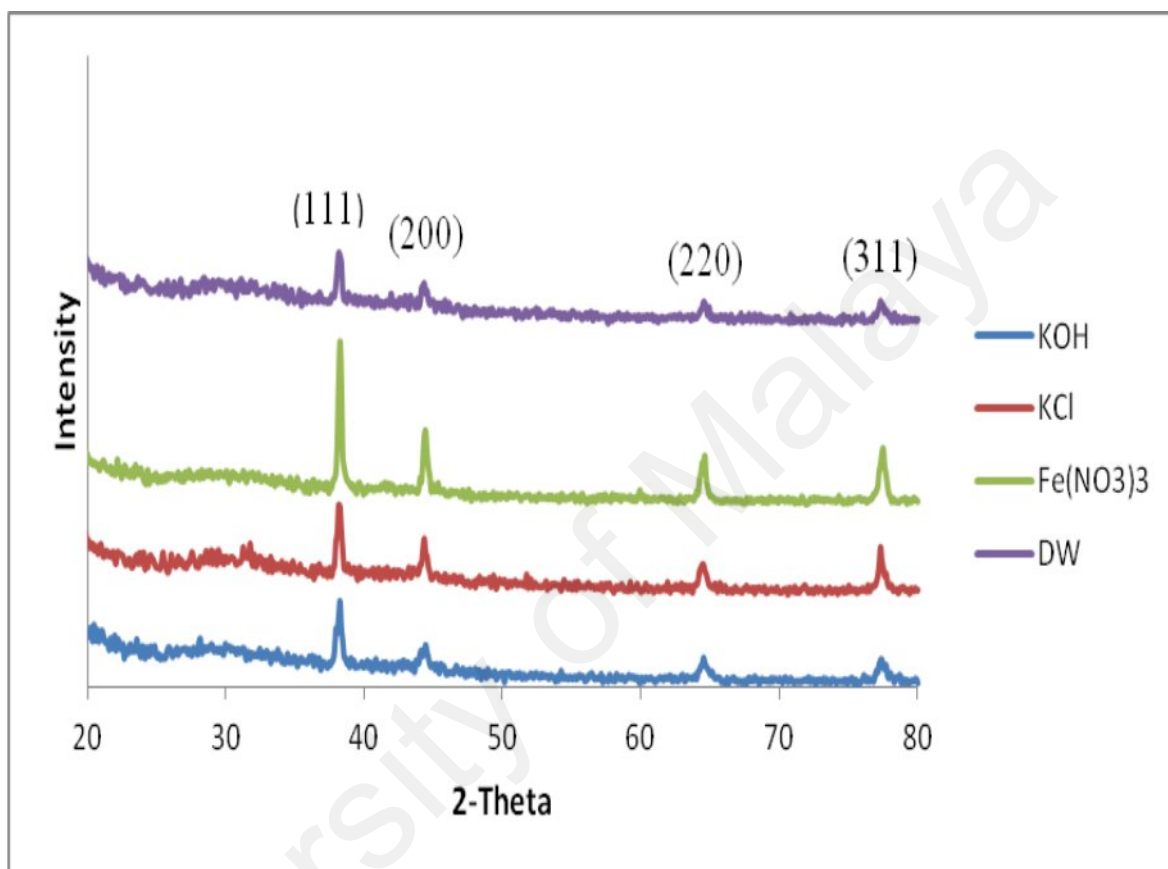


Figure 4.44: XRD patterns of all as-synthesized samples with different control agents KOH, KCl,  $\text{Fe}(\text{NO}_3)_3$  and  $\text{H}_2\text{O}$ .

Figure 4.44 shows the XRD patterns for all samples with four peaks are appeared in each pattern corresponding to the (111), (200), (220) and (311) planes of face-centered-cubic of silver phase. The intensity ratio of (111) to (200) peaks exhibits a relatively high value around 2 to 2.5 (theoretical ratio is 2.5) which indicated the abundance of the (111) crystalline planes in all samples. Besides, no other element was detected other than Ag.

This shows that no impurities were present in the samples and addition of control agents has limited effects on the purity of AgNWs (Chen et al., 2006).

### 4.5.3 Optical studies

#### 4.5.3.1 UV-vis spectroscopy analysis

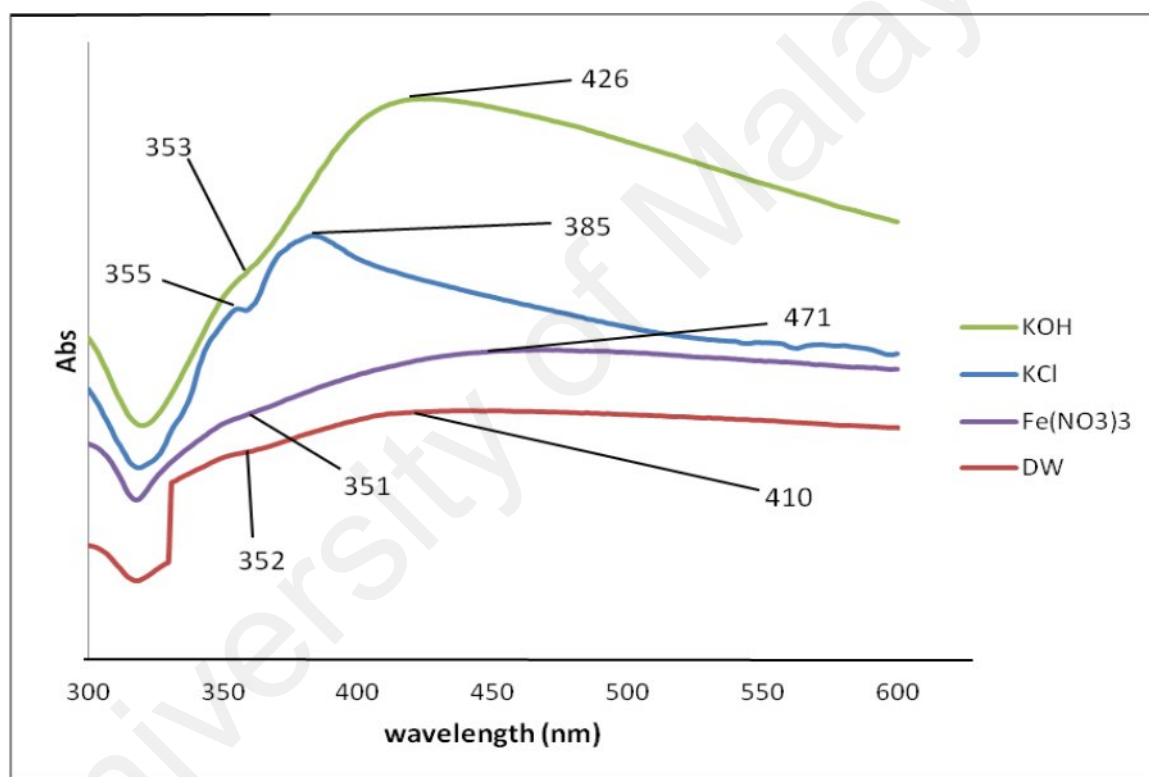


Figure 4.45: UV-vis spectra of as-synthesized AgNWs with control agents KOH, KCl, and Fe(NO<sub>3</sub>)<sub>3</sub> and H<sub>2</sub>O.

Fig. 4.45 shows the UV-vis spectra for all samples with different control agents. It can be seen that all spectra have main and shoulder peaks due to the low symmetry of the

pentagon cross section of AgNWs which belong to its optical signatures (Liu & Yu, 2011). The shoulder peak at around 350 nm regarded to the plasmon resonance of long AgNWs, while the main peak at around 390 nm was attributed to the transverse plasmon mode of AgNWs (You et al., 2009).

University of Malaya



# CHAPTER 5

---

## CONCLUSION

In this dissertation AgNWs were synthesized via polyol process with different mediated agents. Different results of AgNWs were obtained from different mediated agent used. From the research, polyol process successfully proved as a suitable method to synthesis AgNWs. The morphology of the nanowires could be seen clearly from the FESEM and TEM images. The diameter sizes of the AgNWs were in the range between from 60 to 100 nm.

From the XRD results of all the samples, all the diffraction peaks can be assigned to the FCC Ag crystals which according to standard PDF card 04-0783. Four distinct peaks of AgNWs were located at angle of  $2\theta$  around  $38^\circ$ ,  $44^\circ$ ,  $64^\circ$  and  $77.5^\circ$  which corresponding to (111), (200), and (311) plane. This indicated that the AgNWs were finely crystallized and successfully synthesized by the polyol process.

Uv-vis spectra of synthesized AgNWs show that there were two peaks at around 350 and 410 nm. The peaks at around 350 nm called as shoulder peaks, attributed to the plasmon resonance of long AgNWs while other main peaks at around 410 nm were the transverse plasmon mode of AgNWs.

From this research, it shows that the mediated agent was important and should be added into the reaction to get better formation of AgNWs. The present of  $\text{CuCl}_2$  and  $\text{NaCl}$  as mediated agent into the reaction resulted in better formation of nanowires as  $\text{Cl}^-$  provided electrostatic stabilization for the initially formed Ag seeds. The high  $\text{Cl}^-$

concentration during  $\text{CuCl}_2$  and  $\text{NaCl}$  mediated synthesis, help to reduce the concentration of free  $\text{Ag}^+$  in the solution through the formation of  $\text{AgCl}$  nanocrystallites. This decrease in free  $\text{Ag}^+$  during initial  $\text{Ag}$  seed formation and subsequent slow release of  $\text{Ag}^+$ , effectively. The formed  $\text{AgCl}$  can be slowly reduced and decreased rate made anisotropic growth of  $\text{AgNWs}$ . Therefore, these  $\text{CuCl}_2$  and  $\text{NaCl}$  are very good mediated agent to synthesis  $\text{AgNWs}$ .

University of Malaya

## 5.1 Suggestions for future work

As AgNWs were successfully synthesized via this polyol process, it is possible to future the research on the metamaterial behavior of the AgNWs. Almost all materials encountered in optics, such as glass or water, have positive values for both permittivity ( $\epsilon$ ) and permeability ( $\mu$ ). However, metals such as silver and gold have negative permittivity at shorter wavelengths. A material such as a surface plasmon that has either (but not both)  $\epsilon$  or  $\mu$  negative is often opaque to electromagnetic radiation. However, anisotropic materials with only negative permittivity can produce negative refraction due to chirality.

Although the optical properties of a transparent material are fully specified by the parameters  $\epsilon_r$  and  $\mu_r$ , refractive index  $n$  is often used in practice, which can be determined from  $n = \sqrt{\epsilon_r \mu_r}$ . All known non-metamaterial transparent materials possess positive  $\epsilon_r$  and  $\mu_r$ . By convention the positive square root is used for  $n$ . However, some engineered metamaterials have  $\epsilon_r$  and  $\mu_r$  smaller than 0. Because of the product  $\epsilon_r \mu_r$  is positive, so  $n$  is real. Under such circumstances, it is necessary to take the negative square root for  $n$ .

Therefore, further studies should be more focus on the optical properties of the AgNWs especially to get negative value of  $n$ . Moreover, studies on the electromagnetic properties of the AgNWs should also be done as the electromagnetic properties of material is size depending.

## References

Al-Saidi, W., et al. (2012). Adsorption of polyvinylpyrrolidone on Ag surfaces: insight into a structure-directing agent. *Nano Letters*, 12(2), 997-1001.

Bhushan, B. (2010). *Springer handbook of nanotechnology*: Springer Science & Business Media.

Braun, E., et al. (1998). DNA-templated assembly and electrode attachment of a conducting silver wire. *Nature*, 391(6669), 775-778.

Chen, C., et al. (2006). Study on the synthesis of silver nanowires with adjustable diameters through the polyol process. *Nanotechnology*, 17(15), 3933.

Chen, J., et al. (2007). One-dimensional nanostructures of metals: large-scale synthesis and some potential applications. *Langmuir*, 23(8), 4120-4129.

Colvin, V. L. (2003). The potential environmental impact of engineered nanomaterials. *Nature biotechnology*, 21(10), 1166-1170.

Coskun, S., et al. (2011). Polyol synthesis of silver nanowires: an extensive parametric study. *Crystal Growth & Design*, 11(11), 4963-4969.

Day, T. M., et al. (2005). Electrochemical templating of metal nanoparticles and nanowires on single-walled carbon nanotube networks. *Journal of the American Chemical Society*, 127(30), 10639-10647.

Dresselhaus, M., et al. (2003). Nanowires and nanotubes. *Materials Science and Engineering: C*, 23(1), 129-140.

Fiévet, F., & Brayner, R. (2013). The polyol process *Nanomaterials: A Danger or a Promise?* (pp. 1-25): Springer.

Fievet, F., et al. (1989). Preparing monodisperse metal powders in micrometer and submicrometer sizes by the polyol process. *MRS Bull*, 14(12), 29-34.

Foltmann, H., & Quadir, A. (2008). Polyvinylpyrrolidone (PVP)—one of the most widely used excipients in pharmaceuticals: an overview. *Drug Deliv Technol*, 8(6), 22-27.

Han, Y.-J., et al. (2000). Preparation of noble metal nanowires using hexagonal mesoporous silica SBA-15. *Chemistry of Materials*, 12(8), 2068-2069.

Hu, J., et al. (1999). Chemistry and physics in one dimension: synthesis and properties of nanowires and nanotubes. *Accounts of Chemical Research*, 32(5), 435-445.

Huang, M. H., et al. (2000). Ag nanowire formation within mesoporous silica. *Chemical Communications*(12), 1063-1064.

Huang, X., et al. (2011). Synthesis of confined Ag nanowires within mesoporous silica via double solvent technique and their catalytic properties. *Journal of colloid and interface science*, 359(1), 40-46.

Jana, N. R., et al. (2001). Wet chemical synthesis of silver nanorods and nanowires of controllable aspect ratio. Electronic supplementary information (ESI) available: UV–VIS spectra of silver nanorods. See <http://www.rsc.org/suppdata/cc/b1/b100521i>. *Chemical Communications*(7), 617-618.

Korte, K. E., et al. (2008). Rapid synthesis of silver nanowires through a CuCl-or CuCl<sub>2</sub>-mediated polyol process. *J. Mater. Chem.*, 18(4), 437-441.

- Liu, C.-H., & Yu, X. (2011). Silver nanowire-based transparent, flexible, and conductive thin film. *Nanoscale Res. Lett*, 6(1), 75.
- Liu, F.-K., et al. (2005). Gold seed-assisted synthesis of silver nanomaterials under microwave heating. *Materials Letters*, 59(8), 940-944.
- Luu, Q. N., et al. (2011). Preparation and optical properties of silver nanowires and silver-nanowire thin films. *Journal of colloid and interface science*, 356(1), 151-158.
- Malfatti, L., et al. (2010). Writing self-assembled mesostructured films with in situ formation of gold nanoparticles. *Chemistry of Materials*, 22(6), 2132-2137.
- Murphy, C. J., & Jana, N. R. (2002). Controlling the aspect ratio of inorganic nanorods and nanowires. *Advanced materials*, 14(1), 80.
- Oberdörster, E. (2004). Manufactured nanomaterials (fullerenes, C60) induce oxidative stress in the brain of juvenile largemouth bass. *Environmental health perspectives*, 112(10), 1058.
- Roosen, A. R., & Carter, W. C. (1998). Simulations of microstructural evolution: anisotropic growth and coarsening. *Physica A: Statistical Mechanics and its Applications*, 261(1), 232-247.
- Sarkar, R., et al. (2010). Synthesis and photoluminescence properties of silver nanowires. *Current Applied Physics*, 10(3), 853-857.
- Shen, Q., et al. (2007). Fabrication of silver nanorods controlled by a Segmented Copolymer. *The Journal of Physical Chemistry C*, 111(37), 13673-13678.

- Shi, C., et al. (2004). Investigation on the catalytic roles of silver species in the selective catalytic reduction of NO<sub>x</sub> with methane. *Applied Catalysis B: Environmental*, 51(3), 171-181.
- Silva, G. A. (2004). Introduction to nanotechnology and its applications to medicine. *Surgical neurology*, 61(3), 216-220.
- Song, Y.-J., et al. (2014). Applications of Silver Nanowires on Transparent Conducting Film and Electrode of Electrochemical Capacitor. *Journal of Nanomaterials*, 2014.
- Sun, Y., & Xia, Y. (1991). Large-scale synthesis of uniform silver nanowires through a soft, self-seeding, polyol process. *Nature*, 353(1991), 737.
- Sun, Y., et al. (2002). Uniform silver nanowires synthesis by reducing AgNO<sub>3</sub> with ethylene glycol in the presence of seeds and poly (vinyl pyrrolidone). *Chemistry of Materials*, 14(11), 4736-4745.
- Tang, X., & Tsuji, M. (2010). *Syntheses of silver nanowires in liquid phase*: INTECH Open Access Publisher.
- Tang, X., et al. (2009). Rapid and high-yield synthesis of silver nanowires using air-assisted polyol method with chloride ions. *Colloids and Surfaces A: Physicochemical and Engineering Aspects*, 338(1), 33-39.
- Tsuji, M., et al. (2006). Effects of chain length of polyvinylpyrrolidone for the synthesis of silver nanostructures by a microwave-polyol method. *Materials Letters*, 60(6), 834-838.
- You, T., et al. (2009). Controllable synthesis of pentagonal silver nanowires via a simple alcohol-thermal method. *Materials Letters*, 63(11), 920-922.

Zhang, X.-Y., et al. (2012). Fabrication and spectroscopic investigation of branched silver nanowires and nanomeshworks. *Nanoscale research letters*, 7(1), 1-7.

Zhang, Z., et al. (2011). High yield preparation of silver nanowires by CuCl<sub>2</sub>-mediated polyol method and application in semitransparent conduction electrode. *Physica E: Low-dimensional Systems and Nanostructures*, 44(3), 535-540.

Zong, R.-L., et al. (2004). Synthesis and optical properties of silver nanowire arrays embedded in anodic alumina membrane. *The Journal of Physical Chemistry B*, 108(43), 16713-16716.

#### Internet References

[http://en.wikipedia.org/wiki/Silver\\_nitrate](http://en.wikipedia.org/wiki/Silver_nitrate), 16/01/2013a.

<http://en.wikipedia.org/wiki/Polyvinylpyrrolidone>, 16/01/2013b.

[http://en.wikipedia.org/wiki/Ethylene\\_glycol](http://en.wikipedia.org/wiki/Ethylene_glycol), 16/01/2013c.

[http://en.wikipedia.org/wiki/Sodium\\_chloride](http://en.wikipedia.org/wiki/Sodium_chloride), 25/03/2013a.

[http://en.wikipedia.org/wiki/Copper\(II\)\\_chloride](http://en.wikipedia.org/wiki/Copper(II)_chloride), 25/03/2013b.



## Research Article

# Synthesis and Growth Mechanism of Silver Nanowires through Different Mediated Agents ( $\text{CuCl}_2$ and $\text{NaCl}$ ) Polyol Process

**Mohd Rafie Johan, Nurul Azri Khalisah Aznan, Soo Teng Yee, Ing Hong Ho, Soo Wern Ooi, Noorsaiyyidah Darman Singho, and Fatihah Aplop**

*Nanomaterials Engineering Research Group, Advanced Materials Research Laboratory, Department of Mechanical Engineering, University of Malaya, 50603 Kuala Lumpur, Malaysia*

Correspondence should be addressed to Noorsaiyyidah Darman Singho; [ieyda\\_putri@um.edu.my](mailto:ieyda_putri@um.edu.my)

Received 6 February 2014; Revised 23 April 2014; Accepted 23 April 2014; Published 22 May 2014

Academic Editor: Zhenhui Kang

Copyright © 2014 Mohd Rafie Johan et al. This is an open access article distributed under the Creative Commons Attribution License, which permits unrestricted use, distribution, and reproduction in any medium, provided the original work is properly cited.

Silver nanowires (AgNWs) have been synthesized by polyol process through different mediated agents ( $\text{CuCl}_2$  and  $\text{NaCl}$ ). The presence of cations and anions ( $\text{Cu(II)}$ ,  $\text{Na}^+$ , and  $\text{Cl}^-$ ) has been shown to have a strong impact on the shape of silver nanostructures. The field emission scanning electron microscopy (FESEM) and transmission electron microscopy (TEM) show uniform nanowires. The UV-vis spectra show that plasmon peak indicated the formation of nanowires. The X-ray diffraction (XRD) pattern displayed that final product was highly crystallized and pure. The growth mechanism of AgNWs was proposed.

## 1. Introduction

One-dimensional (1-D) metal nanostructures such as nanowires have attracted extensive attention due to their unique magnetic, optical, and electronic properties compared to zero-dimensional (0-D) nanostructures [1–6]. Among these 1-D metal nanostructures, silver nanowires (AgNWs) are particularly of interest because the bulk Ag exhibits the highest electrical and thermal conductivity among all metals. There are many applications where nanowires could be exploited to greatly enhance the functionality of a material [7–9]. In these regards, the synthesis of nanowires has attracted attention from a broad range of researchers [10–14]. Over the last decade, various methods had been used to synthesize AgNWs such as polyol process [12–14], wet chemical synthesis [15, 16], hydrothermal method [17, 18], and ultraviolet irradiation photoreduction techniques [19, 20]. Among these methods, the polyol process is considered due to simple, effective, low cost, and high yield. In the polyol process, an exotic reagent leads to the formation of wire like structure. Xia and Sun [13] have modified the polyol process by generating AgNWs with diameters in the range of 30–50 nm. By controlling the parameters such as reaction time, molar ratio between capping agent and metallic precursor, temperature, and addition

of control agent, a reasonable control growth of AgNWs may be achieved. In this work, AgNWs were synthesized through reducing silver nitrate ( $\text{AgNO}_3$ ) with 1,2-propanediol (Sample 1) and ethylene glycol (EG) (Samples 2 and 3) in the presence of polyvinylpyrrolidone (PVP) as the surfactant which can direct the growth of AgNWs and protect them from aggregation. The mediated agents such as  $\text{CuCl}_2$  (Sample 2) and  $\text{NaCl}$  (Sample 3) are added to facilitate the growth of AgNWs. We believe  $\text{Cu(II)}$ ,  $\text{Na}^+$ , and  $\text{Cl}^-$  ions are necessary for AgNWs production.

## 2. Experimental Method

Anhydrous 1,2-propanediol (99%),  $\text{AgNO}_3$  (99%), and polyvinylpyrrolidone were purchased from Acros. All the chemicals were used as received without any further purification. The first sample (Sample 1) is without any mediated agent. 10 mL of 1,2-propanediol was added into a 50 mL three-necked flask at  $170^\circ\text{C}$  for 2 h. Then 0.5 mL of 1,2-propanediol solution of  $\text{AgNO}_3$  (0.005 M) was injected into the 1,2-propanediol under vigorous magnetic stirring. Later, 3 mL of 1,2-propanediol solution of  $\text{AgNO}_3$  (0.1 M) and 3 mL of 1,2-propanediol solution of PVP (0.45 M) were added dropwise

simultaneously over a period of 5 minutes. The solution immediately turned from colorless to light yellow. The reaction was continued for 1 h and heated at 170°C for 30 min. A grey suspension was obtained and allowed to cool at the room temperature. Then, the mixture was diluted by acetone, centrifuged, washed by deionized water, and dried in a vacuum for 24 hours at room temperature.

The second sample (Sample 2) is with CuCl<sub>2</sub> as the mediated agent. Firstly, 5 mL of ethylene glycol was added into a beaker and heated for 1 hour using silicon oil bath at 150°C. Then, 40 μL of a 4 mM CuCl<sub>2</sub>·H<sub>2</sub>O/ethylene glycol was added into the solution, stirred, and allowed to heat for 15 minutes. After that, 1.5 mL of 114 mM PVP/ethylene glycol was added into the beaker, followed by 1.5 mL of 94 mM AgNO<sub>3</sub>/ethylene glycol. The color changed to yellow and became brownish grey after AgNO<sub>3</sub>/ethylene glycol was added. The solution was heated for another 1 hour. Then, the solution was taken out and let to cool at room temperature. The solution was centrifuged at 3000 rpm and 30 min each with acetone and deionized water. The final product was preserved in deionized water until characterization.

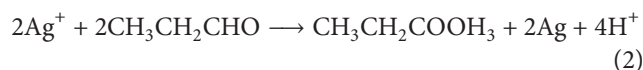
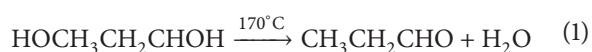
The third sample (Sample 3) is with NaCl as the mediated agent. 15 mL of 0.36 M of ethylene glycol (EG) solution of polyvinylpyrrolidone (PVP) was heated and stirred for 15 minutes. It was then followed by microwave heating at 170°C for an hour. Then, 20 μL of 0.1 M EG solution of NaCl and 20 μL of 0.06 M EG solution of AgNO<sub>3</sub> were injected into this EG solution of PVP to produce AgCl as seeds. After 15 minutes of injection, 15 mL of 0.06 M of EG solution of AgNO<sub>3</sub> was injected into mixture solution within 5 minutes. The mixture solution was stirred to obtain a homogeneous solution. The color of mixture solution slowly changes to light yellow. The mixture solution was then heated under microwave irradiation with temperature maintained at 170°C for approximately 30 minutes. It is allowed to cool naturally to room temperature and turn to gray color. The resulting solution was washed several times using acetone and ethanol and then dried in vacuum at 60°C.

The X-ray diffraction (XRD) patterns were recorded using a Siemens D5000 X-ray diffractometer (Cu-Kα radiation, λ = 0.154 nm). The transmission electron microscopy (TEM) images were taken on a Libra 120 model TEM using accelerating voltage of 400 kV. Field emission scanning electron microscopy (FE-SEM) images were taken using Zeiss Auriga. The UV-visible spectrum of the as-prepared products was recorded on a Varian Cary 50 UV-vis spectroscopy.

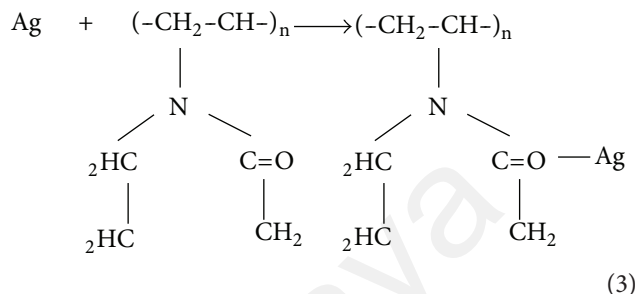
### 3. Results and Discussion

#### 3.1. Mechanism for the Formation of AgNWs

3.1.1. *Scheme 1 (Sample 1 without any Mediated Agent)*. The formation of anisotropic AgNWs involves two steps. In the first step, 1,2-propanediol was converted to propionaldehyde at high temperature (170°C) as shown in (1). Then it reduces Ag<sup>+</sup> ions to Ag atoms as shown in (2). Consider

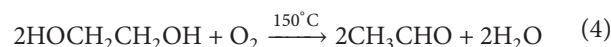


In the second step, AgNO<sub>3</sub> and PVP were added dropwise to the reaction system allowing the nucleation and growth of AgNWs.



Ag atoms are nucleated through the homogeneous nucleation process. These AgNps were well dispersed because of the presence of a polymeric surfactant PVP that could be chemically adsorbed onto the surfaces of Ag through O–Ag bonding (3). PVP has an affinity toward many chemicals to form coordinative compounds due to the structure of polyvinyl skeleton with strong polar group (pyrrolidone ring). In this case, C=O polar groups were interacted with Ag<sup>+</sup> ions and form coordinating complex as shown in (3). When this dispersion of AgNps was continuously heated at 170°C, the small nanoparticles progressively disappeared to the benefit of larger ones via Ostwald ripening process [21]. The critical particle radius increased with temperature. As the reaction continued, the small AgNps were no longer stable in solution, and they started to dissolve and contribute to the growth of larger ones. With the assistance of PVP, some of the larger nanoparticles were able to grow into rod-shaped structures. The growth process would continue until all the AgNps were completely consumed and only nanowires survived.

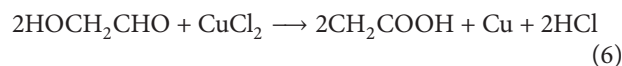
3.1.2. *Scheme 2 (Sample 2 with CuCl<sub>2</sub> Mediated Agent)*. In the initial step, high temperature is crucial for the conversion of ethylene glycol to glycolaldehyde as shown in



AgNps were formed by reducing Ag<sup>+</sup> ions with glycolaldehyde as shown in



It was found that a small amount of Cl<sup>-</sup> must be added to a polyol synthesis to provide electrostatic stabilization for the initially formed Ag seeds [4]:

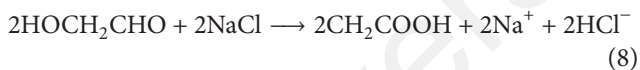


In addition to electrostatically stabilizing the initially formed Ag seeds, the high Cl<sup>-</sup> concentrations during CuCl<sub>2</sub>

mediated synthesis help reduce the concentration of free  $\text{Ag}^+$  ions in the solution through the formation of  $\text{AgCl}$ . Subsequent, it will slowly release the  $\text{Ag}^+$  and subsequent slow release of  $\text{Ag}^+$  effectively. These facilitate the high-yield formation of the thermodynamically more stable multiply twinned Ag seeds that are required for wire length. Valency metal ions ( $\text{Cu}^{2+}$ ) were reduced by EG to low valence ( $\text{Cu}^+$ ) which in turn reacted with and scavenged adsorbed atomic oxygen from the surface of  $\text{AgNps}$ . Here,  $\text{Cu}^{2+}$  can remove oxygen from the solvent which prevents twinned seeds dissolved by oxidative etching and scavenging adsorbed atomic oxygen from the surface of the Ag seeds, facilitating multiply twinned seeds growth [12].

In the final step,  $\text{AgNO}_3$  and PVP were added dropwise to the reaction system allowing the nucleation and growth of silver nanowires as shown in (3).  $\text{AgNps}$  were well dispersed because of the presence of PVP, a polymeric surfactant that could be chemically adsorbed onto the surfaces of Ag through O–Ag bonding. As the reaction continued, the small Ag nanoparticles were no longer stable in solution and they started to dissolve and contribute to the growth of larger ones. When multiple twinned form the nanoparticles during a nuclei period, the PVP was bounded preferentially on  $\{100\}$  then  $\{111\}$  [22, 23]. This inhibited the growth along  $\{111\}$  direction. So the growth took place only in the  $\{110\}$  direction resulting in the fivefold twinned nanowires (Figure 1).

**3.1.3. Scheme 3 (Sample 3 with NaCl Mediated Agent).** Like in Scheme 2, the formation of anisotropic AgNWs involves a number of steps. The first two steps are similar to (4) and (5). Like in Scheme 2, chloride ions were added (8) to stabilize  $\text{AgNps}$  and prevented the growth of nanoparticles [10]. As a result, nanoparticles that can grow will dissolve via Oswald ripening:



The high  $\text{Cl}^-$  concentration during NaCl mediated synthesis helps reduce the concentration of free  $\text{Ag}^+$  in the solution through the formation of  $\text{AgCl}$  (9). Subsequent, it will slowly release the  $\text{Ag}^+$  and subsequent slow release of  $\text{Ag}^+$ , effectively. This facilitates the high yield formation of the thermodynamically stable multiply twinned Ag seeds. So,  $\text{AgCl}$  precipitate that forms in the early stages of the reaction serves as a seed for multitwin particles. The formed  $\text{AgCl}$  nanoparticles can be reduced slowly and decreased reaction rate makes anisotropic growth of Ag nanowires favorable [24]. Meanwhile,  $\text{Na}^+$  can remove oxygen from the solvent which prevents twinned seeds dissolved by oxidative etching and scavenging adsorbed atomic oxygen from the surface of the silver seeds, facilitating multiply twinned seeds growth [12]. In the final step,  $\text{AgNO}_3$  and PVP were added dropwise to the recreation system allowing the nucleation and growth of AgNWs as shown in (3).

With passivation of some facets of particles by PVP, some nanoparticles can grow into multitwin particles. PVP is

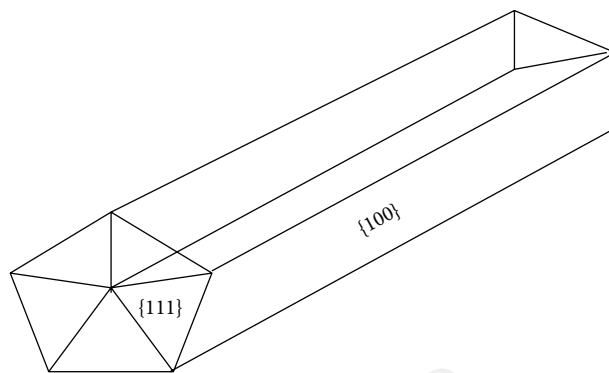


FIGURE 1: Schematic of 5-fold twinned pentagonal nanowires consisting of five elongated  $\{100\}$  facets and 10  $\{111\}$  end facets.

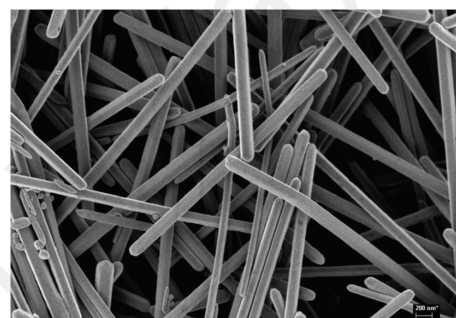


FIGURE 2: FESEM image of AgNWs (without any mediated agent).

believed to passivate (100) faces of these multitwin particles and leave (111) planes achieve for anisotropic growth at  $[110]$  direction [13] (Figure 1). As the addition of  $\text{Ag}^+$  continues, multitwin particles grow into Ag nanowires.

**3.2. FESEM Analysis.** Figure 2 shows the FESEM image of AgNWs without any mediated agents. The image shows straightness along the longitudinal axis, the level of perfection, and the copiousness in quantity that we could routinely achieve using this synthetic approach. The presence of silver nanoparticles ( $\text{AgNps}$ ) is also evident in the figure indicating that not all of  $\text{AgNps}$  are transformed into nanowires.

Figure 3 shows the FESEM image of AgNWs with  $\text{CuCl}_2$  as the mediated agent. The image reveals that the product is entirely composed of a large quantity of uniform nanowires with a mean diameter of 65 nm. The high faces of PVP on all faces of the seeds lead to anisotropic growth mode.

Figure 4 shows the FESEM image of AgNWs with NaCl as the mediated agent. The image shows well-defined wires with mean diameter of 80 nm.

**3.3. TEM Analysis.** Figure 5 shows the TEM image of individual AgNWs without any mediated agents with 84 nm in diameter and 1119 nm in length.

Figure 6 shows a TEM image of an individual AgNW ( $\text{CuCl}_2$  mediated agent) with 87 nm in diameter and 3  $\mu\text{m}$

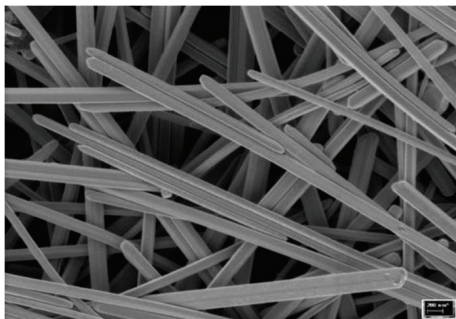


FIGURE 3: FESEM image of AgNWs (with  $\text{CuCl}_2$  mediated agent).

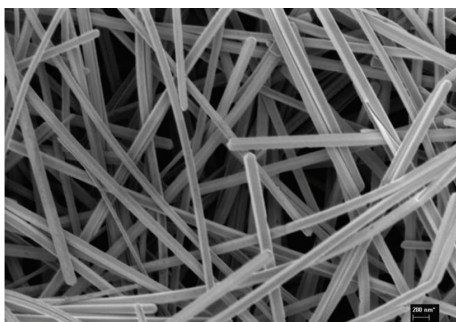


FIGURE 4: FESEM image of AgNWs (with  $\text{NaCl}$  mediated agent).

in length. The insert of Figure 6 reveals a pentagonal cross-section of AgNWs and indicates the multiple-twinned structure of the AgNWs [24].

Figure 7 shows the TEM image of AgNWs with  $\text{NaCl}$  mediated agent. The TEM image displayed a twin boundary in the middle of nanowires and pentagon shape cross-section at the end of nanowires.

**3.4. XRD Analysis.** Figure 8 shows the XRD pattern of AgNWs with and without mediated agent. The peaks at angles of  $2\theta = 38.1^\circ$ ,  $44.2^\circ$ ,  $64.3^\circ$ , and  $77.5^\circ$  correspond to the (111), (200), (220), and (311) crystal planes of the face center cubic (FCC) Ag, respectively. The lattice constant calculated from the diffraction pattern was 0.4086 nm, which is in agreement with the reported value of silver (JCPDS 04-0783). Furthermore, the intensity ratio of the (111) to (200) peaks is 2.0, in good agreement with the theoretical ratio, that is, 2.5 [14].

Figure 9 shows the XRD pattern of highly crystalline AgNWs with  $\text{CuCl}_2$  mediated agent. It has a similar pattern with AgNWs without mediated agent (Figure 8). The XRD pattern reveals that the synthesis AgNWs through polyol process comprise pure phase. The lattice constant,  $a$ , was  $4.07724 \text{ \AA}$  which is almost approaching the literature value of  $4.086 \text{ \AA}$ . The ratio of intensity between (111) and (200) peaks reveals a relatively high value of 3.2 compared to the theoretical ratio value of 2.5. This high value of ratio indicates the enhancement of {111} crystalline planes in the AgNWs.

Figure 10 shows the XRD pattern of AgNWs with  $\text{NaCl}$  mediated agent. It exhibits well-defined peaks without any impurity element peaks detected. This indicated the success

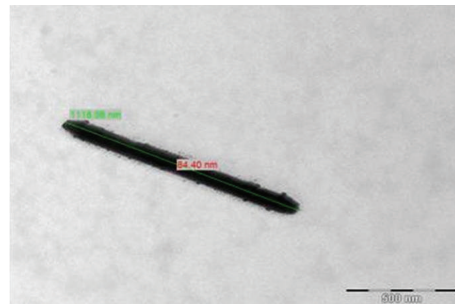


FIGURE 5: TEM image of AgNWs without any mediated agent.

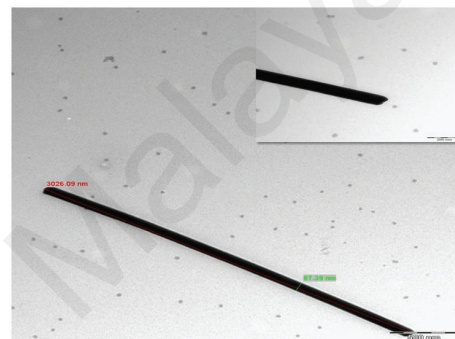


FIGURE 6: TEM image of AgNWs with  $\text{CuCl}_2$  mediated agent (insert: pentagon cross-section of AgNWs).

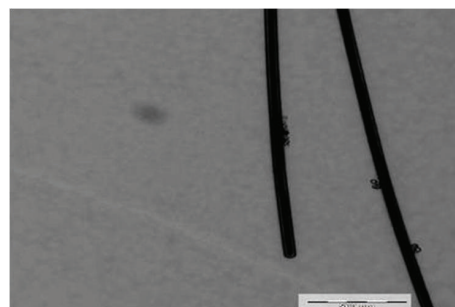


FIGURE 7: TEM image of AgNWs (with  $\text{NaCl}$  mediated agent).

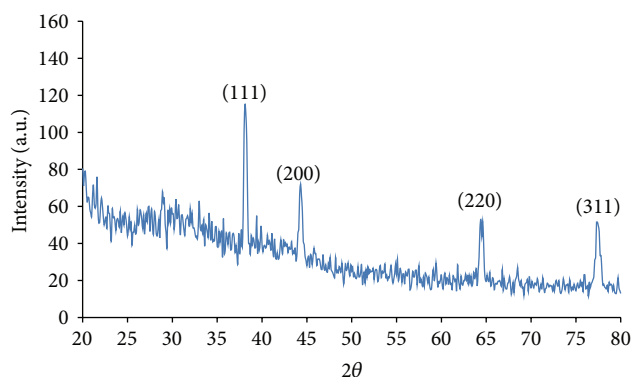
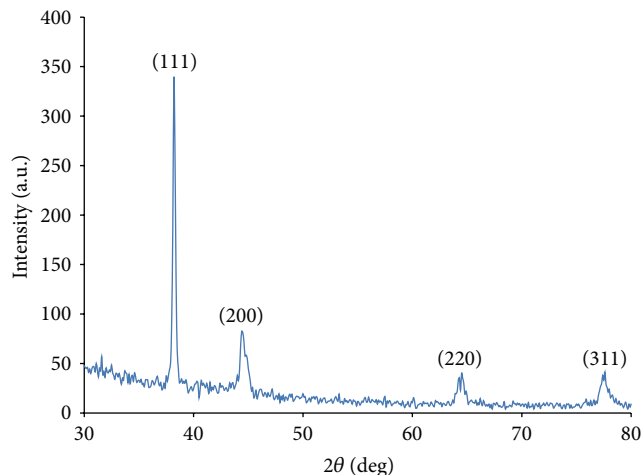
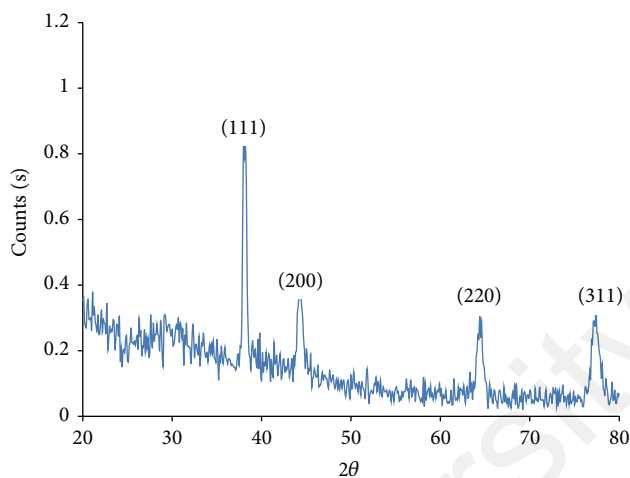
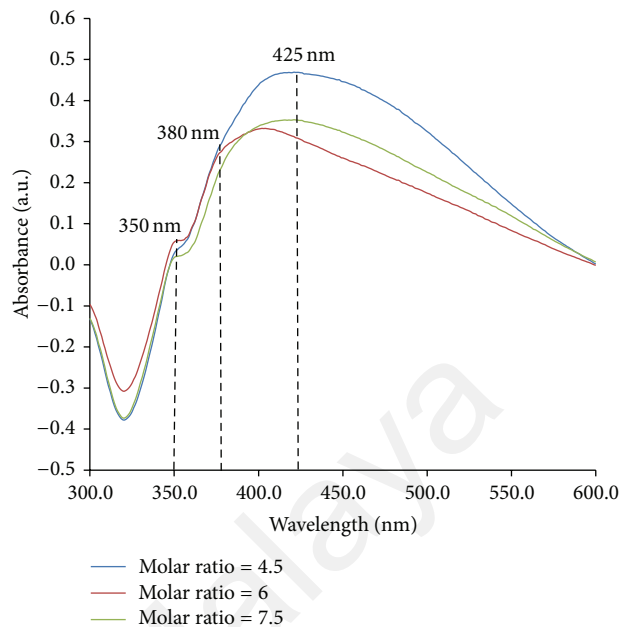
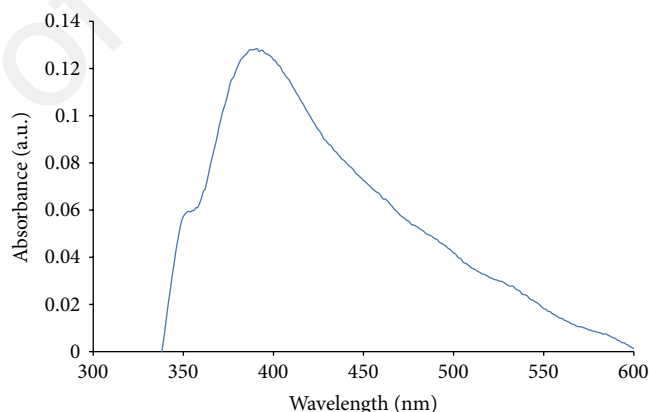


FIGURE 8: XRD pattern of AgNWs without any mediated agent.

FIGURE 9: XRD pattern of AgNWs (with  $\text{CuCl}_2$  mediated agent).FIGURE 10: XRD patterns of the as-synthesized AgNWs (with  $\text{NaCl}$  mediated agent).

in the formation of the crystalline silver nanowires. The four diffraction peaks obtained are similar to peaks in Figures 8 and 9. It is worth noting that the ratio of intensity between (111) and (200) peaks exhibits a relative value of 2.05 (the theoretical ratio is 2.5). It indicated that the sample becomes less crystalline with  $\text{NaCl}$  mediated agent.

**3.5. UV-Vis Spectroscopy Analysis.** Figure 11 shows the absorption spectra of AgNWs without mediated agent at different molar ratio of PVP to  $\text{AgNO}_3$ . The appearance of a weak surface plasmon resonance (SPR) at 425 nm indicated the formation of AgNps [17]. This implies that the final product synthesized under this particular condition was a mixture of AgNps and AgNWs. As the molar ratio increases from 4.5 to 7.5, the intensity of the SPR is slightly decreased. Furthermore, the SPR peak around 425 nm is blue-shifted to 404 nm. The shoulder peak at 380 nm could be considered as the optical signature of AgNWs. At this point, optical signatures similar to those of bulk Ag also began to appear as indicated by the

FIGURE 11: Absorption spectra of AgNWs (without any mediated agent) with different molar ratio of PVP and  $\text{AgNO}_3$ .FIGURE 12: Absorption spectra of AgNWs (with  $\text{CuCl}_2$  mediated agent).

shoulder peak around 350 nm. With increasing molar ratio, the intensity of absorption bands at 350 and 380 nm increased apparently due to increased density of AgNWs.

Figure 12 shows the UV-vis absorption spectra for AgNWs with  $\text{CuCl}_2$  mediated agent. The peak positions at 391 nm could be considered as the optical signature of relatively long AgNWs. At this point, optical signatures similar to those of bulk silver also began to appear as indicated by the shoulder peak around 357 nm [25]. Compared to the previous absorption spectra (Figure 11), no peak for AgNps existed. This indicates that the sample is completely of AgNWs.

Figure 13 shows the absorption spectra of ANWs (with  $\text{NaCl}$  mediated agent) synthesized with different molar of  $\text{AgNO}_3$ . The appearance of a story peak at 384 nm could be considered as the transverse mode of relatively long AgNWs.

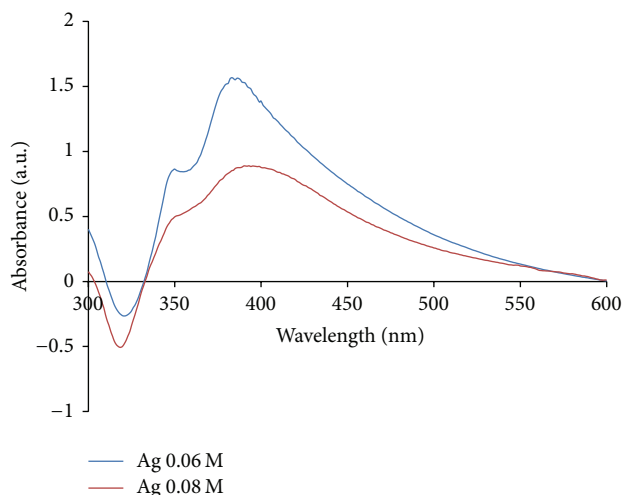


FIGURE 13: Absorption spectra of the as-synthesized AgNWs (with NaCl mediated agent) at different molar of  $\text{AgNO}_3$ : (a) 0.06; (b) 0.08.

At this point, optical signatures similar to those of bulk Ag also began to appear as indicated by the shoulder peak around 350 nm. As the concentration of  $\text{AgNO}_3$  increases from 0.06 to 0.08 M, the intensity of these peaks increased significantly and red-shifted to 394 and 351 nm, respectively. This result indicated that the AgNWs increased in number with apparent growth in length. Again, the spectra show that the sample is completely AgNWs.

#### 4. Conclusion

AgNWs were successfully synthesized by using polyol technique with and without mediated agents. It was found that the addition of  $\text{CuCl}_2$  or NaCl to the polyol reduction of  $\text{AgNO}_3$  in the presence of PVP greatly facilitated the formation of AgNWs. Without the mediated agents, the final product synthesized was a mixture of AgNps and AgNWs. Both the cation and the anions are crucial for the successful production of AgNWs.

#### Conflict of Interests

The authors declare that there is no conflict of interests regarding the publication of this paper.

#### Acknowledgment

The financial support received from University of Malaya Research Grant (RP011C-13AET) is gratefully acknowledged.

#### References

- [1] Y. Xia, P. Yang, Y. Sun et al., "One-dimensional nanostructures: synthesis, characterization, and applications," *Advanced Materials*, vol. 15, no. 5, pp. 353–389, 2003.
- [2] Z. L. Wang, "Characterizing the structure and properties of individual wire-like nanoentities," *Advanced Materials*, vol. 12, no. 17, pp. 1295–1298, 2000.
- [3] P. J. Cao, Y. S. Gu, H. W. Lin et al., "High-density aligned carbon nanotubes with uniform diameters," *Journal of Materials Research*, vol. 18, pp. 1686–1690, 2003.
- [4] J. Hu, T. W. Odom, and C. M. Lieber, "Chemistry and physics in one dimension: synthesis and properties of nanowires and nanotubes," *Accounts of Chemical Research*, vol. 32, no. 5, pp. 435–445, 1999.
- [5] N. A. C. Lah and M. R. Johan, "Facile shape control synthesis and optical properties of silver nanoparticles stabilized by Daxad 19 surfactant," *Applied Surface Science*, vol. 257, no. 17, pp. 7494–7500, 2011.
- [6] N. A. C. Lah and M. R. Johan, "Optical and thermodynamic studies of silver nanoparticles stabilized by Daxad 19 surfactant," *International Journal of Materials Research*, vol. 102, no. 3, pp. 340–347, 2011.
- [7] C. M. Lieber, "One-dimensional nanostructures: chemistry, physics & applications," *Solid State Communications*, vol. 107, no. 11, pp. 607–616, 1998.
- [8] M. S. Gudiksen, L. J. Lauhon, J. Wang, D. C. Smith, and C. M. Lieber, "Growth of nanowire superlattice structures for nanoscale photonics and electronics," *Nature*, vol. 415, no. 6872, pp. 617–620, 2002.
- [9] Y. Cui and C. M. Lieber, "Functional nanoscale electronic devices assembled using silicon nanowire building blocks," *Science*, vol. 291, no. 5505, pp. 851–853, 2001.
- [10] C. R. Martin, "Nanomaterials: a membrane-based synthetic approach," *Science*, vol. 266, no. 5193, pp. 1961–1966, 1994.
- [11] A. M. Morales and C. M. Lieber, "A laser ablation method for the synthesis of crystalline semiconductor nanowires," *Science*, vol. 279, no. 5348, pp. 208–211, 1998.
- [12] K. E. Korte, S. E. Skrabalak, and Y. J. Xia, "Rapid synthesis of silver nanowires through a  $\text{CuCl}^-$  or  $\text{CuCl}_2^-$ -mediated polyol process," *Journal of Materials Chemistry*, vol. 18, pp. 437–441, 2008.
- [13] Y. Xia and Y. Sun, "Large-scale synthesis of uniform silver nanowires through a soft, self-seeding, polyol process," *Advanced Materials*, vol. 14, no. 11, pp. 833–837, 2002.
- [14] Y. Sun, Y. Yin, B. T. Mayers, T. Herricks, and Y. Xia, "Uniform silver nanowires synthesis by reducing  $\text{AgNO}_3$  with ethylene glycol in the presence of seeds and poly(vinyl pyrrolidone)," *Chemistry of Materials*, vol. 14, no. 11, pp. 4736–4745, 2002.
- [15] K. K. Coswell, C. M. Bender, and C. J. Murphy, "Seedless, surfactantless wet chemical synthesis of silver nanowires," *Nano Letters*, vol. 3, no. 5, pp. 667–669, 2003.
- [16] P. S. Mdluli and N. Revaprasadu, "An improved N,N-dimethylformamide and polyvinyl pyrrolidone approach for the synthesis of long silver nanowires," *Journal of Alloys and Compounds*, vol. 469, no. 1–2, pp. 519–522, 2009.
- [17] Z. Wang, J. Liu, X. Chen, J. Wan, and Y. Qian, "A simple hydrothermal route to large-scale synthesis of uniform silver nanowires," *Chemistry—A European Journal*, vol. 11, no. 1, pp. 160–163, 2005.
- [18] J. Xu, J. Hu, C. Peng, H. Liu, and Y. Hu, "A simple approach to the synthesis of silver nanowires by hydrothermal process in the presence of gemini surfactant," *Journal of Colloid and Interface Science*, vol. 298, no. 2, pp. 689–693, 2006.
- [19] Y. Zhou, S. H. Yu, C. Y. Wang, X. G. Li, Y. R. Zhu, and Z. Y. Chen, "A novel ultraviolet irradiation photoreduction technique for the preparation of single-crystal Ag nanorods and Ag dendrites," *Advanced Materials*, vol. 11, no. 10, pp. 850–852, 1999.
- [20] K. Zou, X. H. Zhang, X. F. Duan, X. M. Meng, and S. K. Wu, "Seed-mediated synthesis of silver nanostructures and

- polymer/ silver nanocables by UV irradiation," *Journal of Crystal Growth*, vol. 273, no. 1-2, pp. 285–291, 2004.
- [21] A. R. Roosen and W. C. Carter, "Simulations of microstructural evolution: anisotropic growth and coarsening," *Physica A*, vol. 261, no. 1-2, pp. 232–247, 1998.
- [22] W. A. Al-Saidi, H. Feng, and K. A. Fichthorn, "Adsorption of polyvinylpyrrolidone on Ag surfaces: insight into a structure-directing agent," *Nano Letters*, vol. 12, no. 2, pp. 997–1001, 2012.
- [23] W. A. Al-Saidi, H. Feng, and K. A. Fichthorn, "The binding of PVP to Ag surfaces: insight into a structure-directing agent from dispersion-corrected density-functional theory," *The Journal of Physical Chemistry C*, vol. 117, pp. 1163–1171, 2013.
- [24] K. E. Korte, S. E. Skrabalak, and Y. Xia, "Rapid synthesis of silver nanowires through a CuCl- or CuCl<sub>2</sub>-mediated polyol process," *Journal of Materials Chemistry*, vol. 18, no. 4, pp. 437–441, 2008.
- [25] T. You, S. Xu, S. Sun, and X. Song, "Controllable synthesis of pentagonal silver nanowires via a simple alcohol-thermal method," *Materials Letters*, vol. 63, no. 11, pp. 920–922, 2009.



**Hindawi**

Submit your manuscripts at  
<http://www.hindawi.com>

